

**PERFORMANCE EVALUATION OF MIMO/STBC SYSTEMS
WITH ANTENNA SELECTION TECHNIQUES WORKING
UNDER NAKAGAMI-m FADING CHANNELS**

*A thesis
Submitted in partial fulfillment of the requirements
for the award of degree of*

Master of Engineering
in

Electronics and communication Engineering



Submitted by
Shyamveer

Reg. No: 800961017

Under the guidance of

Dr. Amit Kumar Kohli

Assistant Professor, ECED

**ELECTRONICS AND COMMUNICATION ENGINEERING
DEPARTMENT**

THAPAR UNIVERSITY

(Established under the section 3 of UGC Act, 1956)

PATIALA-147004(PUNJAB)

DECLARATION

I, **Shyamveer** hereby certify that the work which is being presented in this thesis entitle, **"PERFORMANCE EVALUATION OF MIMO/STBC SYSTEM WITH ANTENNA SELECTION TECHNIQUES UNDER NAKAGAMI-m FADING CHANNEL"** is practical fulfillment of requirement for the award of degree of Master of Engineering in Electronics and communication from Thapar University, Patiala, is an authentic record of my own work carried under the supervision of **Dr. Amit Kumar Kohli** during semester 4th, 2011.

The matter presented in this thesis has not been submitted in any University or Institute for the award of Master of Engineering.

Date: 01/07/2011



Shyamveer

Roll.no. 800961017

I certified that the above statement made by the student is correct to the best of my knowledge and belief.



Dr. Amit Kumar Kohli

Assistant Professor

ECED, TU, Patiala-147004, (Punjab)

Date... 01/7/2011



Head of Department

ECED, TU, Patiala-147004, (Punjab)

Date... 1/7/11



Dr. S. K. Mohapatra

Dean of Academic Affairs

ECED, TU, Patiala-147004, (Punjab)

Date... 01/07/11

ACKNOWLEDGEMENT

I would like to express my gratitude to **Dr. Amit Kumar Kohli**, Assistant Professor, Electronic and Communication Engineering Department, Thapar University, Patiala for his patient guidance and support throughout this thesis work. I am truly very fortunate to have the opportunity to work with him. He has provided me help in technical writing and presentation style, and I found this guidance to be extremely valuable.

I am very thankful to head of the Department, **Dr. A. K. Chatterjee**, for his encouragement, support and providing the facilities for the completion of this thesis.

I am also thankful to entire faculty and staff members of Electronic and Communication Engineering Department for their unyielding encouragement.

I am greatly indebted to all my friends, who have graciously applied themselves to the task of helping me with ample morale support and valuable suggestions. Finally, I would like to extend my gratitude to all those persons who directly or indirectly helped me in the process and contributed towards this work.

Shyamveer

ABSTRACT

The latest wireless communication techniques such as high speed wireless internet application demand higher data rates and better quality of service. However, “Multiple-input multiple-output (MIMO) systems can increase the system capacity and improve transmission reliability. By transmitting multiple copies of data, a MIMO system can effectively combat the effects of fading. Moreover, using MIMO system will lead to increase of system cost and complexity, which constrain the development of MIMO technology, however, the antenna selection (AS) techniques have been applied in MIMO system design to reduce the system efficiently reduce the complexity and cost. There are three possible AS scheme namely receive antenna selection (RAS), transmit antenna selection (TAS) and joint antenna selection (T-RAS).

Thus, this thesis presents a comprehensive analysis of antenna selection in MIMO/STBC system over Nakagami- m fading channel. The main work is as following: We briefly explain and analyze performance all three possible antenna selection (TAS, RAS, T-RAS) scheme in MIMO/STBC system and drive the BER expression in close-form, where system select an antenna (at transmitter, receiver or both side) that maximizes the received signal power. This thesis also compares the performance of all three possible antenna selection schemes. Exact bit error rate (BER) expression for binary phase shift keying (BPSK) modulations are derived by using the moment generating function (MGF)-based analysis method of the output signal-to-noise ratios (SNR).

The Nakagami- m distribution has been considered for MIMO channel modeling since a wide range of fading channels, from severe to moderate, can be modeled by using Nakagami- m distribution. The Rayleigh distribution is a special case of the Nakagami- m distribution. In this thesis, we analyze the error performance RAS, TAS & T-RAS of MIMO/STBC schemes over Nakagami- m fading channels. Our approach can be used over not only independent but also arbitrary correlated Rayleigh, Nakagami- m and Rician fading channels.

Key words: - Multiple input multiple output (MIMO), space time block code (STBC), Moment generating function (MGF), Nakagami- m fading, transmit antenna selection (TAS), receive antenna selection (RAS), joint transmit and receive antenna selection (T-

RAS), Binary Phase-Shift Keying (BPSK), bit error rate (BER), symbol error rate (SER), signal to noise ratio (SNR)

TABLE OF CONTENTS

Declaration	i
Acknowledgement	ii
Abstract	iii-iv
List of Figures	viii-ix
List of Tables	x
List of Acronyms	xi-xii
Chapter 1: Introduction	1
1.1 Background	1
1.1.1 Need of antenna selection	3
1.2 Literature Review	3
1.3 Thesis Objectives	7
1.4 Thesis Outline	7
Chapter 2: Digital Wireless Transmission Schemes	9
2.1 Introduction	9
2.2 Digital Communication Systems	9
2.3 Digital Modulation Schemes	11
2.3.1 Introduction	11
2.3.2 M-ray Phase Shift Keying	11
2.3.3 M-ray Quadrature Amplitude Modulation	12
2.4 Multiple-Input Multiple-Output System Model	12
2.5 Antenna Selection Techniques	17
2.5.1 Introduction	17
2.5.2 Transmit Antenna Selection	17
2.5.3 Receive Antenna Selection	19
2.5.4 Joint Transmit and Receive Antenna Selection	20
2.6 Fading Channels	22
2.6.1 Multipath Fading	22
2.6.1.1 Slow Fading and Fast Fading	22
2.6.1.2 Flat Fading and Frequency Selective Fading	23

2.6.2 Statistical Models for Fading Channels	23
2.6.2.1 Rayleigh Fading	23
2.6.2.2 Nakagami-m Fading	24
2.7 Diversity Combining Techniques	25
2.7.1 Introduction	25
2.7.2 Selection Combining	26
2.7.3 Maximal-Ratio Combining	26
2.7.4 Equal Gain Combining	27
2.8 Coding Gain and Diversity Gain	27
2.9 Space-Time Block Codes	29
2.10.1 Alamouti Scheme	29
2.10.2 Extension to Multiple Transmit Antennas	33
2.10 Chapter Summary	37
Chapter 3: Performance of the RAS Scheme under Nakagami-m	
Fading Channels	38
3.1 Introduction	38
3.2 System and Channel Model	39
3.3 Error Performance Analysis of the RAS Scheme	44
3.4 Chapter Summary	47
Chapter 4: Performance of the TAS Scheme over Nakagami-m	
Fading Channels	48
4.1 Introduction	48
4.2 System and Channel Model	48
4.3 Error Performance Analysis of the TAS Scheme	50
4.4 Chapter Summary	55
Chapter 5: Performance of the T-RAS Scheme over Nakagami-m	
Fading Channels	56
5.1 Introduction	56
5.2 System and Channel Model	57
5.3 Error Performance Analysis of the T-RAS Scheme	60
5.4 Chapter Summary	63

Chapter 6: Simulation Result and Discussion	64
Chapter 7: Conclusion and future scope	74
7.1 Conclusion	74
7.2 Future Scope	76
Reference	77

List of Figures

2.1: Block diagram of a typical digital communication system	10
2.2: Constellations for MPSK modulation, $M=2, 4, 8$	12
2.3: Constellations for MQAM modulation, $M=8, 16$	14
2.4: A diagram of a MIMO system	15
2.5: A diagram of single transmit antenna selection	18
2.6: A diagram of multiple transmit antenna selection	19
2.7: A diagram of single receive antenna selection	20
2.8: A diagram of multiple receive antenna selection	20
2.9: A diagram of joint transmit and receive selection	21
2.10: A diagram of a transmission system with fading and noise	22
2.11: Selection Combining Model	26
2.12: Maximal-Ratio Combining Model	27
2.13: Illustration of diversity order and coding gain	28
2.14: A block diagram of the Alamouti scheme encoder	30
2.15: The Alamouti scheme with two transmit antennas and one receive antenna	31
2.16: The Alamouti scheme with two transmit antennas and two receive antenna	33
2.17: A system block diagram of the space-time block codes	35
3.1: A model of MIMO-STBC with receiver antenna selection	40
4.1: A model of MIMO-STBC with transmitter antenna selection	49
6.1: MIMO channel capacity with n_T and n_R antenna in Rayleigh channel ($m=1$)	64
6.2: Bit error probability of BPSK modulation	65
6.3: Improvement of SNR Vs BER using MIMO/STC code in Rayleigh channel ($m=1$)	66
6.4: Improvement of SNR in MIMO system with n_T and n_R antenna in Rayleigh Channel ($m=1$)	67
6.5: SNR Vs BER curve in MIMO/STBC system with RAS in Rayleigh channel ($m=1$)	68
6.6: Improvement of SNR in MIMO/STBC system with n_T selected antenna in Rayleigh channel ($m=1$)	69
6.7: SNR Vs BER curve in MIMO/STBC system with TAS in Rayleigh channel ($m=1$)	70
6.8: Improvement of SNR in MIMO/STBC system with n_R and n_T selected antenna in Rayleigh channel ($m=1$)	71

6.9: SNR Vs BER curve in MIMO/STBC system with T-RAS in Rayleigh Channel (m=1)	72
6.10: SNR Vs BER curve in MIMO/STBC system with all three possible AS in Rayleigh channel (m=1)	73

List of Tables

2.1 The notation of fading coefficient for the Alamouti scheme	32
2.2 The notation of received signals for the Alamouti scheme	32

List of Acronyms

AM	Amplitude Modulation
PM	Phase modulation
AWGN	Additive White Gaussian Noise
BER	Bit Error Rate
BPSK	Binary Phase-Shift Keying
CDF	cumulative distribution function
CSI	Channel State Information
EGC	Equal Gain Combining
i.i.d.	Independent identically distributed
MGF	Moment Generating Function
SISO	Single input single output
MIMO	Multiple-Input Multiple-Output
MPSK	M-ray Phase-Shift Keying
BPSK	Binary Phase-Shift Keying
MQAM	M-ray Quadrature Amplitude Modulation
MMSE	Minimum Mean Square Error
MRC	Maximal-Ratio Combining
pdf	probability density function
PSK	Phase-Shift Keying
QAM	Quadrature Amplitude Modulation
RF	Radio-Frequency
SC	Selection Combining
SEP	Symbol Error Probability
SER	Symbol Error Rate
SNR	Signal-to-Noise Ratio
STC	Space-Time Coding
STBC	Space-Time Block Code
STTC	Space-Time Trellis Code
TAS	Receive Antenna Selection
RAS/STBC	Receive Antenna Selection/Space-Time Block Code

TAS	Transmit Antenna Selection
TAS/STBC	Transmit Antenna Selection/Space-Time Block Code
JAS	Joint Antenna Selection
T-RAS	Receive-Transmit Antenna Selection
3G	Third Generations

Introduction

1.1 Background

Current wireless systems like cellular mobile phones, wireless local area network (WLAN), Bluetooth, mobile low earth orbit (LEO) satellite etc. all require very high data rate (>100 mbps), lower delay, greater transmission reliability and wider coverage. So we can say that latest wireless services demand higher data rates and better quality of service. But the limitations are fading, limited available spectrum and battery life of wireless portable devices. However, transmission reliability in wireless channels is a challenging issue as wireless links represent a harsh medium with high path loss, time-varying multipath fading and power and bandwidth limitations. Together with thermal noise, these factors severely degrade the quality of data transmission. Utilizing more than one antenna at a transmitter and receiver sides of the wireless communication is known as MIMO (multiple-input, multiple-output). This technique Promises significant enhancements of system performance without requiring the allocation of extra spectrum [1, 2]. By transmitting multiple copies of data, a MIMO system can effectively combat the effects of fading. The fundamental theoretical research of this new approach which utilizes multiple antennas to increase network capacity was pioneered by Winter [3], Telatar [1], Foschini [4] and Gans [2]. Their work predicted that enormous capacity gains can be obtained for MIMO systems in fading channels.

Utilizing more than one antenna at a transmitter and receiver sides (i.e. MIMO) in the wireless communication can be applied in various ways. A technique called **spatial multiplexing** seeks to enhance the spectrum efficiency by simultaneous transmission of independent data streams. One alternative method called **space-time coding** [5, 6] improves the link reliability by introducing spatial diversity (also referred to as antenna diversity). A single data stream is encoded and the resulting signals transmitted from the multiple antenna elements are highly correlated. This redundancy in time and space enables the receiver to optimally combine the signal components picked up by the respective receive antennas [7].

The spatial multiplexing directly improve the data-rate of the system, one can attain a similar benefit with the help of space-time coding. In a multipath fading situation the additional

diversity increases the average quality of the received signal. Within given transmit-power constraints this can for instance be exploited by applying higher modulation formats, thus indirectly enhancing the achievable spectrum efficiency [8].

Generally, space-time codes can be divided into two classes. The first is called **space-time trellis codes** (STTC) [6]. As the name implies their coding procedure involves trellis stages to derive the transmit symbol streams. The incoming bits select the current state transition, every possible transition is then mapped onto a vector of transmit symbols components are sent via the individual antennas [8]. This scheme offers diversity gain as well as additional coding gain but it also decreases the data rate since the total number of valid transmit signal vectors is lowered. Moreover, the decoding procedure requires a trellis search and its complexity grows exponentially with the number of used antennas and the length of the trellis.

The second category of space-time codes is based on **block** orientated processing [9, 10]. In the first trivial encoding step the bit sequence is mapped onto a symbol sequence. Subsequently, a block of successive symbols is linearly combined to a space-time coding matrix whose columns represent the symbol vectors transmitted via the individual antennas over time. Compared to their trellis-based counterparts these space-time block codes (STBC) are easier to decode but they do not exhibit any coding gain.

Although the use of multiple antennas at the transmitter and the receiver improves the overall system performance, but the main challenge of engineers are faced with when actually implementing MIMO devices is the cost is concomitantly increased with number of antenna and increased complexity. This complexity stems from the following two facts.

1. Increased processing effort

Both transmitter and receiver need to be equipped with powerful signal processors in order to handle the algorithmic intricacy Introduced by the use of multiple antennas.

2. Multiple radio-frequency (RF) front ends

The simultaneous utilization of multiple antennas also implies that the number of costly analog-circuitry elements integrated on both sides of the link is significantly higher compared to the multiple antenna case.

However, multiple expensive radio frequency (RF) chains are required to be implemented for multiple antennas in MIMO systems. In order to deal with this drawback, previous

researchers proposed antenna selection techniques which are capable of selecting a subset of the available antennas in a MIMO system to transmit or receive data. It has been used to alleviate the hardware costs of MIMO systems. The number of required RF chains is reduced to the number of selected antennas and thus the cost of the system decreases significantly while exploiting the advantages of the full-complexity MIMO system.

1.1.1 Need of Antenna Selection

One attractive way to reduce the number of RF chains is antenna selection [11, 12, 13, and 14]. Systems equipped with this capability optimally choose a subset of the available transmit and receive antennas and only process the signals associated with them. This allows maximally benefiting from the multiple antennas within given RF complexity and costing constraints.

This thesis is dedicated to the analysis of the performance of various antenna selection algorithms in a space-time block coding context. For a given set of codes the optimum selection criteria, minimizing the instant bit error ratio (BER) will be formulated. Using numerical Monte-Carlo simulations written in MATLAB1 the resulting system performances are evaluated and compared. These comparisons will also partly incorporate performance results for non-selective systems.

Antenna selection for multiple-input–multiple-output (MIMO) Systems a Promising low-complexity technology has received much attention in the Wireless community. -selection strategies may be classified into three categories as: transmit antenna selection, receive antenna selection and simultaneous selection on both transmit and receive antennas. The Hybrid selection/maximal-ratio combining (HS/MRC) system is introduced as an application of receive antenna selection. Unlike receive antenna selection, transmit antenna selection requires feedback from the receiver to the transmitter. The transmit antennas which maximize the total received signal-to-noise ratio (SNR) are selected. In this thesis there is more emphasis on transmit antenna selection.

1.2 Research Methodology

To mitigate against the destructive effects of fading channels and accommodate the demands of the latest wireless applications, it is important for wireless researchers to design new communication systems. In this thesis we present two MIMO schemes that achieve excellent error performance and high data rates.

The RAS, TAS and T-RAS in STBC scheme have been researched in several papers []. In [] the bit error rate (BER) expression for binary phase shift keying (BPSK) of the TAS scheme in flat Rayleigh fading channels was derived and the manner in which the feedback delays degraded the performance of the TAS scheme was numerically analyzed. In [], the close-form exact and asymptotic BER expressions for BPSK of the TAS scheme in flat Rayleigh fading channels were presented. The close-form outage probability of the TAS/MRC scheme was also derived]. An interesting **conclusion** is drawn that the diversity order was equal to the product of the number of the transmit antennas L_t and receive antennas L_r in flat Rayleigh fading channels at high SNRs [].

In [] Yang investigated the error performance of the TAS/MRC scheme in correlated Rayleigh fading channels and presented the BER expression for BPSK of the TAS scheme r in correlated Rayleigh fading channels. In [15] and [16] the exact BER expression for BPSK of the TAS/STBC scheme was derived. It was proven that the TAS/STBC scheme can provide a full diversity order in Rayleigh fading channels.

However, all of these are focused on flat Rayleigh fading channels. The emphasis of the work presented here is on error performance analysis of the RAS/STBC scheme and the TAS/STBC scheme over Nakagami- m fading channels [17]. The Nakagami- m distribution has been widely used as a useful and important model for physical radio fading channels [18]. A series of fading channels from severe to moderate can be modeled by using Nakagami- m distribution via parameter m in the range $m = 0.5$. Rayleigh distribution is a special case of Nakagami- m distribution with $m = 1$. The practical importance of Nakagami- m fading channels motivated researchers to investigate the performance of digital communication systems over Nakagami- m fading channels.

The error performance of the digital communication systems over generalized fading channels has been analyzed for at least forty years. In early years, most of the fading channels investigated were simple multipath fading such as Rayleigh fading channels. However, the models of digital communication systems and fading channels have become more complicated in recent years. By using the previous mathematical tools such as Gaussian and Marcum Q-functions, the close-form solution is difficult to be obtained or in such a very complex mathematical form that cannot provide much insight into the dependence of the error performance on the system parameters. In 1998, Simon and Alouini developed a unified

approach that can simplify the previously complicated results analytically and computationally and derived the new results for some special case in a simple form [19]. By using alternate representations of classic Gaussian and Marcum Q-functions, the expressions for the error rate of digital communication systems in fading channels are in a simple mathematical form which is usually no more complex than a single integral with finite limits and an integrand composed of elementary functions. This analytical approach is referred to as the moment generating function based (MGF-based) approach because the integrand contains the MGF of the instantaneous fading SNR. Since 1998, the MGF-base approach has been widely applied by researchers to investigate various digital communication systems including coherent, differentially.

In this thesis, we apply the MGF-based approach to analyze the performance of the TAS/MRC scheme over Nakagami- m fading channels with arbitrary and integer fading parameters m . First of all, the MGF of the TAS/STBC scheme over Nakagami- m fading channels with arbitrary and integer fading parameters m are obtained. Then the BER expression for BPSK and SER expressions for M-ray phase shift keying (MPSK) of the TAS/MRC scheme are presented.

These BER and SER expressions consist of infinite series and Gauss and Appell hypergeometric functions [20]. Using the method from [21], the asymptotic performance of the TAS/MRC scheme over Nakagami- m fading channels is evaluated. Our analytical results of asymptotic error rate expressions of the TAS/MRC scheme over Nakagami- m fading channels show that an asymptotic diversity order which is equal to the product of Nakagami- m fading parameter m , the number of transmit antennas L_t and the number of receive antennas L_r can be achieved.

Based on a Gaussian and Marcum Q-functions approach and a mathematical method to simplify multiple integrals by [22], we derive the BER expressions for BPSK of the TAS/STBC schemes with three and four transmit antennas over Nakagami- m fading channels and show that the TAS/STBC scheme can provide a full diversity order of mL_rL_t over Nakagami- m fading channels.

1.3 Thesis Objectives

The main objective of the thesis is to study the performance analysis of Antenna selection in multiple input multiple output (MIMO) space time block code (STBC) systems in Nakagami-m fading channel. To tackle the problem, we have subdivided our main objective into the following three different goals:

- (1) Performance analysis of receive antenna selection in MIMO/STBC systems in Nakagami-m fading channel.
- (2) Performance analysis of transmit antenna selection in MIMO/STBC systems in Nakagami-m fading channel.
- (3) Performance analysis of joint transmit and receive antenna selection in MIMO systems in Nakagami-m fading channel.

Thus the objective is to analyze such systems one by one, develop analytical expressions for different performance metrics and verify the derived relations through comprehensive simulation studies.

1.3 Thesis Outline

The rest of the thesis is organized as follows. The primary goal of chapter 2 is to introduce basic concepts, models and notations that will be used throughout the thesis. We begin in chapter 2 with a brief overview on the current and future requirements of wireless services and some methods to fulfill those criteria in section 2.1. The next section 2.2 briefly discusses on wireless channel, specifically large scale fading and small scale fading. Section 2.3 tells us about the digital modulation schemes mainly MPSK and MQAM, their constellation diagrams and a brief comparison, whereas section 2.4 is devoted to performance metrics, i.e. capacity, outage probability and symbol error rate (SER). Section 2.5 talks about different types of receiver diversity schemes. Under section 2.6 we discuss about MIMO systems. Section 2.7 tells us about the space-timecode (STC) used in MIMO systems. The next section, section 2.8 provides a brief literature survey i.e. works on diversity, MIMO and STC on last ten years. Lastly the chapter concludes with a chapter summary in section 2.9. The primary goal of chapter 3 is to analyze the system employing Alamouti coding, a type of diversity, at the transmitter side and multibank switch-and-examine combining (SEC) at the receiver side. In chapter 4 we derive the performance metrics of a system employing transmit antenna selection and Alamouti code. In chapter 5, we show how a system performs if we employ both transmit antenna selection and Alamouti code at the transmitter side and SEC as receiver diversity.

The thesis ends with chapter 6, which consists of a comparative study among the schemes that are presented in chapters 3, 4 and 5. Also some limitations we have discussed that should be kept in mind when we are adopting such schemes. We end the chapter with future scopes.

Background Materials

2.1 Introduction

Current wireless systems require higher transmission rate with lower delay, higher link reliability and wider coverage. The traditional resources that have been used to add capacity to wireless systems are radio bandwidth and transmitter power. Unfortunately, these two resources are among the most severely limited parameters during design: radio bandwidth because of the very tight situation with regard to useful radio spectrum, and transmitter power because mobile radio and other portable devices must be small, low-power, and lightweight, which restrict their capabilities. Also, wireless systems operate over a complex and harsh time-varying radio channel which introduces severe multipath fading and shadowing, rendering the link budget expensive for a typical symbol error rate (SER)/ bit error rate (BER) requirement.

Given these circumstances, there has been considerable research effort in recent years aimed at development of novel signal transmission techniques and advanced receiver signal processing methods that allow significant increase in wireless capacity without an increase in the transmitted bandwidth and power.

Diversity combining is such a sophisticated spectral and power efficient fade mitigation technique, which are used to improve radio link performance.

Diversity, where signal replicas are obtained through the use of either temporal, frequency, spatial, or polarization spacing, is an effective technique to mitigate the multipath fading. For example, an information bit can be transmitted simultaneously from two antennas (linked by some form of coding), and then the signals can be combined coherently at the receiver. If one of the spatial sub channels experiences a deep fade, it may be possible to recover the information from the signal on the other spatial sub channel. For each additional diversity branch, the chance of the combined signals being severely attenuated decreases.

2.2 Digital Communication Systems

Digital communication has become the predominant method of communication since then 70s of the last century. Morse invented the telegraph machine in 1838 which was an early form of modern digital communication. Messages can thus be transmitted over long distances. In 1948, Shannon developed information theory which formed the basic theory of digital communication [25]. Information theory had a strong impact on academic research

and practical system design for digital communication systems. It was a significant revolution in digital communication history. In his classic paper [25], a mathematical foundation for information transmission was established and the fundamental limits for digital communication systems was derived [26].

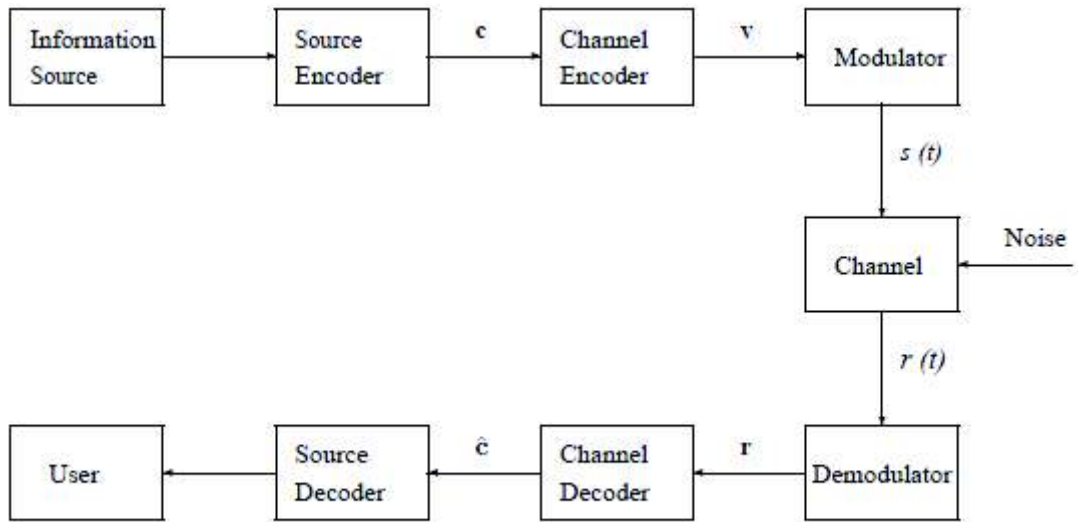


Figure 2.1: Block diagram of a typical digital communication system.

The block diagram of a typical digital communication system with basic elements is presented in Fig. 2.1 [26]. The input information source is what needs to be transmitted through digital communication systems and it includes such different types as voice, video, pictures and document files. The information source is usually modeled as a sample function of a random process in Shannon's theory. Shannon focuses on the set of possible input source instead of any particular input [25]. The source encoder removes the unnecessary details from the input source in order to enable the input message to be processed and carried through the channel more efficiently. If the source information is in analog format, the source encoder also converts an analog signal to a digital signal. The source decoder at the receiver performs the reverse operation to restore the original signal. The pair of source encoder and decoder should reduce unnecessary redundancy as much as possible without corrupting the original signal. The channel encoder adds controlled redundancy to the information sequence for error detection or correction. At the receiver, the channel decoder performs the inverse

operation to construct an estimation of the information sequence. The role of the modulator is to map the transmit information from bit or symbol stream to an appropriate electrical waveform. Then the modulated waveform is transmitted through the channels. The communication channel is the physical medium through which the transmit signals go and it always contains noise. Normally the communication channel is regarded in terms of its input, its output and some description on how the input affects the output.

2.4 Digital Modulation Schemes

2.4.1 Introduction

Digital modulation schemes are widely utilized in modern wireless communication. Compared with analog modulation, digital modulation has several advantages which include the possibility to apply advanced signal processing, such as error correction coding, higher data rate, better security and diversity. Based on the carrier attribute, digital modulation can be classified into phase modulation (PM), amplitude modulation (AM) and frequency modulation (FM). FM has better power efficiency and resistance to channel impairments while AM and PM have the advantage of better spectral efficiency [27]. In this thesis, we mainly focus on two types of AM and FM, MPSK and MQAM.

2.3.2 M-ray Phase Shift Keying

In contemporary communication systems, MPSK is one of the most popular modulation schemes. The signal amplitudes are constant and the signals can be amplified by a nonlinear device without significant distortion [28]. MPSK modulation uses M distinct phases to represent digital data. Each of these phases encodes $\log_2 M$ binary bits and represents the particular symbol. The constellations of some special cases of MPSK, when $M=2, 4$ and 8 are illustrated in Fig.2.2 [26]. In these Gray mappings, each adjacent symbol only differs by one bit. Every constellation symbol (X, Y) is given by $X = A \cos \left[\frac{2\pi(t-1)}{M} \right]$ and $Y = A \sin \left[\frac{2\pi(t-1)}{M} \right]$, $i = 1, 2, \dots, M$ where A is the amplitude. The transmit signal over one symbol time T_s is given by [27]

$$s_i(t) = \Re \{ A g(t) e^{j2\pi(t-1)/M} e^{j2\pi f_c t} \}, 0 \leq t \leq T_s$$

$$\begin{aligned}
&= Ag(t) \cos \left[2\pi f_c t + \frac{2\pi(i-1)}{M} \right] \\
&= Ag(t) \cos \left[\frac{2\pi(i-1)}{M} \right] \cos 2\pi f_c t - Ag(t) \sin \left[\frac{2\pi(i-1)}{M} \right] \sin 2\pi f_c t \quad (2.1)
\end{aligned}$$

where A is the amplitude, f_c is the frequency of the carrier and $g(t)$ is the pulse shape.

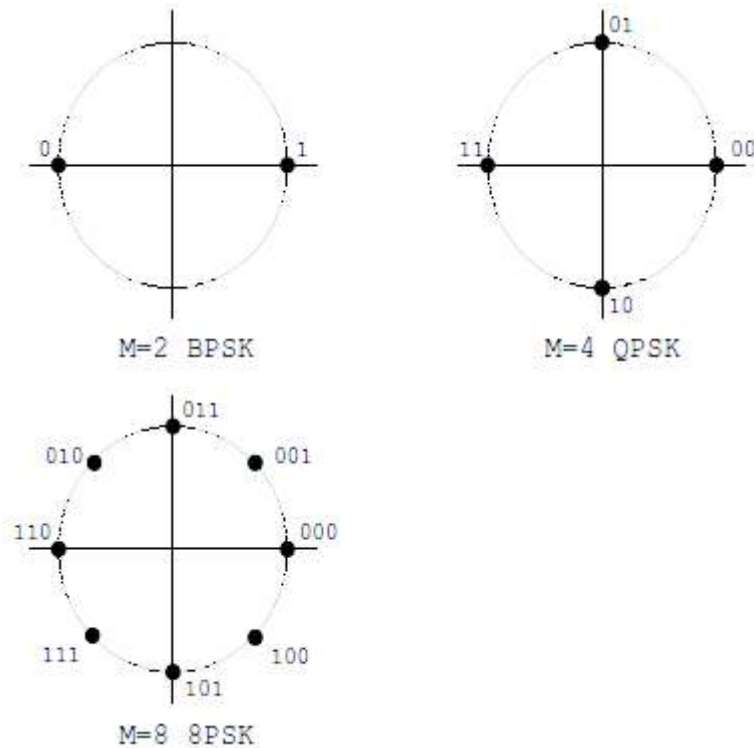


Figure 2.2: Constellations for MPSK modulation M=2, 4 & 8

2.2.3 M-ray Quadrature Amplitude Modulation

A MPSK modulation scheme maps all the symbols on M constellation points on a circle. This method lacks energy efficiency for large M. Thus MQAM is an alternative for that situation. QAM combines two AM signals into one channel in order to achieve double effective bandwidth. The information bits are encoded in the amplitude and phase of the transmit signal. A QAM signal has two carriers which have the same frequency but are out of phase with each other by 90°. Those two quadrature signals are referred to as I signals and Q signals which can be represented by a sine wave and a cosine wave respectively. Therefore

MQAM has two degrees of freedom in which to encode the information bits while MPSK has only one degree of freedom [27]. The transmitted signal is given by [27]

$$s_i(t) = \Re\{A_i e^{j\theta_i} g(t) e^{j2\pi f_c t}\}, 0 \leq t \leq T_s$$

$$= A_i \cos(\theta_i) g(t) \cos(2\pi f_c t) - A_i \sin(\theta_i) g(t) \sin(2\pi f_c t) \quad (2.2)$$

Where A_i is the amplitude, f_c is the frequency of the carrier and $g(t)$ is the pulse shape. Normally the constellation diagrams of MQAM are rectangular but other constellation diagrams such as circular MQAM still exist. Although the rectangular MQAM constellation does not maximally space the constellation points for a given energy, it is much easier to modulate and demodulate compared with a circular MQAM constellation. The non-rectangular constellations achieve marginally better BER but are harder to modulate and demodulate. Higher-order constellations transmit more bits per symbol but as the Constellation points become closer, so the BER are higher than the lower-order QAM constellations [26]. The constellation diagrams for rectangular MQAM and non-rectangular MQAM are shown in Fig.2.3 [26].

2.3 Multiple-Input Multiple-Output System Model

Let us consider a MIMO system employing L_t transmit antennas and L_r receive antennas. A system model diagram is presented in Fig.2.4. In each symbol period, the transmitted signals are represented as an $L_t \times 1$ column matrix \mathbf{X} , in which the i_{th} entry X_i , $i = 1, \dots, L_t$, is the transmitted signal from the i_{th} transmit antenna. Here we consider an additive Gaussian channel for which the optimum distribution of the transmitted signals in \mathbf{x} is still Gaussian. Therefore the i_i component X_i , $i = 1, \dots, L_t$, can be zero mean independent identically distributed (i.i.d) Gaussian random variables. The covariance matrix of \mathbf{X} is expressed as below [29]

$$\mathbf{R}_{xx} = E\{\mathbf{X}\mathbf{X}^H\} \quad (2.3)$$

where $E\{\cdot\}$ is the expectation and $(\mathbf{X})^H$ denotes the Hermitian of matrix \mathbf{X} . The total transmit power is constrained to P , regardless of transmit antennas L_t . It is given as [29]

$$P = \text{tr}(\mathbf{R}_{xx}) \quad (2.4)$$

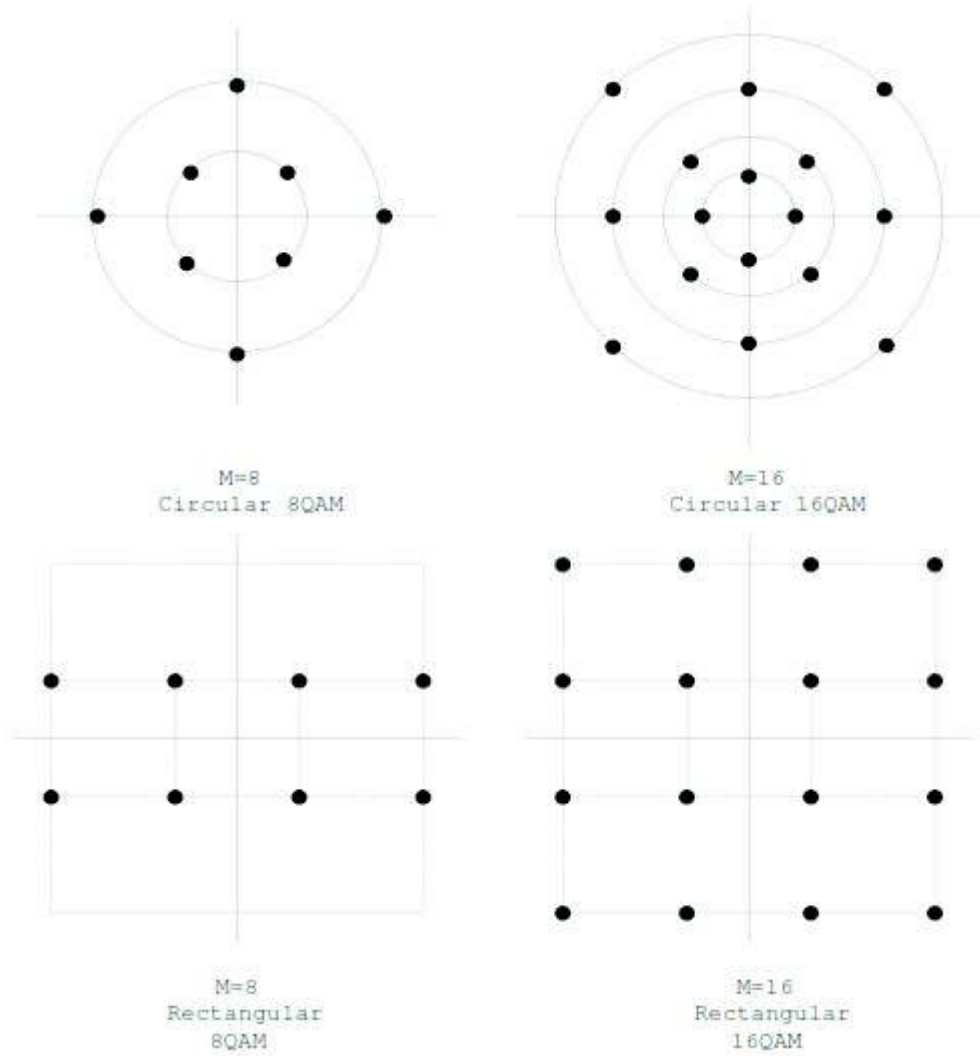


Figure 2.3: Constellations for MQAM modulation, $M=8, 16$.

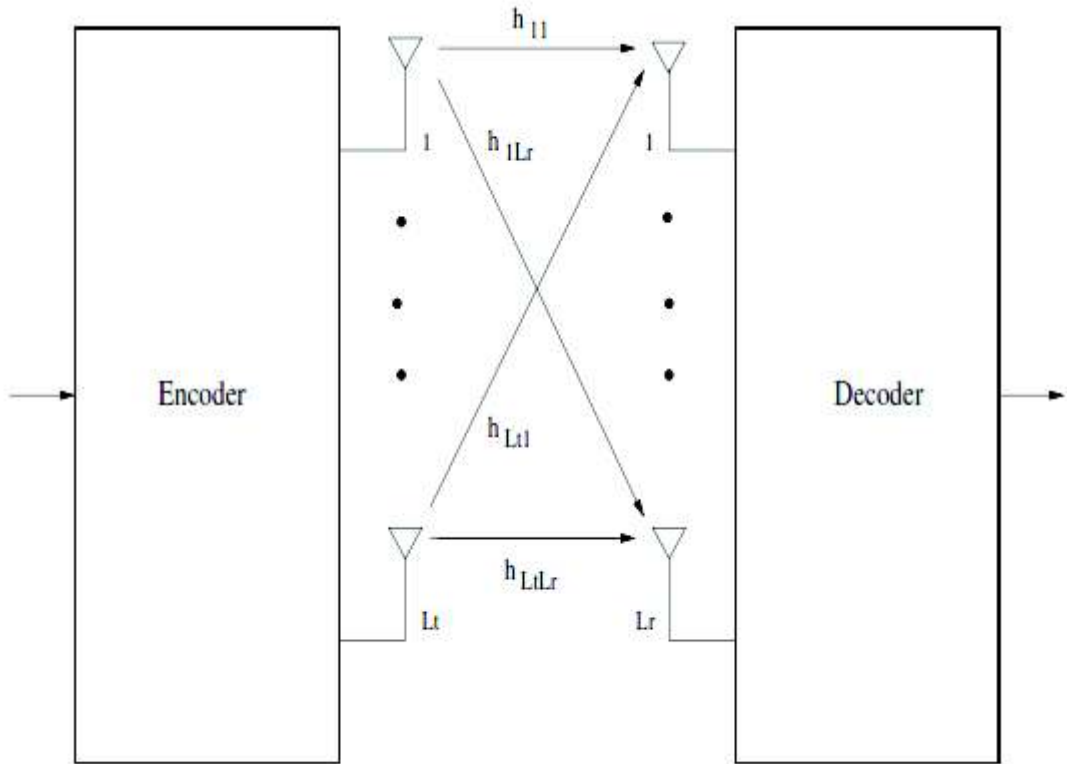


Figure 2.4: A diagram of a MIMO system

Where $\text{tr}(\cdot)$ is the trace operation of a matrix.

We assume that the channel coefficients are known at the transmitter and the signals transmitted from each transmit antenna is the same and equal to P/L_t . The covariance matrix of the transmitted signal can be expressed as [29]

$$\mathbf{R}_{xx} = \frac{P}{L_t} \mathbf{I}_{L_t} \quad (2.5)$$

Where the \mathbf{I}_{L_t} is the $L_t \times L_t$ identity matrix.

The channel is represented by an $L_r \times L_t$ complex matrix \mathbf{H} , whose entries $h_{i,j}$, $1 \leq i \leq L_r$, $1 \leq j \leq L_t$, are the channel coefficients between the i th receive antenna and the j th transmit antenna. Let us assume that the received power at each of L_r receive antennas is equal to the transmitted power from L_t transmit antennas. For a channel with fixed channel coefficient, we have the normalization constraint for elements of \mathbf{H} as [29]

$$\sum_{j=1}^{L_r} |h_{i,j}|^2 = L_t \quad (2.6)$$

for $i = 1, \dots, L_r$. For a channel with random **variables**, this normalization will apply to the expected value of the expression in (2.6).

The channels matrix is assumed to be known at the receiver but not always at the transmitter. By using a feedback channel, the channel information can be communicated to the transmitter to estimate the channel matrix. The entries of the channel matrix H can be deterministic or random. We consider the fading channels in which the channel matrix elements have Rayleigh distribution since it is an excellent model for non-line-of-sight radio propagation.

Let us denote the noise at the receive antennas as \mathbf{n} which is a $L_r \times 1$ column. The entries of matrix \mathbf{n} are statistically independent and equal variance real and imaginary parts. The covariance matrix of the receiver noise is presented as [29]

$$\mathbf{R}_{nn} = E\{\mathbf{nn}^H\} \quad (2.7)$$

If no correlation exists between components n , the covariance matrix can be derived as [29]

$$\mathbf{R}_{nn} = \sigma^2 \mathbf{I}_{L_r} \quad (2.8)$$

Where σ^2 is the identical noise power of each L_r receive branches. The receiver is based on a maximum likelihood principle operating at L_r receive antennas. We denote received signals as \mathbf{r} which is a $L_r \times 1$ column matrix. The average signal-to-noise ratio (SNR) at each receive antenna is obtained as [29]

$$\gamma = \frac{P_r}{\sigma^2} \quad (2.9)$$

Where P_r is the average power at the output of each receive antenna.

The total received power of each receive antenna is assumed to be equal to the total transmitted power. The SNR at each receive antenna is equal to the ratio of the total transmitted power and the noise power per receive antenna. (2.9) can be rewritten as [14]

$$\gamma = \frac{P}{\sigma^2} \quad (2.10)$$

the receive vector \mathbf{r} can be shown as [29]

$$\mathbf{r} = \mathbf{H}\mathbf{x} + \mathbf{n} \quad (2.11)$$

The received signal covariance matrix which is defined as $E\{\mathbf{r}\mathbf{r}^H\}$ is given as [29]

$$\mathbf{R}_{\mathbf{r}\mathbf{r}} = \mathbf{H}\mathbf{R}_{\mathbf{x}\mathbf{x}} + \mathbf{H}^H \quad (2.12)$$

The total received signal power can be given as $t_r(R_{\mathbf{r}\mathbf{r}})$.

2.5 Antenna Selection Techniques

2.5.1 Introduction

MIMO systems, which employ multiple transmit and receive antennas, can improve the capacity and transmission reliability even in challenging propagation environments. A diversity order that is equal to the product of the number of transmit antennas L_t and the number of receive antennas L_r can be achieved [30]. However, one of the drawbacks of the MIMO systems is that they require an equivalent number of RF chains for multiple antennas. The RF chain, which consists of a low noise amplifier, frequency up and down converters, analog-to-digital and digital-to-analog converters, and filters, is usually very expensive, thus increasing the hardware costs of MIMO systems. Antenna selection techniques are the most efficient approach to reducing the hardware complexity and costs of MIMO systems. In antenna selection techniques, a subset of transmit and/or receive antennas is selected for signal transmission based on selection criteria including maximizing the received SNR and maximizing the channel capacity. After antenna selection, the required number of RF chains is reduced from the number of total antennas to the number of the selected antennas. Antenna selection techniques can be classified as transmit antenna selection, receive antenna selection and antenna selection of both transmit and receive antennas.

2.5.2 Transmit Antenna Selection

Let us assume a MIMO system with transmit antenna selection which has L_t transmit antennas and one receive antenna. A diagram of signal transmit antenna selection is

presented in Fig.2.5. Transmit antenna selection requires feedback from the receiver to

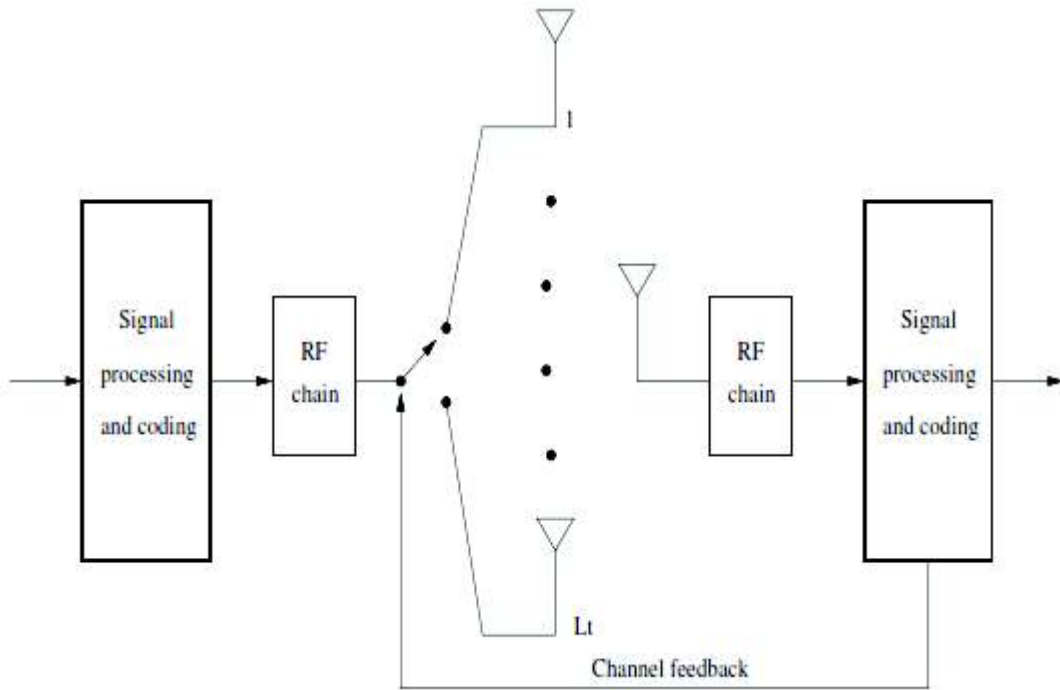


Figure 2.5: A diagram of single transmit antenna selection

transmitter. The channel feedback includes channel state information, channel correlation, and selection-decision. Besides the single transmit antenna selection, we may also have multiple transmit antenna selection. In multiple transmit antenna selection, let us assume that the number of RF chains N ($N > 1$) is smaller than the number of transmits antennas L_t and only one receive antenna exists.

A diagram of multiple transmit antenna selection is shown in Fig.2.6. In multiple transmit antenna selection, the N transmit antennas, which maximize the total received SNR, are selected from the L_t transmit antennas for data transmission. The transmitter needs to know the N most suitable transmit antennas and the complex-value channel coefficients from every transmit antenna to the receive antennas. More feedback is needed for multiple antenna selection than single antenna selection [31].

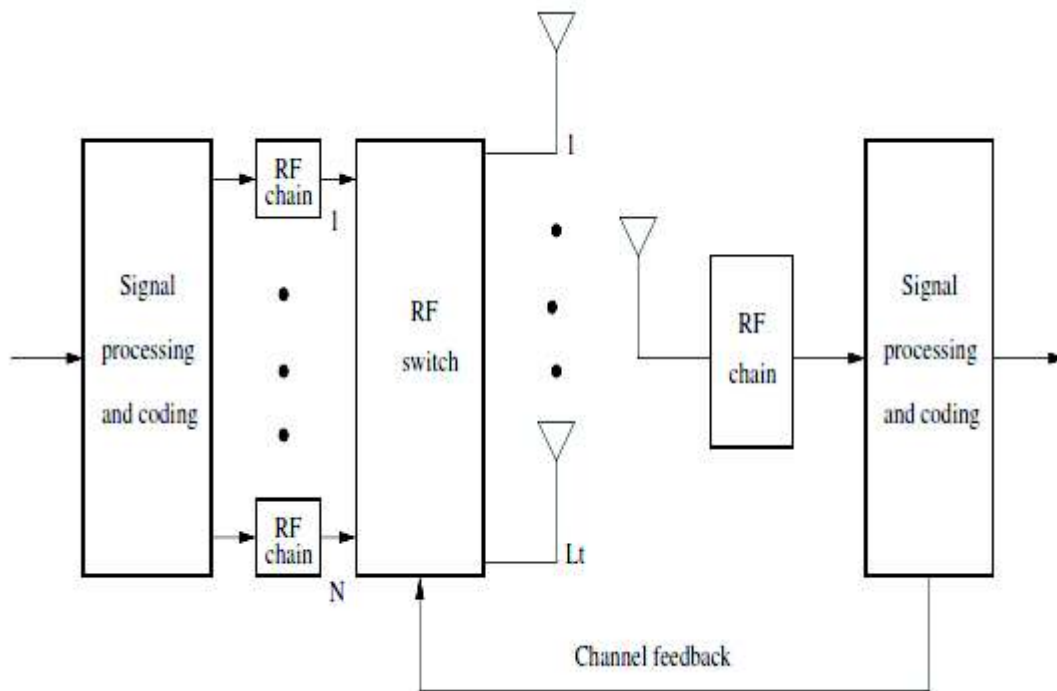


Figure 2.6: A diagram of multiple transmit antenna selection

2.5.3 Receive Antenna Selection

Fig.2.7 shows a signal receive antenna selection in which only one receive antenna is selected among L_r antennas to receive signals. In signal receive antenna selection, the receiver needs to know all the SNR at each receive antenna. A training signal is used in a preamble to the transmitted data. Then the receiver scans all the antennas to find the antenna with the highest channel gain, and chooses it for receiving the next data burst [31].

If N ($N > 1$) RF chains are available, a subset of N receive antennas that have the largest SNR will be selected to receive signals. This is known as generalized selection diversity or hybrid selection/maximal-ratio combining. A diagram of generalized selection diversity is illustrated in Fig.2.8. MRC and EGC can be used to combine the selected branches. Compared with EGC, MRC has better performance but larger complexity.

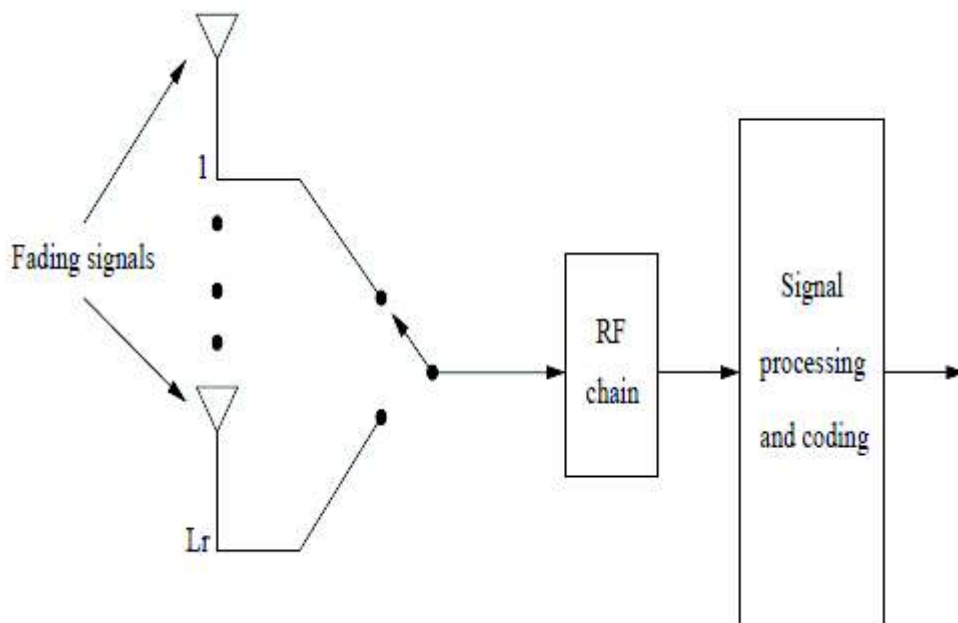


Figure 2.7: A diagram of single receive antenna selection

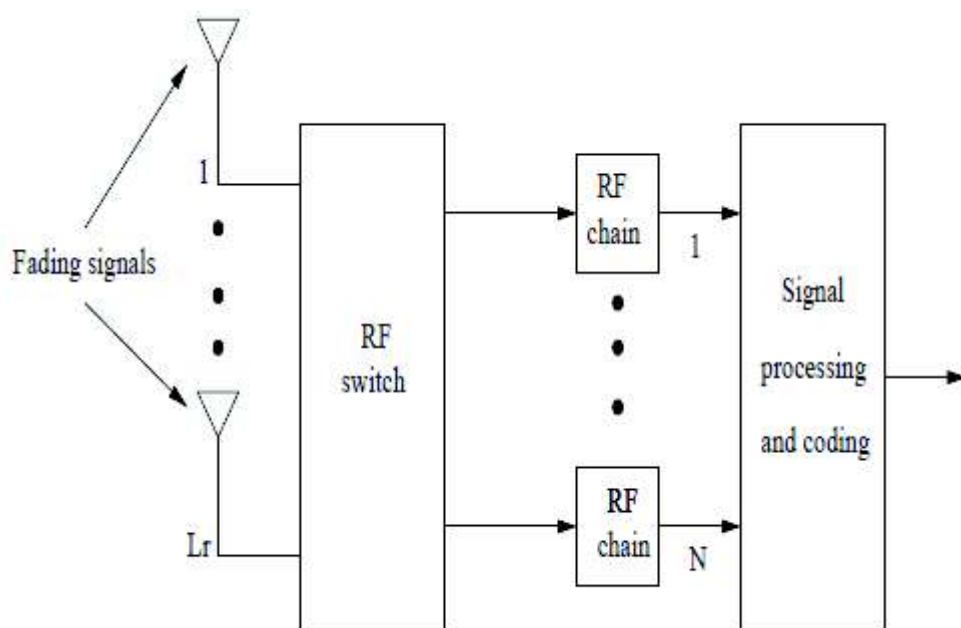


Figure 2.8: A diagram of multiple receive antenna selection

2.5.4 Joint Transmit and Receive Antenna Selection

Selection diversity can be applied to both the transmitter and receiver simultaneously. In this scenario, N_{L_t} transmit antennas from all L_t transmit antennas and N_{L_r} receive antennas from all L_r receive antennas are selected to transmit and receive signals. Let us denote the $L_t \times L_r$ channel matrix by \mathbf{H} and $N_{L_t} \times N_{L_r}$ by \tilde{H} . Space-time codes must be used to provide diversity. A joint transmit and receive selection scheme chooses a subset of \mathbf{H} to maximize the sum of the squared magnitudes of transmit-receive gains [31]. A diagram of joint transmit and receive selection is presented in Fig.2.9. However, successively choosing the best receive antennas and then the best transmit antennas does not necessarily result in an overall optimal selection. Currently no systematic solution to a joint transmits and re Figure 2.9: A diagram of joint transmits and receives selection scheme is known [31].

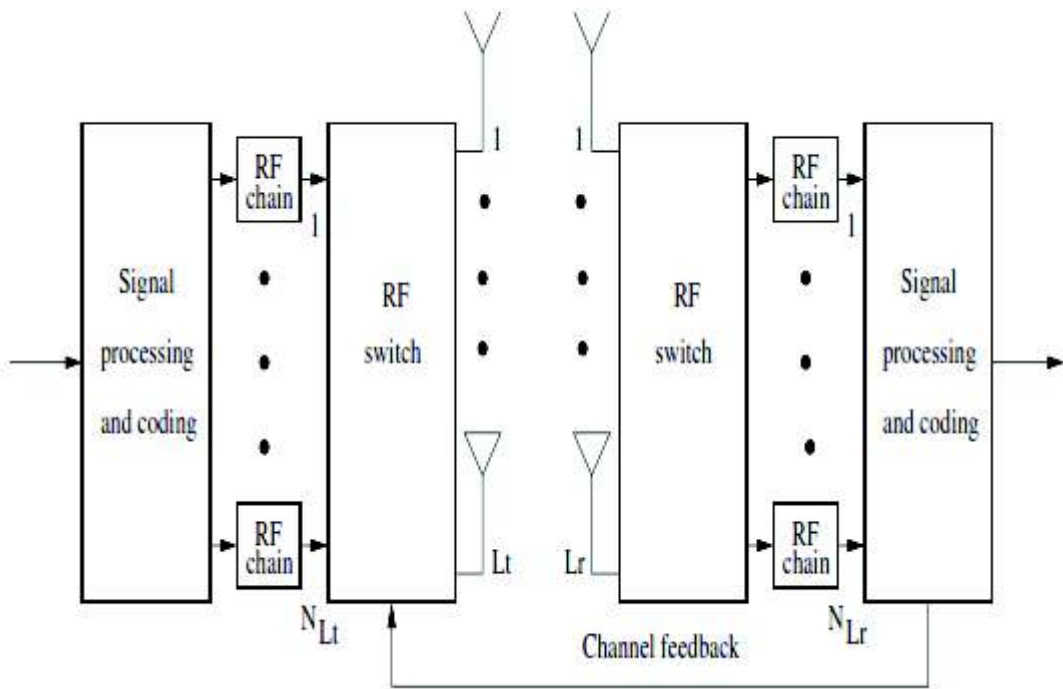


Figure 2.9: A diagram of joint transmit and receive selection

2.6 Fading Channels

2.6.1 Multipath Fading

In practical mobile communication, the base station antenna is sometimes below that of the surrounding buildings. So there is no line-of-sight (LOS) path between the base station antenna and the mobile handset. The handset will receive the reflected, diffracted and scattered signals from all directions. Those signals experience not only noise but also rapid amplitude and phase fluctuation over a period of time when multipath propagating. The signals arriving at the receiver have different amplitudes and phases because of the different attenuations, delays and phase shifts they experience. This effect is called multipath fading. A simple diagram of a transmission system over a fading channel is presented in Fig.2.10. The output signal at a receiver can be expressed as:

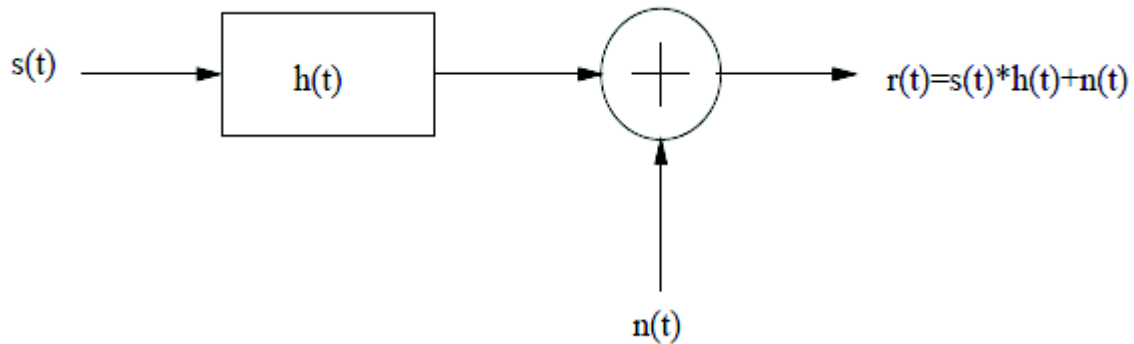


Figure 2.10: A diagram of a transmission system with fading and noise.

$$r(t) = s(t) * h(t) + n(t) \quad (2.13)$$

Where $s(t)$ is the input signal, $(*)$ is the convolution process, $h(t)$ is the channel fading coefficient and $n(t)$ is the additive random noise process.

2.6.1.1 Slow Fading and Fast Fading

In mobile communication there are two kinds of fading which are very important: slow fading and fast fading [32]. Slow fading is caused by prominent obstruction (buildings, mountains and so on) and large movements of a mobile during propagation. The slow fading channel coefficients change at a rate that is much slower than the rate of the transmitted

signal. Therefore the slow fading channels can be assumed to remain static over one or more transmitted signal symbol durations. Fast fading appears when small changes, as small as half wavelength, happen in the amplitudes and phases of the signals. Fast fading represents the rapid fluctuations of the signals' amplitudes and phases in a short time or distance. The fading coefficients of a fast fading channel change rapidly in one transmit time period. The channel coherence time T_c is used to distinguish slow fading and fast fading.

$$T_c \approx \frac{1}{f_d} \quad (2.14)$$

Where f_d is the channel Doppler spread. The fast fading has a high Doppler spread and if the channel coherence time T_c is smaller than the symbol time duration T_s , the fading is fast fading otherwise it is slow fading.

2.6.1.2 Flat Fading and Frequency Selective Fading

Based on multipath time delay spread there are two important fading: flat fading and frequency selective fading. In flat fading, the bandwidth of a transmitted signal is smaller than the coherence bandwidth of channels f_c . The coherence bandwidth is given by [32]

$$f_c \approx \frac{1}{\tau_{\max}} \quad (2.15)$$

where max is the maximum delay spread. The coherence bandwidth illustrates the amount of bandwidth that will fade in a correlated fashion at any instant in time [26]. In contrast, frequency selective fading affects the transmitted signal by different amplitude gains and phase shifts and the transmit bandwidth is greater than the channel's coherent bandwidth [32]. Certain frequency components are produced in the received signal spectrum with greater gains than others.

2.6.2 Statistical Models for Fading Channels

2.6.2.1 Rayleigh Fading

To design and investigate the performance of digital communication systems, statistical models for multipath fading channels are developed by extensive measurements of received signals envelopes in rural, urban and suburban environments [33]. Rayleigh fading is a statistical model for the fading caused by multipath which is approximated by Rayleigh distribution in radio propagation [34–39]. Rayleigh fading is small scale fading and is the most applicable to model heavily built-up city centers such as Manhattan where there is no light of sight (LOS) path between transmitter and receiver [41]. Signal propagation in tropospheric, ionospheric and ship-to-ship radio links may also approximate Rayleigh fading [26]. The square root of a sum of squares of two zero-mean identically distributed Gaussian random variables has a Rayleigh distribution [26]. It can be assumed that the real and imaginary parts of the response are modeled by independent and identically distributed zero-mean Gaussian processes so that the amplitude of the response is the sum of two such processes. If r is defined as a Rayleigh distribution random variable, the pdf is given by [26] as

$$P_R(R) = \frac{r}{\sigma^2} \cdot e^{-r^2/2\sigma^2} \quad (2.16)$$

where σ^2 is the variance of two zero-mean identically distributed Gaussian random variables.

2.6.2.2 Nakagami-m Fading

Nakagami-m distribution is a widely used statistical model for fading envelopes of signals due to its great versatility. With a parameter m ranging from 0.5 to infinite, it can model different fading scenarios from severe to moderate. Rayleigh distribution is a special case when $m = 1$. There is no fading when $m = \infty$. Nakagami-m distribution fits certain urban path strength data better than Rayleigh, Rice or lognormal distributions [33] [42]. Therefore performance analysis of a communication scheme over Nakagami-m fading channels has been investigated recently [43–48]. The pdf of the Nakagami-m distribution is given by [32]

$$P_R(R) = \frac{2m^m r^{2m-1}}{\Gamma(m)\Omega^m} e^{-(m/\Omega)r^2} \quad (2.17)$$

Where

$$\Omega = E[R^2] \quad (2.18)$$

and parameter m is defined as

$$m = \frac{\Omega^2}{E[(R^2 - \Omega)^2]} \geq \frac{1}{2} \quad (2.19)$$

When m is an integer or half-integer, the Nakagami-m distribution can be expressed as a square root of the sum of 2m independent identically distributed (i.i.d) Gaussian random variables with zero mean and variance σ^2 . It is given by [49] as

$$R = \sqrt{X_1^2 + X_2^2 + \dots + X_{2m}^2} \quad (2.20)$$

Where X_i , $i = 1, 2, \dots, 2m$ are i.i.d Gaussian random variables.

2.8 Diversity Combining Techniques

2.8.1 Introduction

Diversity techniques are important methods to improve the transmission reliability of digital communication systems by combating the effect of fading. By applying diversity combining techniques, a large number of copies of transmitted signals can be sent over fading channels from a transmitter. Then a receiver combines these multiple copies to maximize the power of received signals. The success of diversity schemes depends on the degree to which the signals are uncorrelated. If these multiple signal copies have low or no correlation of fading coefficients, the effect of fading is significantly reduced.

Diversity techniques can be classified into time diversity, frequency diversity, space diversity and receive diversity. Time diversity uses a method of transmitting signal copies at different time slots. So the receiver can receive uncorrelated signal repetitions that will provide performance improvement due to diversity. However, time diversity loses bandwidth

efficiency so that it needs a larger symbol constellation or larger bandwidth to maintain a set throughput. Time diversity is usually effective for fast fading channel since the coherence time of this channel is small. For slow fading, time interleaving causes problems in decoding delay which is a significant problem for delay sensitive applications such as voice transmission.

In frequency diversity, a number of different frequencies are used to transmit the same signal. The frequencies need to be separated enough to ensure independent fading coefficients associated with a guarantee that the fading coefficients for different frequencies will be uncorrelated. The drawback of frequency diversity is a loss in bandwidth efficiency due to a redundancy introduced in the frequency domain.

Space diversity, which arranges multiple antennas at a proper distance to obtain independent replicas of the transmitted signals, is a very popular technique in wireless communications because space diversity does not induce any loss in bandwidth efficiency.

This thesis is mostly concerned with receive diversity combining. Three main diversity combining techniques: SC, MRC and EGC [50] are discussed below.

2.8.2 Selection Combining

In selection combining, the diversity branch with the highest SNR is selected. Therefore the output SNR of the SC combiner is equal to the SNR of the selected diversity branch. SC does not need knowledge of the signal phase of each diversity branch so it can be used with coherent or noncoherent modulation schemes. SC is extended to a generalized SC in which N branches from all L branches are selected. A SC model is shown in Fig.2.11.

In i.i.d Rayleigh fading channels, the average SNR of the output combiner is given by [51] as

$$\bar{\gamma}_{out} = \bar{\gamma} \sum_{k=1}^M \frac{1}{k} \quad (2.21)$$

Where $\bar{\gamma}$ is the average SNR of each diversity branch and M is the number of diversity branches. The output SNR does not increase with M linearly.

2.8.3 Maximal-Ratio Combining

Compared with SC, MRC [52-53] is an optimal diversity scheme with greater complexity. It gives the best fading reduction performance of all linear diversity combiners. In MRC, all the signals from diversity

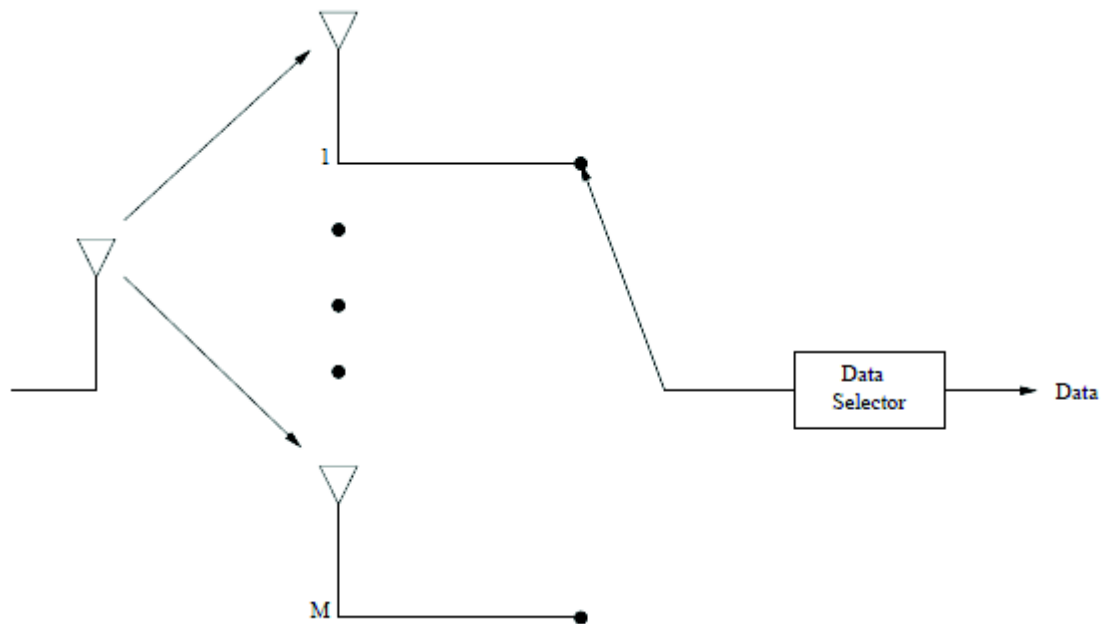


Figure 2.11: Selection Combining Model

branches are weighted proportionately to the signal strength and then added together so that the output SNR can be maximized. The SNR of the output combiner is the sum of SNRs of all the diversity branches. Thus the SNR of the output combiner is given by [51] as

$$\bar{\gamma}_{out} = \sum_{k=1}^M \gamma_k \quad (2.22)$$

where γ_k is the SNRs of each diversity branches. A MRC model is depicted in Fig.2.12.

2.8.4 Equal Gain Combining

EGC [53, 54] achieves a good performance following MRC in these three main diversity techniques. MRC yields the best performance but it is the most complicated since it needs the

knowledge of the channel fading amplitudes. EGC reduces system complexity because it does not need to estimate the

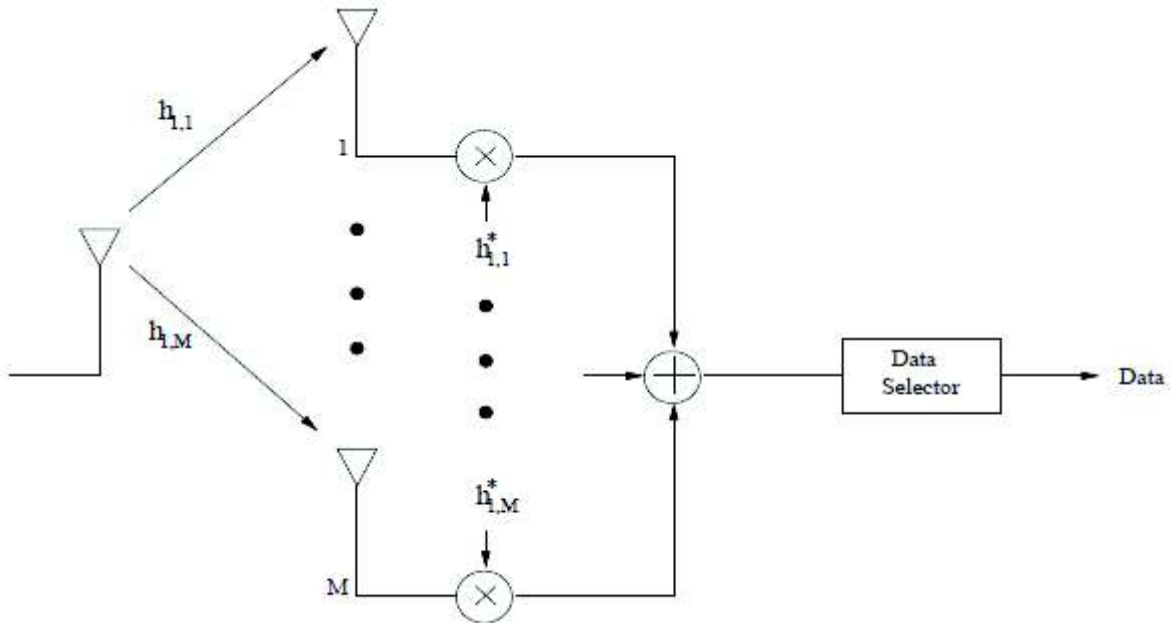


Figure 2.12: Maximal-Ratio Combining Model

fading channel amplitudes and EGC provides almost as good performance as MRC. In some situations, EGC is an excellent alternative for MRC. If M and k are defined as the number of diversity branches and the average SNR of each diversity branch respectively, the average output SNR in i.i.d Rayleigh fading channels is given by [51] as

$$\bar{\gamma}_{out} = \bar{\gamma} \left[1 + \frac{\pi}{4} (M-1) \right] \quad (2.23)$$

2.9 Coding Gain and Diversity Gain

Performance analysis of coded or uncoded transmissions over fading channels is usually carried out in two steps. First, for a fixed channel realization, the instantaneous error rate expression is expressed as a Q function, defined by [26] as

$$Q(x) = \frac{1}{\sqrt{2\pi}} \int_x^{\infty} e^{-t^2/2} dt \quad (2.24)$$

This is a function of the instantaneous channel SNR. In the second step, this instantaneous error rate expression is integrated over the pdf of the instantaneous channel SNR to obtain the average performance.

At high SNRs, the average error rate of a transmission system can be approximated by

$$P_E \approx (G_c \cdot \bar{\gamma})^{-G_d} \quad (2.25)$$

where G_c is the coding gain, G_d is referred to as the diversity gain or diversity order and $\bar{\gamma}$ is the average SNR. When in log-log scale, the coding gain G_c determines the horizontal location of the error performance curve and the diversity gain G_d determines the slope of the error rate versus the average SNR curve.

Let us assume the three error performance expressions below

$$\begin{aligned} P_{E_1} &\approx (G_{c_1} \cdot \bar{\gamma})^{-G_{d_1}} \\ P_{E_2} &\approx (G_{c_2} \cdot \bar{\gamma})^{-G_{d_2}} \\ P_{E_3} &\approx (G_{c_3} \cdot \bar{\gamma})^{-G_{d_3}} \end{aligned} \quad (2.26)$$

in which $G_{c_2} > G_{c_1}, G_{d_3} > G_{d_1}$. These three curves are presented in Fig. 2.13. P_{E_1} and P_{E_2} are parallel to each other at high SNRs and separated by $10 \log \frac{G_{c_2}}{G_{c_1}}$ dB, which is referred to as the coding gain of P_{E_2} over P_{E_1} . P_{E_3} has a higher diversity order and a corresponding sharper slope graphically.

For an uncoded MIMO system, the diversity order is equal to the number of independent fading paths that a symbol passes through, or, the number of independent fading coefficients that can be averaged to detect a symbol [54]. It has been shown in [55] that for an (L_t, L_r) MIMO system with space-time coding in quasi-static flat Rayleigh fading channels, the

maximum achievable diversity order is $L_t L_r$. In this case, we say that a full diversity order is achieved.

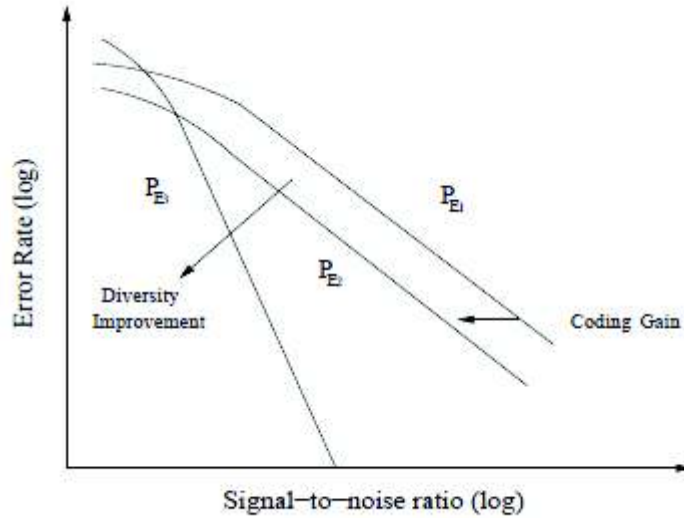


Figure 2.13: Illustration of diversity order and coding gain.

2.10 Space-Time Block Codes

2.10.1 Alamouti Scheme

A new simple scheme which uses two transmit antennas and a maximum-likelihood decoding (MLD) to achieve full diversity order was proposed by Alamouti [56]. This scheme does not require any bandwidth expansion or any feedback from the receiver to the transmitter [56]. It also ensures a full transmit diversity and has a simple MLD based on linear processing. A new research area of space-time block coding is therefore opened up. The block diagram of Alamouti space-time encoder is shown in [29]. Fig 2.15 presents the Alamouti scheme with two transmit antennas and one receive antenna. In the Alamouti scheme with two transmit antennas and one receive antenna, each of two transmit antennas transmits two signals in two consecutive symbol periods. In the first transmission period, transmit antenna 0 and transmit 1 transmit signals s_0 and s_1 respectively. Then in the next

period, signals $-s_1^*$ and s_0^* are transmitted from transmit antenna 0 and transmit antenna 1 respectively, where $*$ is complex conjugate operation.

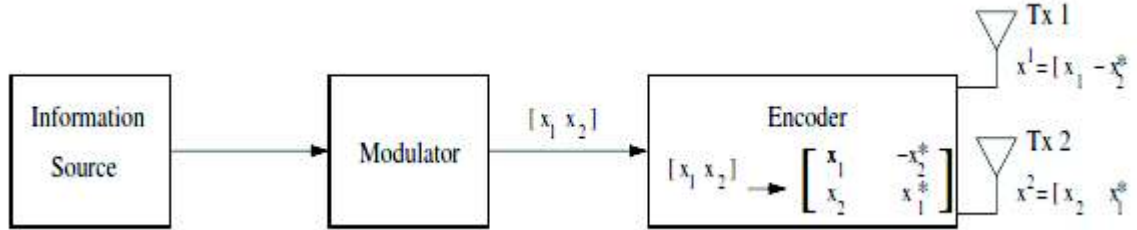


Figure 2.14: A block diagram of the Alamouti scheme encoder

Let us denote $h_0(t)$ and $h_1(t)$ as the fading coefficients from transmit antenna 0 and transmit antenna 1 to receive antenna 0 at time t respectively. It is assumed that the fading coefficients remain constant in two consecutive transmission periods. Thus the fading coefficients are written by [56] as

$$\begin{aligned}
 h_0(t) &= h_0(t+T) = h_0 = \alpha e^{j\theta_0} \\
 h_1(t) &= h_1(t+T) = h_1 = \alpha e^{j\theta_1}
 \end{aligned}
 \tag{2.27}$$

where T is the symbol duration.

Therefore the received signals at the time t and $t + T$ which are denoted as r_0 and r_1 are presented by [56] as

$$\begin{aligned}
 r_0 &= r(t) = h_0 s_0 + h_1 s_1 + n_0 \\
 r_1 &= r(t+T) = -h_0 s_1^* + h_1 s_0^* + n_1
 \end{aligned}
 \tag{2.28}$$

Where n_0 and n_1 are channel interference and noise.

Two combined signals, \tilde{s}_0 and \tilde{s}_1 are sent to the maximum likelihood detector [56],

$$\begin{aligned}\tilde{s}_0 &= h_0^* r_0 + h_1 r_1^* = (\alpha_0^2 + \alpha_1^2) s_0 + h_0^* n_0 + h_1 n_1^* \\ \tilde{s}_1 &= h_1^* r_0 - h_0 r_1^* = (\alpha_0^2 + \alpha_1^2) s_1 - h_0 n_1^* + h_1^* n_0\end{aligned}\tag{2.29}$$

For PSK constellation, the maximum likelihood detector will choose signals s_0 and s_1

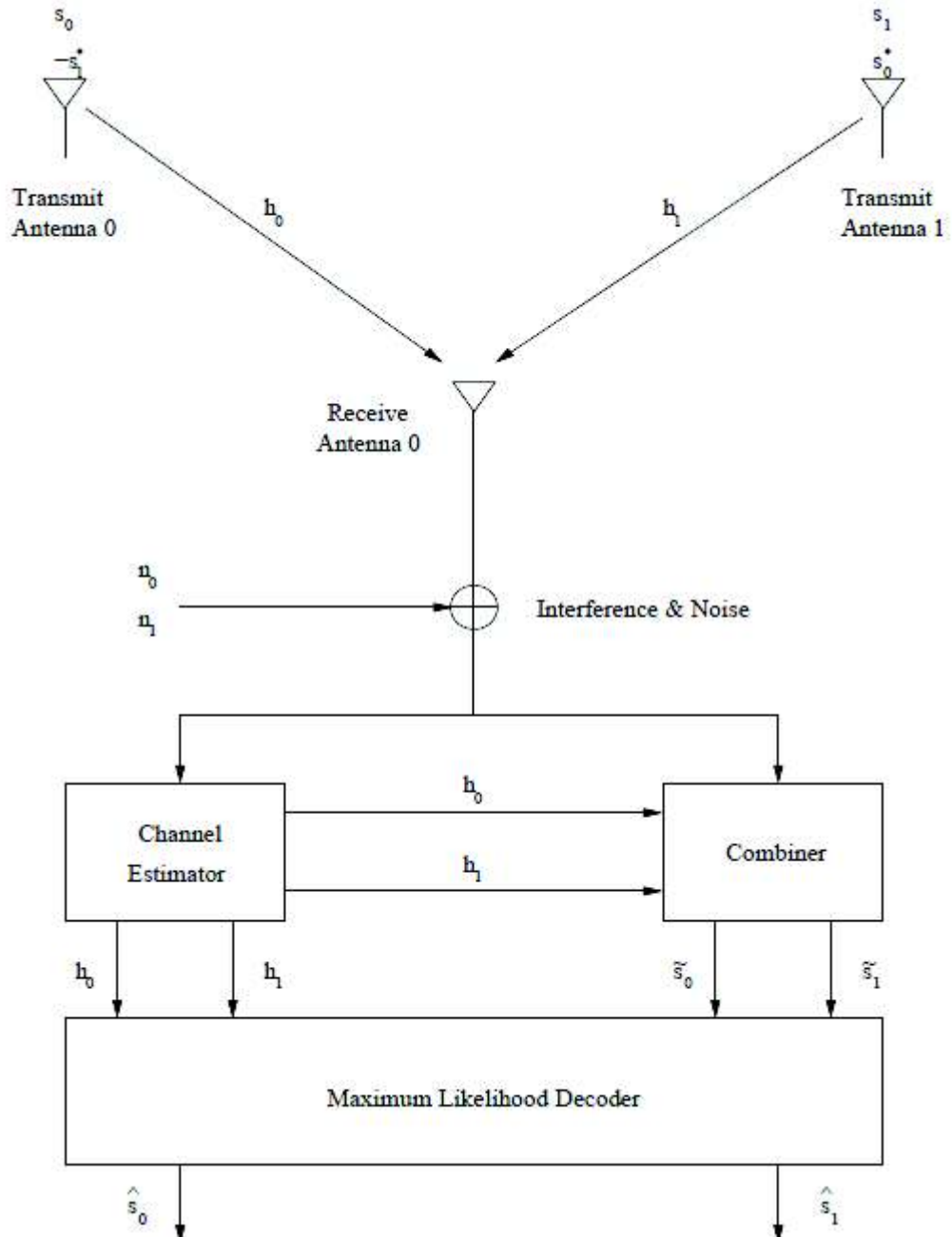


Figure 2.15: The Alamouti scheme with two transmit antennas and one receive antenna

using the decision rule below [56]

$$\begin{aligned}\hat{s}_0 &= \arg \max_{\hat{s}_0 \in \mathcal{S}} [d^2(\tilde{s}_0, \hat{s}_0)] \\ \hat{s}_1 &= \arg \max_{\hat{s}_1 \in \mathcal{S}} [d^2(\tilde{s}_1, \hat{s}_1)]\end{aligned}\tag{2.30}$$

The Alamouti scheme can achieve a full diversity order of $2L_r$ when the number of receive antennas is extended from 1 to L_r . In [56] the author investigated a special case with two receive antennas. The Alamouti scheme with two transmit and two receive antenna is shown in Fig.2.16. The encoding and transmission for this scheme are identical to the scheme with one receive antenna. If we denote h_i and r_i , $i = 0, 1, 2, 3$,

Table 2.1: The notation of fading coefficient for the Alamouti scheme.

	receive antenna 0	receive antenna 1
transmit antenna 0	h_0	h_2
transmit antenna 1	h_1	h_3

Table 2.2: The notation of received signals for the Alamouti scheme.

	receive antenna 0	receive antenna 1
time t	r_0	r_0
time t + T	r_0	r_0

the received signals are expressed by [56] as

$$\begin{aligned}r_0 &= h_0 s_0 + h_1 s_1 + n_0 \\ r_1 &= -h_0^* s_1 + h_1^* s_0 + n_1 \\ r_2 &= h_2 s_0 + h_3 s_1 + n_2 \\ r_3 &= -h_2^* s_1 + h_3^* s_0 + n_3\end{aligned}\tag{2.31}$$

Where n_i , $i = 0, 1, 2, 3$ are channel interference and noise. Two signals which are sent to

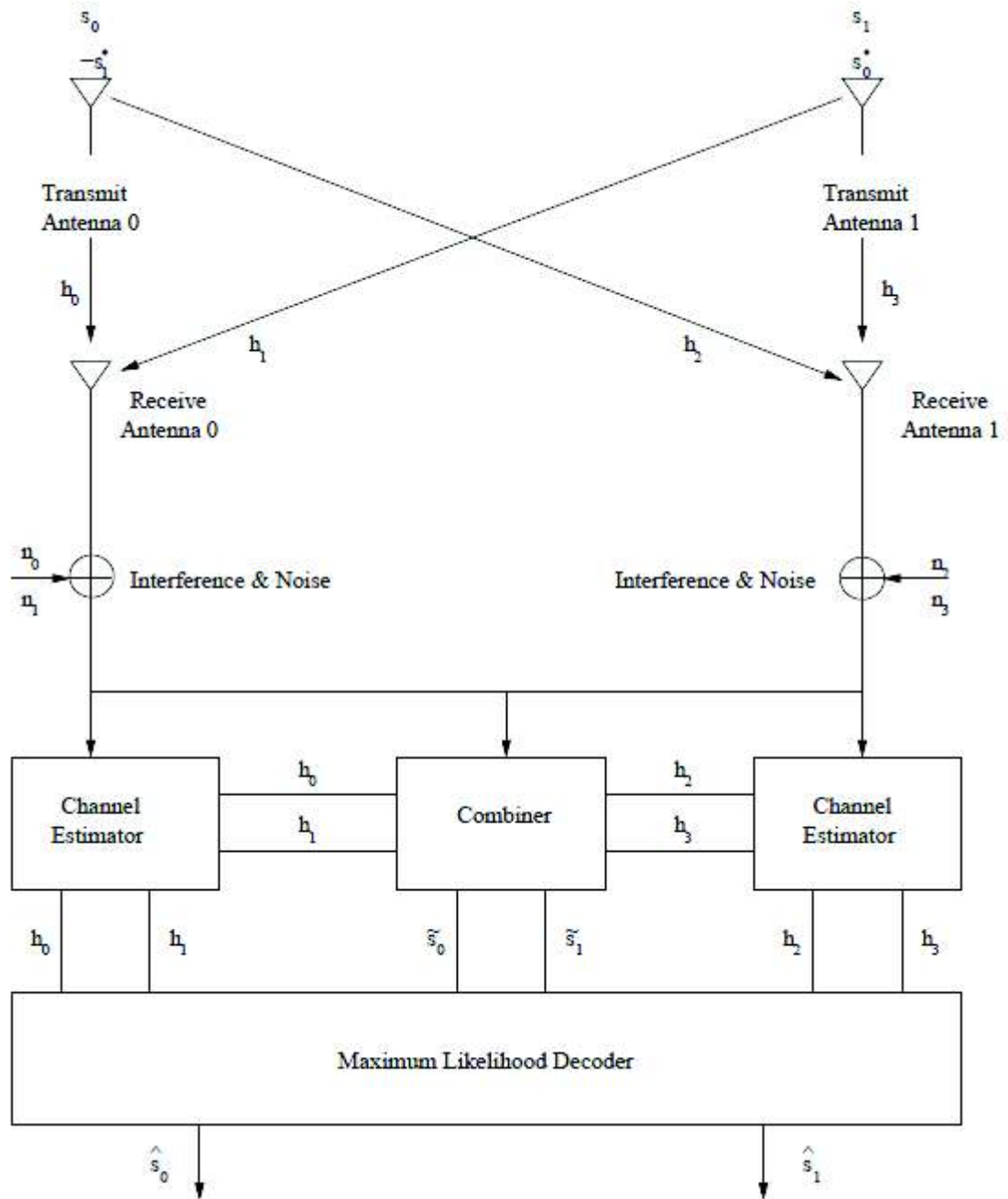


Figure 2.16: The Alamouti scheme with two transmit antennas and two receive antenna

the maximum likelihood detector are given by [56] as

$$\begin{aligned} \tilde{s}_0 &= h_0^* r_0 + h_1 r_1^* + h_2^* r_2 + h_3 r_3^* \\ &= (\alpha_0^2 + \alpha_1^2 + \alpha_2^2 + \alpha_3^2) s_0 + h_0^* n_0 + h_1 n_1^* + h_2^* n_2 + h_3 n_3^* \end{aligned}$$

$$\begin{aligned}
\tilde{s}_1 &= h_1^* r_0 - h_0 r_1^* + h_3^* r_2 - h_2 r_3^* \\
&= (\alpha_0^2 + \alpha_1^2 + \alpha_2^2 + \alpha_3^2) s_1 - h_0 n_1^* + h_1^* n_0 - h_2 n_3^* + h_3^* n_2
\end{aligned} \tag{2.32}$$

For PSK signals, the decision rule is presented in [29] as

$$\begin{aligned}
\hat{s}_0 &= \arg \max_{\hat{s}_0 \in \mathcal{S}} [d^2(\tilde{s}_0, \hat{s}_0)] \\
\hat{s}_1 &= \arg \max_{\hat{s}_1 \in \mathcal{S}} [d^2(\tilde{s}_1, \hat{s}_1)]
\end{aligned} \tag{2.33}$$

2.10.2 Extension to Multiple Transmit Antennas

Space-time coding is a technique that greatly improves performance in wireless networks by using multiple antennas at the transmitter and receiver [75]. The block codes were utilized by Alamouti [56], and later by Tarokh, Seshadri, Jafarkhani and Calderbank [55, 57, 58, 59] to develop space-time block codes (STBC). In the previous section, the Alamouti scheme uses a two transmit antennas system with a very simple maximum likelihood decoding algorithm to achieve full diversity order. The coding matrix of the Alamouti scheme is given by [56] as

$$C_2 = \begin{bmatrix} x_1 & x_2 \\ -x_2^* & x_1^* \end{bmatrix} \tag{2.34}$$

where * is complex conjugate.

In [57], Tarokh generalized the two transmit antennas Alamouti scheme to an arbitrary number of transmit antennas. Fig 2.17 shows the system block diagram for space-time block codes. We assume that a MIMO system with L_t transmit antennas and L_r receive antennas. Let us denote $h_{i,j}$ as the path gain from the i_{th} transmit antenna to the j_{th} receive antennas which is constant over a frame of length l . At each time slot t , signals

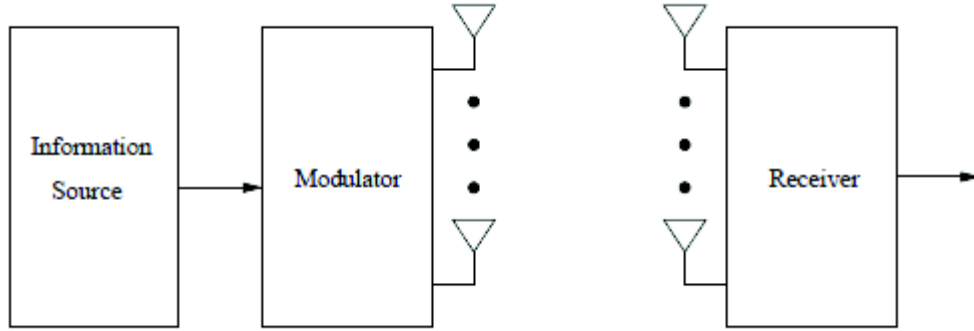


Figure 2.17: A system block diagram of the space-time block codes

c_i^t , $i = 1, 2, \dots, L_t$ are transmitted from L_t transmit antennas. The received signal r_j^t at the j^{th} receive antenna is shown by [60]

$$r_t^j = \sum_{i=1}^{L_t} h_{i,j} c_i^i + \eta_t^j \quad (2.35)$$

where η_t^j is a sample of additive white Gaussian noise (AWGN).

The receiver computes the decision metric [57]

$$\sum_{t=1}^l \sum_{j=1}^{L_r} \left| r_t^j - \sum_{i=1}^{L_t} h_{i,j} c_i^i \right|^2 \quad (2.36)$$

over all the code words

$$c_1^1 c_1^2 \dots c_1^{L_t} c_2^1 c_2^2 \dots c_l^1 c_l^2 \dots c_l^{L_t} \quad (2.37)$$

and decides in favor of the code word that minimizes the sum.

For three and four transmit antennas, the transmission matrices which have a code rate 1/2 are given below [57]

$$C_3 = \begin{bmatrix} x_1 & x_2 & x_3 \\ -x_2 & x_1 & -x_4 \\ -x_3 & x_4 & x_1 \\ -x_4 & -x_3 & x_2 \\ x_1^* & x_2^* & x_3^* \\ -x_2^* & x_1^* & -x_4^* \\ -x_3^* & x_4^* & x_1^* \\ -x_4^* & -x_3^* & x_2^* \end{bmatrix} \quad (2.38)$$

And

$$C_4 = \begin{bmatrix} x_1 & x_2 & x_3 & x_4 \\ -x_2 & x_1 & -x_4 & x_3 \\ -x_3 & x_4 & x_1 & -x_2 \\ -x_4 & -x_3 & x_2 & x_1 \\ x_1^* & x_2^* & x_3^* & x_4^* \\ -x_2^* & x_1^* & -x_4^* & x_3^* \\ -x_3^* & x_4^* & x_1^* & x_3^* \\ -x_4^* & -x_3^* & x_2^* & x_1^* \end{bmatrix} \quad (2.39)$$

The transmission matrices which have a code rate 3/4 are shown in [57]

$$H_3 = \begin{bmatrix} x_1 & x_2 & \frac{x_3}{\sqrt{2}} \\ -x_2^* & x_1^* & \frac{x_3}{\sqrt{2}} \\ \frac{x_3^*}{\sqrt{2}} & \frac{x_3^*}{\sqrt{2}} & \frac{(-x_1 - x_1^* + x_2 - x_2^*)}{2} \\ \frac{x_3^*}{\sqrt{2}} & -\frac{x_3^*}{\sqrt{2}} & \frac{(x_2 + x_2^* + x_1 - x_1^*)}{2} \end{bmatrix} \quad (2.40)$$

And

$$H_4 = \begin{bmatrix} x_1 & x_2 & \frac{x_3}{\sqrt{2}} & \frac{x_3}{\sqrt{2}} \\ -x_2^* & x_1^* & \frac{x_3}{\sqrt{2}} & -\frac{x_3}{\sqrt{2}} \\ \frac{x_3^*}{\sqrt{2}} & \frac{x_3^*}{\sqrt{2}} & \frac{(-x_1 - x_1^* + x_2 - x_2^*)}{2} & \frac{(-x_2 - x_2^* + x_1 - x_1^*)}{2} \\ \frac{x_3^*}{\sqrt{2}} & -\frac{x_3^*}{\sqrt{2}} & \frac{(x_2 + x_2^* + x_1 - x_1^*)}{2} & -\frac{(x_1 + x_1^* + x_2 - x_2^*)}{2} \end{bmatrix} \quad (2.41)$$

The decision rule for three and four transmit antennas is shown in [57].

2.11 Chapter Summary

This chapter introduces some fundamental concepts related to this thesis. A brief overview of digital communication systems, digital modulation schemes, MIMO system models, antenna selection techniques and fading channels is presented. Diversity combining techniques, the Alamouti scheme and space-time block codes are also discussed in this chapter.

Performance of the RAS/STBC Scheme under Nakagami-m fading channel

3.1 Introduction

Multiple-input multiple-output (MIMO) systems offer numerous benefits over conventional single-input single-output (SISO) systems, such as the potential to facilitate considerably higher data rates or to significantly improve the reliability of a wireless link. However, this superior performance generally comes along with an increased signal processing complexity as well as substantially higher hardware requirements, what hence represents a limiting factor for the production and widespread deployment of low-cost MIMO devices. A promising approach for partially alleviating these drawbacks is to make use of some form of antenna selection. Antenna selection technique [1] in MIMO systems reduces the hardware cost and computational complexity while retaining the high performance in fading environment.

The core idea for antenna selection is to select optimally a small number of best antennas from a larger set of available antennas. By utilizing low-cost RF switches, only a limited number of RF chains are adaptively switched to a best subset of antennas which can be identified during the training phase by probing all antennas. However, the computational complexity required for such optimal selection grows exponentially with the total number of antennas. Various fast antenna selection algorithms have been studied [61]. A promising approach for fast receive antenna selection was proposed by Gorokhov [62] which finds a near optimal subset selection based on the channel capacity maximization. An improved algorithm which achieves same performance but lower computational complexity was proposed in [63]. Both methods assume perfect Channel State Information (CSI) at the receiver. In practical implementation, inaccurate channel estimation in the presence of unknown interference will inevitably affect antenna selection performance.

In this chapter, we analyze the performance of MIMO systems employing space-time block codes (STBC) combined with antenna selection at the receiver-side. This might be an

attractive solution for the downlink of cellular networks, for example, where the complexity and the costs of the mobile user equipment generally should be kept as low as possible whereas this is usually only of secondary importance for the base stations. Previous studies dealing with the combination of antenna selection and STBCs have mainly focused on performing antenna subset selection at the transmitter-side (see for example [64], [65] and references therein), but only very few results have been reported concerning the performance of orthogonal STBC with receive antenna selection so far. In [66], for instance, the authors present upper bounds on the average bit error rates for binary modulation in uncorrelated Rayleigh fading as well as an exact expression for the special case that the well-known Alamouti scheme is employed. Besides, the effects of channel estimation errors on the performance of orthogonal STBCs combined with receive antenna selection recently have been investigated in [67]. However, to the best of our knowledge, a comprehensive performance analysis of orthogonal STBCs with receive antenna selection has not been presented yet, what we therefore will do herein. In particular, we derive exact analytical closed-form expressions for the capacity of such a system as well as the average symbol error rates (SER) in case of M-ary quadrature amplitude modulation (M-QAM) and M-ary phase shift keying (MPSK), considering Nakagami-m fading channels with possible spatial correlation at the transmitter-side. In addition, we compare the performance of our system with the performance of a full-complexity system as well as a single-input multiple output (SIMO) system with selection combining.

3.2 System and Channel Model

We consider a multiuser MIMO system, equipped with L_t transmit antennas at the base station, and L_r receive antennas. Depending on the channel conditions, the user scheduler selects the best user and then the discrete-rate adaptive modulator chooses the highest bit-rate modulation scheme for that user that satisfies a target BER. We assume that the MIMO channel between the receive antennas and transmit antennas at the base station is a Nakagami-m flat fading channel. It is assumed that channel state information (CSI) is perfectly available only at the receiver. The RAS in MIMO/STBC scheme model is presented in Fig. 3.1.

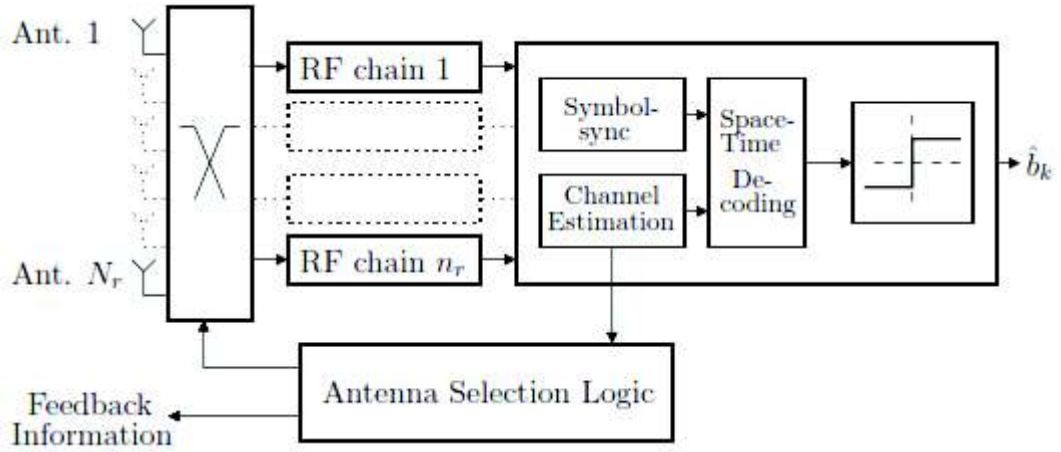


Figure 3.1 MIMO-STBC with receiver antenna selection

The channel can be expressed by matrix H of size $L_r \times L_t$ with elements corresponding to the fading coefficients $h_{i,j}$, ($1 \leq i \leq L_r, 1 \leq j \leq L_t$) The amplitude $|h_{i,j}|$ follows a Nakagami distribution with fading parameter $m \geq 1/2$ between the j -th transmit antenna and the i -th receive antenna. The phase of each channel coefficient is assumed to be uniformly distributed in $[0; 2\pi)$ whereas the magnitudes are supposed to be Nakagami- m variates with unity average power gain and integer fading parameter m .

The transmitter encodes the data to be sent by means of an orthogonal STBC with code rate R_c while the receiver—which is assumed to have perfect knowledge of the channel—selects always only the best out of the available L_r receive antenna elements for processing the faded received signals, which are additionally perturbed by additive white Gaussian noise. It is well known that after appropriate signal combining, orthogonal STBCs transform a MIMO system into a set of equivalent SISO channels [66] and in case that the i -th receive antenna is selected, it can easily be shown that these equivalent SISO channels have the effective signal-to-noise ratio (SNR).

$$\gamma_i = \frac{\bar{\gamma}}{R_c L_t} \sum_{j=1}^{L_t} |h_{i,j}|^2 = \gamma_0 \sum_{j=1}^{L_t} |h_{i,j}|^2 \quad (3.1)$$

where γ_i denotes the instantaneous output SNR of the of the i -th selected receiver antenna and short-hand notation $\gamma_0 = \bar{\gamma}/(R_c L_t)$, where $\bar{\gamma}$ denotes the average SNR per receive

antenna. Clearly, selecting the best antenna hence corresponds to selecting the antenna for which this effective SNR is maximized.

The PDF of channel amplitudes $h_{i,j}$ in Nakagami-m fading is given by

$$p_\gamma(\gamma) = \frac{\gamma^{mL_r-1} \exp(-m\frac{\gamma}{\bar{\gamma}})}{\left(\frac{\bar{\gamma}}{m}\right)^{mL_r} \Gamma(mL_r)} \quad (3.2)$$

Where the average SNR $\bar{\gamma} = E_s/N_0$ in which E_s is the average energy per symbol at the transmitter and N_0 is the power spectral density of the AWGN at each receive antenna.

For an arbitrary real-valued fading parameter m , the cumulative distribution function (cdf) of γ is calculated as

$$P_\gamma(\gamma) = \frac{\gamma(mL_r, m\frac{\gamma}{\bar{\gamma}})}{\Gamma(mL_r)} \quad (3.3)$$

where $\gamma(\alpha, x) = \int_0^x e^{-t} t^{\alpha-1} dt$ is the lower incomplete Gamma function.

$$\begin{aligned} P_{(L_t)}(\gamma) &= L_t \left[P_{(\gamma)}(\gamma) \right]^{L_t-1} P_{(\gamma)}(\gamma) \\ &= L_t \left(\frac{m}{\bar{\gamma}} \right)^{mL_r} \frac{\gamma^{mL_r-1} \exp(-m\frac{\gamma}{\bar{\gamma}})}{\Gamma(mL_r)} \left[\frac{\gamma(mL_r, m\frac{\gamma}{\bar{\gamma}})}{\Gamma(mL_r)} \right]^{L_t-1} \end{aligned} \quad (3.4)$$

Using the infinite series representation of the incomplete gamma function in [69, (8.3541)]

$$\gamma(\alpha, x) = \sum_{n=0}^{\infty} \frac{(-1)^n x^{\alpha+n}}{n!(\alpha+n)} \quad (3.5)$$

the MGF associated with γ is expressed as

$$M_\gamma(s) = \int_0^{\infty} P_{(L_t)}(\gamma) e^{s\gamma} d\gamma$$

$$\begin{aligned}
&= \int_0^{\infty} \frac{L_t}{\Gamma(mL_r)} \left(\frac{m}{\bar{\gamma}}\right)^{mL_r} \gamma^{mL_r-1} \left[\frac{\gamma \left(mL_r, m \frac{\gamma}{\bar{\gamma}}\right)}{\Gamma(mL_r)} \right]^{L_t-1} \exp\left[-\left(\frac{m}{\bar{\gamma}} - s\right)\gamma\right] d\gamma \\
&= \frac{L_t}{[\Gamma(mL_r)]^{L_t}} \left(\frac{m}{\bar{\gamma}}\right)^{mL_r L_t} \sum_{n_1=0}^{+\infty} \sum_{n_2=0}^{+\infty} \cdots \sum_{n_{L_t-1}=0}^{+\infty} \left(\frac{m}{\bar{\gamma}}\right)^{\sum_{k=1}^{L_t-1} n_k} \prod_{i=1}^{L_t-1} \frac{(-1)^{n_i}}{n_i!(mL_r + n_i)} \\
&\quad \times \int_0^{+\infty} \gamma^{mL_r L_t + \sum_{k=1}^{L_t-1} n_k - 1} \exp\left[-\left(\frac{m}{\bar{\gamma}} - s\right)\gamma\right] d\gamma \tag{3.6}
\end{aligned}$$

Using the identity below [69, (3.381-4)]

$$\int_0^{\infty} x^{\nu-1} e^{-\mu x} dx = \frac{1}{\mu^{\nu}} \Gamma(\nu), \quad \text{Re } \mu > 0, \tag{3.7}$$

the MGF of the RAS scheme over Nakagami-m fading channels with arbitrary parameter m in (3.6) can be further written as

$$\begin{aligned}
M_{\gamma}(s) &= \frac{L_t}{[\Gamma(mL_r)]^{L_t}} \left(\frac{m}{\bar{\gamma}}\right)^{mL_r L_t} \sum_{n_1=0}^{+\infty} \sum_{n_2=0}^{+\infty} \cdots \sum_{n_{L_t-1}=0}^{+\infty} \left(\frac{m}{\bar{\gamma}}\right)^{\sum_{k=1}^{L_t-1} n_k} \prod_{i=1}^{L_t-1} \frac{(-1)^{n_i}}{n_i!(mL_r + n_i)} \\
&\quad \times \Gamma\left(mL_r L_t + \sum_{k=1}^{L_t-1} n_k\right) \times \left(\frac{m}{\bar{\gamma}} - s\right)^{-(mL_r L_t + \sum_{k=1}^{L_t-1} n_k)} \tag{3.8}
\end{aligned}$$

For Nakagami-m fading channels with integer m , the cdf of γ can be expressed as

$$\begin{aligned}
P_{\gamma}(\gamma) &= \int_0^{\gamma} P(y) dy = \int_0^{\gamma} \frac{y^{mL_r-1}}{\left(\frac{\bar{\gamma}}{m}\right)^{mL_r} \Gamma(mL_r)} \exp\left(-m \frac{y}{\bar{\gamma}}\right) dy \\
&= \frac{1}{\Gamma(mL_r)} \left(\frac{m}{\bar{\gamma}}\right)^{mL_r} \int_0^{\gamma} y^{mL_r-1} \exp\left(-m \frac{y}{\bar{\gamma}}\right) dy \tag{3.9}
\end{aligned}$$

Applying [69, (8.339-1)] and [69, (8.351-1)] into (3.9)

$$\Gamma(n) = (n-1)! \quad [n = 1, 2, \dots] \tag{3.10}$$

$$\int_0^u x^n e^{-\mu x} dx = \frac{n!}{\mu^{n+1}} - e^{-u\mu} \sum_{k=0}^n \frac{n!}{k!} \frac{u^k}{\mu^{n-k+1}} \quad [u > 0, \text{Re } \mu > 0, n = 1, 2, \dots] \quad (3.11)$$

we have

$$\begin{aligned} P_\gamma(\gamma) &= \frac{1}{(mL_r - 1)!} \left(\frac{m}{\bar{\gamma}}\right)^{mL_r} \left[\frac{(mL_r - 1)!}{\left(\frac{m}{\bar{\gamma}}\right)^{mL_r}} - e^{-\frac{m\gamma}{\bar{\gamma}}} \sum_{k=0}^{mL_r-1} \frac{(mL_r - 1)!}{k!} \frac{\gamma^k}{\left(\frac{m}{\bar{\gamma}}\right)^{mL_r-k}} \right] \\ &= 1 - e^{-\frac{m\gamma}{\bar{\gamma}}} \sum_{k=0}^{mL_r-1} \frac{\gamma^k}{k!} \left(\frac{m}{\bar{\gamma}}\right)^k \end{aligned} \quad (3.12)$$

Therefore, the pdf of the instantaneous post-processing SNR of the (L_t, L_r) RAS system can be derived as [68]

$$\begin{aligned} P_{(L_t)}(\gamma) &= L_t [P_\gamma(\gamma)]^{L_t-1} P_\gamma(\gamma) \\ &= L_t \left[1 - e^{-\frac{m\gamma}{\bar{\gamma}}} \sum_{k=0}^{mL_r-1} \frac{\gamma^k}{k!} \left(\frac{m}{\bar{\gamma}}\right)^k \right]^{L_t-1} \left(\frac{m}{\bar{\gamma}}\right)^{mL_r} \frac{\gamma^{mL_r-1}}{(mL_r - 1)!} e^{-\frac{m\gamma}{\bar{\gamma}}} \\ &= \frac{L_t}{(mL_r - 1)!} \sum_{k=0}^{L_t-1} (-1)^k \binom{L_t - 1}{k} \sum_{t=0}^{k(mL_r-1)} \left(\frac{m}{\bar{\gamma}}\right)^{mL_r+t} b_t(mL_r, k) \gamma^{mL_r+t+1} e^{-\frac{(k+1)m\gamma}{\bar{\gamma}}} \end{aligned} \quad (3.13)$$

in which $b_t(mL_r, k)$ is the coefficient of z^t , $t = 0, 1, \dots, k(mL_r - 1)$ in the expansion of

$$\left(\sum_{i=0}^{mL_r-1} \frac{z^i}{i!} \right) \quad (3.14)$$

The MGF is derived as [70]

$$\begin{aligned} M_\gamma(s) &= \int_0^\infty P_{(L_t)}(\gamma) e^{-s\gamma} d\gamma \\ &= \int_0^\infty \frac{L_t}{(mL_r - 1)!} \sum_{k=0}^{L_t-1} (-1)^k \binom{L_t - 1}{k} \sum_{t=0}^{k(mL_r-1)} \left(\frac{m}{\bar{\gamma}}\right)^{mL_r+t} b_t(mL_r, k) \\ &\quad \times \gamma^{mL_r+t+1} e^{-\frac{(k+1)m\gamma}{\bar{\gamma}}} d\gamma \end{aligned}$$

$$\begin{aligned}
&= \frac{L_t}{(mL_r - 1)!} \sum_{k=0}^{L_t-1} (-1)^k \binom{L_t-1}{k} \sum_{t=0}^{k(mL_r-1)} \left(\frac{m}{\bar{\gamma}}\right)^{mL_r+t} b_t(mL_r, k) \\
&\quad \times \int_0^\infty \gamma^{mL_r+t-1} e^{-\frac{(k+1)m}{\bar{\gamma}}\gamma} d\gamma
\end{aligned} \tag{3.15}$$

Substituting the identity [9, (3.351-3)] into (3.15)

$$\int_0^\infty x^n e^{-\mu x} dx = n! \mu^{-n-1}, \quad [\operatorname{Re} \mu > 0, n = 0, 1, 2, \dots] \tag{3.16}$$

we can derive the MGF of the RAS scheme over Nakagami-m fading channels with integer parameter m in (3.15) as

$$\begin{aligned}
M_\gamma(s) &= \frac{L_t}{(mL_r - 1)!} \sum_{k=0}^{L_t-1} (-1)^k \binom{L_t-1}{k} \sum_{t=0}^{k(mL_r-1)} \left(\frac{m}{\bar{\gamma}}\right)^{mL_r+t} b_t(mL_r, k) \\
&\quad \times (mL_r + t - 1)! \left[\frac{(k+1)m}{\bar{\gamma}} - s \right]^{-(mL_r+t)}
\end{aligned} \tag{3.17}$$

3.3 Error Performance Analysis of the RAS Scheme

Exact BER of BPSK of the RAS Scheme for the (L_t , L_r) RAS scheme with BPSK modulation, the BER expression can be presented as [70]

$$P_{BPSK} = \int_0^{\pi/2} M_\gamma \left(-\frac{g}{\sin^2 \theta} \right) d\theta \tag{3.18}$$

where $g = 1$ for BPSK modulation.

Substituting (3.8) into (3.18) gives

$$\begin{aligned}
P_{BPSK} &= \frac{L_t}{[\Gamma(mL_r)]^{L_t}} \left(\frac{m}{\bar{\gamma}}\right)^{mL_r L_t} \sum_{n_1=0}^{+\infty} \sum_{n_1=0}^{+\infty} \dots \sum_{n_{L_t-1}=0}^{+\infty} \left(\frac{m}{\bar{\gamma}}\right)^{\sum_k^{L_t-1} n_k} \prod_{i=1}^{L_t-1} \frac{(-1)^{n_i}}{n_i! (mL_r + n_i)} \\
&\quad \times \Gamma \left(mL_r L_r + \sum_k^{L_t-1} n_k \right) \underbrace{\frac{1}{\pi} \int_0^{\pi/2} \left(\frac{m}{\bar{\gamma}} + \frac{g}{\sin^2 \theta} \right)^{-(mL_r L_r + \sum_k^{L_t-1} n_k)} d\theta}_{A_1}
\end{aligned} \tag{3.19}$$

A_1 can be further written as

$$A_1 = \left(\frac{m}{\bar{\gamma}}\right)^{-(mL_r L_r + \sum_k^{L_t-1} n_k)} \underbrace{\frac{1}{\pi} \int_0^{\pi/2} \left(\frac{\sin^2 \theta}{\sin^2 \theta + \frac{\bar{\gamma}}{m}} \right)^{-(mL_r L_r + \sum_k^{L_t-1} n_k)} d\theta}_{A_2} \tag{3.20}$$

Using Eq. [11] the integral A_2 can be simplified as

$$A_2 = \left(1 + \frac{\bar{\gamma}}{m}\right)^{-(mL_r L_t + \sum_k^{L_t-1} n_k)} \frac{1}{2\sqrt{\pi}} \frac{\Gamma\left(mL_r L_t + \sum_k^{L_t-1} n_k + \frac{1}{2}\right)}{\Gamma\left(mL_r L_t + \sum_k^{L_t-1} n_k + 1\right)} \times {}_2F_1\left(mL_r L_t + \sum_k^{L_t-1} n_k, \frac{1}{2}; mL_r L_t + \sum_k^{L_t-1} n_k + 1; \frac{1}{1 + \frac{\bar{\gamma}}{m}}\right) \quad (3.21)$$

Therefore, the BER expression for BPSK modulation is presented as

$$P_{BPSK} = \frac{L_t}{[\Gamma(mL_r)]^{L_t}} \sum_{n_1=0}^{+\infty} \sum_{n_2=0}^{+\infty} \dots \sum_{n_{L_t-1}=0}^{+\infty} \left(\prod_{i=1}^{L_t-1} \frac{(-1)^{n_i}}{n_i! (mL_r + n_i)} \right) \left(1 + \frac{\bar{\gamma}}{m}\right)^{-(mL_r L_t + \sum_k^{L_t-1} n_k)} \times \Gamma\left(mL_r L_t + \sum_k^{L_t-1} n_k\right) \left\{ \frac{1}{2\sqrt{\pi}} \frac{\Gamma\left(mL_r L_t + \sum_k^{L_t-1} n_k + \frac{1}{2}\right)}{\Gamma\left(mL_r L_t + \sum_k^{L_t-1} n_k + 1\right)} \times {}_2F_1\left(mL_r L_t + \sum_k^{L_t-1} n_k, \frac{1}{2}; mL_r L_t + \sum_k^{L_t-1} n_k + 1; \frac{1}{1 + \frac{\bar{\gamma}}{m}}\right) \right\} \quad (3.22)$$

If the fading parameter m is an integer, substituting (3.17) into (3.18) gives

$$P_{BPSK}(E) = \frac{L_t}{(mL_r - 1)!} \sum_{k=1}^{L_t-1} (-1)^k \binom{L_t-1}{k} \sum_{t=0}^{mL_r-1} \left(\frac{m}{\bar{\gamma}}\right)^{mL_r-1} b_t(mL_r, k) \times (mL_r + t - 1)! \underbrace{\frac{1}{\pi} \int_0^{\pi/2} \left[\frac{(k+1)m}{\bar{\gamma}} + \frac{g}{\sin^2 \theta} \right]^{-(mL_r+t)} d\theta}_{B_1} \quad (3.23)$$

B_1 can be written

$$B_1 = \left[\frac{(k+1)m}{\bar{\gamma}} \right]^{-(mL_r+t)} \underbrace{\frac{1}{\pi} \int_0^{\pi/2} \left[\frac{\sin^2 \theta}{\sin^2 \theta + \frac{\bar{\gamma}}{(k+1)m}} \right]^{-(mL_r+t)} d\theta}_{B_2} \quad (3.24)$$

Using Eq.[71,(46)], the integral B_2 can be derived as

$$B_2 = \left[1 + \frac{\bar{\gamma}}{(k+1)m} \right]^{-(mL_r+t)} \frac{1}{2\sqrt{\pi}} \frac{\Gamma\left(mL_r + t + \frac{1}{2}\right)}{\Gamma(mL_r + t + 1)} {}_2F_1\left(mL_r + t, \frac{1}{2}; mL_r + t + 1; \frac{1}{1 + \frac{\bar{\gamma}}{(k+1)m}}\right) \quad (3.25)$$

Therefore, the BER expression for BPSK modulation can be written as

$$P_{BPSK}(E) = \frac{L_t}{(mL_r - 1)!} \sum_{k=0}^{L_t-1} (-1)^k \binom{L_t-1}{k} \sum_{t=0}^{k(mL_r-1)} \left(\frac{m}{\bar{\gamma}}\right)^{mL_r-1} b_t(mL_r, k)(mL_r + t - 1)! \\ \times \frac{\left(k + 1 + \frac{\bar{\gamma}}{m}\right)^{-(mL_r+t)}}{2\sqrt{\pi}} \frac{\Gamma\left(mL_r + t + \frac{1}{2}\right)}{\Gamma(mL_r + t + 1)} {}_2F_1\left(mL_r + t, \frac{1}{2}; mL_r + t + 1; \frac{1}{1 + \frac{\bar{\gamma}}{(k+1)m}}\right) \quad (3.26)$$

3.4 Chapter Summary

This chapter primarily focuses on deriving the exact error rate expression for performance evaluation of the RAS/STBC scheme over Nakagami- m fading channels. This chapter starts by deriving the MGF of the RAS/STBC scheme over Nakagami- m fading channels with arbitrary and integer fading parameters m and then proceeds to obtain the exact and asymptotic error probability expressions of the RAS/STBC scheme for BPSK modulations. It is revealed that in Nakagami- m fading channels the RAS/STBC scheme can achieve full diversity order which is equal to the product of Nakagami fading parameter m , the number of transmit antennas L_t and the number of receive antennas L_r . The simulation results of the RAS/STBC scheme over Nakagami- m fading channels are given in chapter 6.

Performance of the TAS/STBC Scheme under Nakagami-m Fading Channels

4.1 Introduction

In the TAS/STBC scheme, two transmit antennas which maximize the total received signal power at the receiver are selected for data transmission. Antenna selection techniques have been investigated to maximize the system capacity [85–89]. In this chapter, we use antenna selection to minimize the error rate for the Alamouti scheme. In [30] and [31] Chen derived the exact and asymptotic BER expressions for BPSK modulation of the TAS/STBC scheme in Rayleigh fading channels and showed that the diversity order is equal to the product of the number of the transmit antennas L_t and the number of the receive antennas L_r in flat Rayleigh fading channels at high SNRs.

In this chapter we analyze the error performance of the TAS/STBC scheme over Nakagami-m fading channels by using a Gaussian and Marcum Q-functions approach. The exact and asymptotic BER expressions for BPSK are derived for the TAS/STBC schemes with three and four transmit antennas. The analytical and numerical results are shown. We also present the performance comparison between the TAS/STBC scheme and the TAS/MRC scheme.

4.2 System and Channel Model

Let us consider an (L_t, L_r) TAS/STBC system with L_t transmit and L_r receive antenna under i.i.d Nakagami-m fading channels. We assume that the CSI is perfectly available at the receiver and partially known at the transmitter through a feedback channel. The TAS/STBC scheme model is shown in Fig. 4.1.

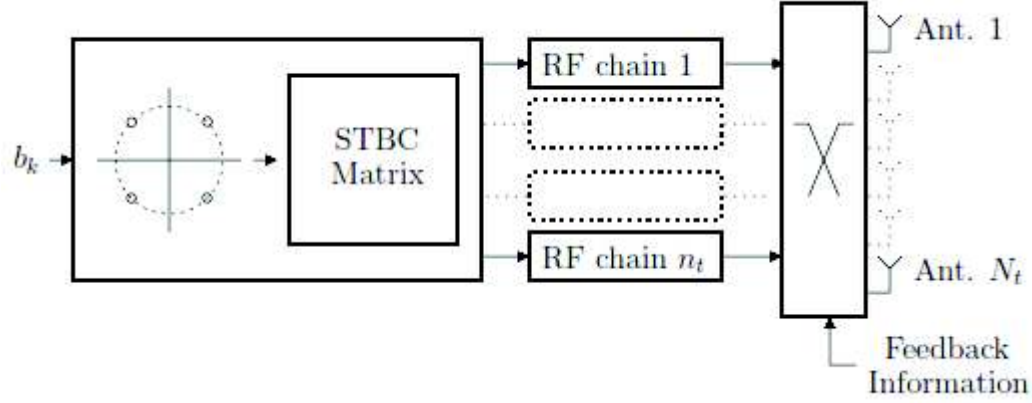


Figure 4.1: MIMO-STBC transmitter with antenna selection

Let \mathbf{H} denote the $L_r \times L_t$ channel matrix. Its entries are the fading coefficients $h_{i,j}$, $1 \leq i \leq L_r$, $1 \leq j \leq L_t$. The amplitude $|h_{i,j}|$ has a Nakagami distribution with fading parameter $m \geq 1/2$. An $L_r \times 1$ matrix \mathbf{H} , which is a column of \mathbf{H} , is used to denote the channel between a single selected transmit antenna and L_r receive antennas. The two selected transmit antennas, denoted by X and Y , are selected by

$$\{X, Y\} = \arg \max_{1 \leq x, y \leq L_t, x \neq y} \left\{ \gamma(t) = \frac{E_s}{N_0} \sum_{t=1}^{L_r} (|h_{x,t}|^2 + |h_{y,t}|^2) \right\} \quad (4.1)$$

E_s is the average energy per symbol and N_0 is the power spectral density of the AWGN at each receive antenna. The instantaneous SNR of the output of Alamouti scheme with two transmit antennas is given by [56]

$$\gamma_b = \frac{\gamma(t)}{2} \quad (4.2)$$

We rearrange the SNRs $\gamma(i)$, $1 \leq i \leq L_t$, in ascending order of magnitude and denote them by $\gamma_{(p)}$, where $1 \leq p \leq L_t$ and $\gamma_{(1)} \leq \gamma_{(2)} \leq \dots \leq \gamma_{(L_t)}$. According to (4.1), the two transmit antennas corresponding to the L_t th order statistic, (L_t) , and the $(L_t - 1)$ th order statistic $(L_t - 1)$ will be selected for uncoded transmission.

$\gamma_{(i)}$ follows a Nakagami- m distribution. The pdf of (i) is given as

$$P_{\gamma_{(i)}}(\gamma_{(i)}) = \left(\frac{m}{\bar{\gamma}}\right)^{mL_r} \frac{\gamma_{(i)}^{mL_r-1}}{\Gamma(mL_r)} \exp\left(-m\frac{\gamma_{(i)}}{\bar{\gamma}}\right) \quad (4.3)$$

where the average SNR $\bar{\gamma} = E_s/N_0$, in which E_s is the average energy per symbol at the transmitter and N_0 is the power spectral density of the AWGN at each receive antenna.

For arbitrary real-value fading parameter m , the cdf of $\gamma_{(i)}$ is shown as

$$P_{\gamma}(\gamma) = \frac{\gamma(mL_r, m\frac{\gamma}{\bar{\gamma}})}{\Gamma(mL_r)} \quad (4.4)$$

Where $\gamma(\alpha, x) = \int_0^x e^{-t} t^{\alpha-1} dt$ is the lower incomplete Gamma function.

The joint pdf of $\gamma_{(L_t)}$ and (L_t-1) of $(L_t, 2; L_r)$ TAS/STBC system can be expressed as [72]

$$P_{\gamma_1, \gamma_2}(\gamma_1, \gamma_2) = L_t(L_t-1)[P_{\gamma_2}(\gamma_2)]^{L_t-2} P_{\gamma_1}(\gamma_1) P_{\gamma_2}(\gamma_2) \quad (4.5)$$

In this chapter, we focus on the error performance of the TAS/STBC scheme with three and four antennas. Therefore when the number of transmit antennas $L_t=3$ and 4 the joint pdf expressions can be simplified as

$$P_{\gamma_1, \gamma_2}(\gamma_1, \gamma_2) = 6P_{\gamma_2}(\gamma_2)P_{\gamma_1}(\gamma_1)P_{\gamma_2}(\gamma_2) \quad (4.6)$$

and

$$P_{\gamma_1, \gamma_2}(\gamma_1, \gamma_2) = 12[P_{\gamma_2}(\gamma_2)]^2 P_{\gamma_1}(\gamma_1) P_{\gamma_2}(\gamma_2) \quad (4.7)$$

4.3 Error Performance Analysis of TAS/STBC Scheme

The average BER expression for BPSK of the (L_t, L_r) TAS/STBC scheme can be expressed as [26]

$$P_{BPSK} = \int_0^{\infty} Q(\sqrt{2\gamma_b}) P_{\gamma_b}(\gamma_b) d\gamma_b \quad (4.8)$$

Substituting (4.2) into (4.8) we have

$$P_{BPSK} = \int_0^{\infty} \int_0^{\gamma_1} Q(\sqrt{2\gamma_1 + \gamma_2}) P_{\gamma_1 + \gamma_2}(\gamma_1 + \gamma_2) d\gamma_2 d\gamma_1 \quad (4.9)$$

Using the alternative representation of Gaussian Q function [67], (4.9) can be further written as

$$P_{BPSK} = \frac{1}{\pi} \int_0^{\frac{\pi}{2}} \int_0^{\infty} \int_0^{\gamma_1} Q(\sqrt{2\gamma_1 + \gamma_2}) P_{\gamma_1 + \gamma_2}(\gamma_1 + \gamma_2) \exp\left(-\frac{\gamma_1 + \gamma_2}{2\sin^2 \phi}\right) d\gamma_2 d\gamma_1 d\phi \quad (4.10)$$

For the (3, 2; L_r) TAS/STBC scheme, substituting (4.6) and (4.3) into (4.10), yields

$$\begin{aligned} P_{BPSK} &= \frac{1}{\pi} \int_0^{\frac{\pi}{2}} \int_0^{\infty} \int_0^{\gamma_1} 6P_{\gamma_2}(\gamma_2) P_{\gamma_1}(\gamma_1) P_{\gamma_2}(\gamma_2) \exp\left(-\frac{\gamma_1 + \gamma_2}{2\sin^2 \phi}\right) d\gamma_2 d\gamma_1 d\phi \\ &= \frac{1}{\pi} \int_0^{\frac{\pi}{2}} \int_0^{\infty} \frac{6P_{\gamma_1}(\gamma_1)}{\Gamma(mL_r)} \underbrace{\int_0^{\gamma_1} P_{\gamma_2}(\gamma_2) \gamma \left(mL_r, m\frac{\gamma_2}{\gamma}\right) \exp\left(-\frac{\gamma_2}{2\sin^2 \phi}\right) d\gamma_2}_{C_1} \\ &\quad \times \exp\left(-\frac{\gamma_1}{2\sin^2 \phi}\right) d\gamma_1 \end{aligned} \quad (4.11)$$

Using (4.3) and [82, (8.354-1)] C_1 can be further written

$$\begin{aligned} C_1 &= \left(\frac{m}{\gamma}\right)^{2mL_r} \frac{1}{\Gamma(mL_r)} \sum_{n=0}^{\infty} \frac{(-1)^n}{n!(mL_r + n)} \left(\frac{m}{\gamma}\right)^n \int_0^{\gamma_1} \gamma_2^{2mL_r + n - 1} \exp\left(-\left(\frac{m}{\gamma} + \frac{1}{2\sin^2 \phi}\right)\gamma_2\right) d\gamma_2 \\ &= \left(\frac{m}{\gamma}\right)^{2mL_r} \frac{1}{\Gamma(mL_r)} \sum_{n=0}^{\infty} \frac{(-1)^n}{n!(mL_r + n)} \left(\frac{m}{\gamma}\right)^n \left(\frac{m}{\gamma} + \frac{1}{2\sin^2 \phi}\right)^{-(2mL_r + n)} \\ &\quad \times \gamma \left(2mL_r + n, \left(\frac{m}{\gamma} + \frac{1}{2\sin^2 \phi}\right)\gamma_1\right) \end{aligned} \quad (4.12)$$

Therefore (4.11) can be simplified as

$$\begin{aligned}
P_{BPSK} &= \frac{1}{\pi} \int_0^{\frac{\pi}{2}} \frac{6}{(\Gamma(mL_r))^3} \left(\frac{m}{\bar{\gamma}}\right)^{3mL_r} \sum_{n=0}^{\infty} \frac{(-1)^n}{n!(mL_r+n)} \left(\frac{m}{\bar{\gamma}}\right)^n \left(\frac{m}{\bar{\gamma}} + \frac{1}{2\sin^2\phi}\right)^{-(2mL_r+n)} \\
&\quad \times \int_0^{\gamma_1} \gamma_2^{2mL_r+n-1} \exp\left(-\left(\frac{m}{\bar{\gamma}} + \frac{1}{2\sin^2\phi}\right)\gamma_2\right) \gamma \left(2mL_r+n, \left(\frac{m}{\bar{\gamma}} + \frac{1}{2\sin^2\phi}\right)\gamma_1\right) d\gamma_1 d\phi
\end{aligned} \tag{4.13}$$

Using [73, (6.455-2)] and Eq. [74, (46)], the BER expression for BPSK of the TAS/STBC scheme with three transmit antennas can be obtained a

$$\begin{aligned}
P_{BPSK} &= \frac{3}{(\Gamma(mL_r))^3} \sum_{n=0}^{\infty} \frac{(-1)^n \Gamma(3mL_r+n+\frac{1}{2})}{n!(mL_r+n)(2mL_r+n)(3mL_r+n)2^{3mL_r+n}\sqrt{\pi}} \left(1+\frac{\bar{\gamma}}{2m}\right)^{-(3mL_r+n)} \\
&\quad \times {}_2F_1\left(1, 3mL_r+n; 2mL_r+n; \frac{1}{2}\right) {}_2F_1\left(3mL_r+n, \frac{1}{2}; 3mL_r+n+1; \frac{1}{1+\frac{\bar{\gamma}}{2m}}\right)
\end{aligned} \tag{4.14}$$

From (4.14), the BER expressions for BPSK of the (3,2;1) and (3,2;2) TAS/STBC scheme are derived as

$$\begin{aligned}
P_{BPSK} &= \frac{3}{(\Gamma(m))^3} \sum_{n=0}^{\infty} \frac{(-1)^n \Gamma(3mL_r+n+\frac{1}{2})}{n!(m+n)(2m+n)(3m+n)2^{3m+n}\sqrt{\pi}} \left(1+\frac{\bar{\gamma}}{2m}\right)^{-(3m+n)} \\
&\quad \times {}_2F_1\left(1, 3m+n; 2m+n; \frac{1}{2}\right) {}_2F_1\left(3m+n, \frac{1}{2}; 3m+n+1; \frac{1}{1+\frac{\bar{\gamma}}{2m}}\right)
\end{aligned} \tag{4.15}$$

and

$$P_{BPSK} = \frac{3}{(\Gamma(2m))^3} \sum_{n=0}^{\infty} \frac{(-1)^n \Gamma(6m+n+\frac{1}{2})}{n!(2m+n)(4m+n)(6m+n)2^{6m+n}\sqrt{\pi}} \left(1+\frac{\bar{\gamma}}{2m}\right)^{-(6m+n)}$$

$$\times {}_2F_1\left(1, 6m+n; 4m+n+1; \frac{1}{2}\right) {}_2F_1\left(6m+n, \frac{1}{2}; 6m+n+1; \frac{1}{1+\frac{\bar{\gamma}}{2m}}\right) \quad (4.16)$$

For the (4, 2; Lr) TAS/STBC scheme, substituting (4.7) and (4.3) into (4.10), (4.10) is expressed as

$$\begin{aligned} P_{BPSK} &= \frac{1}{\pi} \int_0^{\frac{\pi}{2}} \int_0^{\infty} \int_0^{\gamma_1} 12 (P_{\gamma_2}(\gamma_2))^2 P_{\gamma_1}(\gamma_1) P_{\gamma_2}(\gamma_2) \exp\left(-\frac{\gamma_1 + \gamma_2}{2 \sin^2 \phi}\right) d\gamma_2 d\gamma_1 d\phi \\ &= \frac{1}{\pi} \int_0^{\frac{\pi}{2}} \int_0^{\infty} \frac{12 P_{\gamma_1}(\gamma_1)}{(\Gamma(mL_r))^2} \underbrace{\int_0^{\gamma_1} P_{\gamma_2}(\gamma_2) \left(\gamma\left(mL_r, m\frac{\gamma_2}{\bar{\gamma}}\right)\right)^2}_{D_1} \exp\left(-\frac{\gamma_2}{2 \sin^2 \phi}\right) d\gamma_2 \\ &\quad \times \exp\left(-\frac{\gamma_1}{2 \sin^2 \phi}\right) d\gamma_1 d\phi \end{aligned} \quad (4.17)$$

Using (4.3) and [73, (8.354-1)] D_1 is equivalent to

$$\begin{aligned} D_1 &= \left(\frac{m}{\bar{\gamma}}\right)^{3mL_r} \frac{1}{\Gamma(mL_r)} \sum_{n_1=0}^{\infty} \sum_{n_2=0}^{\infty} \frac{(-1)^{n_1+n_2}}{n_1! n_2! (mL_r + n_1)(mL_r + n_2)} \left(\frac{m}{\bar{\gamma}}\right)^{n_1+n_2} \\ &\quad \times \int_0^{\gamma_1} \gamma_2^{3mL_r+n_1+n_2-1} \exp\left(-\left(\frac{m}{\bar{\gamma}} + \frac{1}{2 \sin^2 \phi}\right) \gamma_2\right) d\gamma_2 \\ &= \left(\frac{m}{\bar{\gamma}}\right)^{3mL_r} \frac{1}{\Gamma(mL_r)} \sum_{n_1=0}^{\infty} \sum_{n_2=0}^{\infty} \frac{(-1)^{n_1+n_2}}{n_1! n_2! (mL_r + n_1)(mL_r + n_2)} \left(\frac{m}{\bar{\gamma}}\right)^{n_1+n_2} \\ &\quad \times \left(\frac{m}{\bar{\gamma}} + \frac{1}{2 \sin^2 \phi}\right)^{-(3mL_r+n_1+n_2)} \gamma\left(3mL_r + n_1 + n_2, \left(\frac{m}{\bar{\gamma}} + \frac{1}{2 \sin^2 \phi}\right) \gamma_1\right) \end{aligned} \quad (4.18)$$

Thus the BER expression in (4.17) is reduced to

$$P_{BPSK} = \frac{1}{\pi} \int_0^{\frac{\pi}{2}} \frac{12}{(\Gamma(mL_r))^4} \left(\frac{m}{\bar{\gamma}}\right)^{4mL_r} \sum_{n_1=0}^{\infty} \sum_{n_2=0}^{\infty} \frac{(-1)^{n_1+n_2}}{n_1! n_2! (mL_r + n_1)(mL_r + n_2)} \left(\frac{m}{\bar{\gamma}}\right)^{n_1+n_2}$$

$$\begin{aligned}
& \times \left(\frac{m}{\bar{\gamma}} + \frac{1}{2 \sin^2 \phi} \right)^{-(3mL_r + n_1 + n_2)} \int_0^\infty \gamma_1^{mL_r - 1} \exp \left(- \left(\frac{m}{\bar{\gamma}} + \frac{1}{2 \sin^2 \phi} \right) \gamma_1 \right) \\
& \times \gamma \left(3mL_r + n_1 + n_2, \left(\frac{m}{\bar{\gamma}} + \frac{1}{2 \sin^2 \phi} \right) \gamma_1 \right) d\gamma_1 d\phi \tag{4.19}
\end{aligned}$$

By using [73, (6.455-2)] and Eq. [74, (46)], we can have the BER expression for BPSK of the TAS/STBC scheme with four transmit antennas as

$$\begin{aligned}
P_{BPSK} &= \frac{6}{(\Gamma(2m))^4} \sum_{n_1=0}^{\infty} \sum_{n_2=0}^{\infty} \frac{(-1)^{n_1+n_2} \Gamma \left(4mL_r + n_1 + n_2 + \frac{1}{2} \right) 2^{-(4mL_r + n_1 + n_2)}}{n_1! n_2! (mL_r + n_1) (mL_r + n_2) (3mL_r + n_1 + n_2) (4mL_r + n_1 + n_2)} \\
& \times \frac{1}{\sqrt{\pi}} \left(1 + \frac{\bar{\gamma}}{2m} \right)^{-(4mL_r + n_1 + n_2)} {}_2F_1 \left(1, 4mL_r + n_1 + n_2; 3mL_r + n_1 + n_2 + 1; \frac{1}{2} \right) \\
& \times {}_2F_1 \left(4mL_r + n_1 + n_2, \frac{1}{2}; 4mL_r + n_1 + n_2 + 1; \frac{1}{1 + \frac{\bar{\gamma}}{2m}} \right) \tag{4.20}
\end{aligned}$$

Substituting $L_r=1$ and 2 into (4.20) We have the BER expressions

$$\begin{aligned}
P_{BPSK} &= \frac{6}{(\Gamma(m))^4} \sum_{n_1=0}^{\infty} \sum_{n_2=0}^{\infty} \frac{(-1)^{n_1+n_2} \Gamma \left(4m + n_1 + n_2 + \frac{1}{2} \right) 2^{-(4m + n_1 + n_2)}}{n_1! n_2! (m + n_1) (m + n_2) (3m + n_1 + n_2) (4m + n_1 + n_2)} \\
& \times \frac{1}{\sqrt{\pi}} \left(1 + \frac{\bar{\gamma}}{2m} \right)^{-(4m + n_1 + n_2)} {}_2F_1 \left(1, 4m + n_1 + n_2; 3m + n_1 + n_2 + 1; \frac{1}{2} \right) \\
& \times {}_2F_1 \left(4m + n_1 + n_2, \frac{1}{2}; 4m + n_1 + n_2 + 1; \frac{1}{1 + \frac{\bar{\gamma}}{2m}} \right) \tag{4.21}
\end{aligned}$$

for the (4,2;1) TAS/STBC scheme and

$$\begin{aligned}
P_{BPSK} &= \frac{6}{(\Gamma(2m))^4} \sum_{n_1=0}^{\infty} \sum_{n_2=0}^{\infty} \frac{(-1)^{n_1+n_2} \Gamma\left(8m+n_1+n_2+\frac{1}{2}\right) 2^{-(8m+n_1+n_2)}}{n_1! n_2! (2m+n_1)(2m+n_2)(6m+n_1+n_2)(8m+n_1+n_2)} \\
&\quad \times \frac{1}{\sqrt{\pi}} \left(1 + \frac{\bar{\gamma}}{2m}\right)^{-(8m+n_1+n_2)} {}_2F_1\left(1, 8m+n_1+n_2; 6m+n_1+n_2+1; \frac{1}{2}\right) \\
&\quad \times {}_2F_1\left(8m+n_1+n_2, \frac{1}{2}; 8m+n_1+n_2+1; \frac{1}{1+\frac{\bar{\gamma}}{2m}}\right) \tag{4.22}
\end{aligned}$$

for the (4,2;2) TAS/STBC scheme.

For the TAS/STBC scheme with three and four transmit antennas, considering that

$$\lim_{\bar{\gamma} \rightarrow \infty} P_{BPSK} \bar{\gamma}^{mL_t L_r} = \frac{m^{mL_t L_r} \Gamma\left(mL_t L_r + \frac{1}{2}\right)}{\sqrt{\pi} [\Gamma(mL_r + 1)]^{L_t}}, \dots \dots [L_t = 3, 4] \tag{4.23}$$

(4.14) and (4.20) can be approximated as

$$P_{BPSK} = \frac{m^{mL_t L_r} \Gamma\left(mL_t L_r + \frac{1}{2}\right)}{\sqrt{\pi} [\Gamma(mL_r + 1)]^{L_t}} \bar{\gamma}^{-mL_t L_r} + o\left(\bar{\gamma}^{-mL_t L_r}\right), \dots \dots [L_t = 3, 4] \tag{4.24}$$

which clearly shows that the TAS/STBC scheme can achieve a full diversity order of $mL_t L_r$.

For some special cases, we have

$$P_{BPSK} = \frac{m^{3m} \Gamma\left(3m + \frac{1}{2}\right)}{\sqrt{\pi} [\Gamma(m+1)]^3} \bar{\gamma}^{-3m} + o\left(\bar{\gamma}^{-3m}\right) \tag{4.25}$$

for the (3,2;1) TAS/STBC scheme,

$$P_{BPSK} = \frac{m^{6m} \Gamma\left(6m + \frac{1}{2}\right)}{\sqrt{\pi} [\Gamma(2m+1)]^3} \bar{\gamma}^{-6m} + o(\bar{\gamma}^{-6m}) \quad (4.26)$$

for the (3,2;2) TAS/STBC scheme,

$$P_{BPSK} = \frac{m^{4m} \Gamma\left(4m + \frac{1}{2}\right)}{\sqrt{\pi} [\Gamma(m+1)]^4} \bar{\gamma}^{-4m} + o(\bar{\gamma}^{-4m}) \quad (4.27)$$

for the (4,2;1) TAS/STBC scheme,

$$P_{BPSK} = \frac{m^{8m} \Gamma\left(8m + \frac{1}{2}\right)}{\sqrt{\pi} [\Gamma(2m+1)]^4} \bar{\gamma}^{-8m} + o(\bar{\gamma}^{-8m}) \quad (4.28)$$

for the (4,2;2) TAS/STBC scheme.

(4.24) can be written as

$$P_{BPSK} = \frac{m^{mL_t L_r} \Gamma\left(mL_t L_r + \frac{1}{2}\right)}{2\sqrt{\pi} [\Gamma(mL_r + 1)]^{L_t}} \left(2^{mL_t L_r + 1} \bar{\gamma}\right)^{-mL_t L_r} + o(\bar{\gamma}^{-mL_t L_r}), \dots \dots [L_t = 3, 4] \quad (4.29)$$

4.4 Chapter Summary

In this chapter, we derive the exact error rate expression for performance evaluation deriving the exact error rate expression for performance evaluation error performance of the TAS/STBC schemes with three and four transmit antennas over Nakagami-m fading channels, begins by deriving the probability density functions (pdf) of the TAS/STBC scheme. The Gaussian and Marcum Q-functions approach is then applied to obtain the exact and BER expressions for BPSK are given. In Nakagami-m fading channels, the TAS/STBC scheme can achieve the same full diversity order as the RAS/STBC scheme. The numerical results and the performance comparison between the TAS/STBC scheme and the RAS/MRC scheme are shown in this chapter 6.

Chapter 5

Performance of the JAS/STBC Scheme under Nakagami-m Fading Channel

5.1 Introduction

Multi-antenna systems have attracted great attention for the system capacity and error performance enhancements that they provide. Nevertheless, they suffer from hardware and signal processing complexity. Transmit and/or receive antenna selection (TAS and/or RAS) have been suggested to maintain the advantages of multi-antenna systems with lower complexity. By performing the signal transmission and/or reception through a selected antenna subset that maximizes the instantaneous received SNR, full-diversity transmission can be achieved with reduced signal processing complexity [76]-[77].

In chapter 3 we evaluated the numerical performances of a RAS in MIMO/STBC system equipped with L_r antenna at the receiver side. Again in chapter 4 we showed the performance analysis of transmit antenna selection in Alamouti coded MISO systems. In the current chapter we have combined both TAS at the transmitter side and RAS at the receiver side to see the improvement in performance metrics. [90].

Previously, both RAS and TAS have been extensively investigated. In particular, RAS (also known as selection diversity or selection combining) has been researched for several decades and RAS performances in various channel/correlation models have been comprehensively treated. In TAS is analyzed for selecting one antenna at the transmitter. The probability of symbol error rate (SER) and bit error rate (BER) of TAS and RAS is derived in previous chapter 3^{ed} and 4th respectively.

Previous works on antenna selection in Rayleigh MIMO channel have introduced some antenna selection schemes and obtained exact/approximate bit/symbol error rate (BER/SER) performances for binary/ M -ary modulations [76]-[77]. In [76] and [78], authors have provided exact BER results for different antenna selection algorithms with selection diversity transmission (i.e., single TAS)/maximal ratio combining (SDT/MRC) for binary phase shift keying (BPSK). Also, in [79], exact SER performances of systems which use combined SDT and generalized selection combining (GSC) have been examined for M -ary modulations. A pair wise-error probability (PEP)-based analysis of TAS with space-time coding [79] has been given in [80] and [81]. In [81], authors have also carried out the PEP-based SER analysis of joint transmit and receive antenna selection case. [82] has considered a diversity

system with single antenna selection at both transmit and receive ends. Exact BER/SER analyses of TAS/space-time block coding (STBC) systems have been given in [83] and [84]. In [83], the exact SER expressions have been derived for BPSK, binary frequency shift keying (BFSK), M -ary phase shift keying (M -PSK) and M -ary quadrature amplitude modulation (M -QAM) signals with Alamouti coded transmission. [84] has presented the BER analysis of M -PSK signals by generalizing the number of selected transmit antennas. For independent and identically distributed (i.i.d.) Nakagami- m fading, MGF-based SER analysis of SDT/MRC scheme using M -ary modulations has been well investigated in [85] and [86]. Also a more extensive study on the SDT/MRC scheme for independent but non-identically distributed Nakagami- m fading case has been reported in [87].

In this chapter, by using the MGF-based analysis method, exact average BER expressions of joint SDT&SC (i.e., single TAS & single RAS) scheme are derived for BPSK modulations in i.i.d. and flat Nakagami- m MIMO fading channels, which have drawn considerable attention since it is a generic fading model covering both severe and weak fading scenarios via the parameter m [88]. Besides, derivation of upper bounds for BER expressions has paved the way for observing the diversity order of the systems. Our results are not restricted to independent MIMO channels but can also handle arbitrary correlated Rayleigh, Nakagami- m , or Rician fading channels.

4.2 System and Channel Model

We consider a multi-antenna system that has N_t transmit and N_r receive antennas. So we can say that is $N_t \times N_r$ MIMO system. The MIMO channel is assumed to be slow fading. The slow-fading channel gains are available at the receiver. Since receiver knows the channel gains and selects a subset of L_t transmit antennas and L_r receive antennas. The selection information is conveyed to the transmit side via a feedback link. The number of feedback bits required is $\log_2\left[\binom{N_t}{L_t}\right]$. Orthogonal space-time block code (OSTBC) signal matrices are sent over the subset of selected transmit antennas.

Antenna selection for multiple-input–multiple-output (MIMO) Systems a Promising low-complexity technology has received much attention in the Wireless community. One attractive way to reduce the number of RF chains is antenna selection [85, 86, 87, 88]. Systems equipped with this capability optimally choose a subset of the available transmit and

receive antennas and only process the signals associated with them. This allows maximally benefiting from the multiple antennas within given RF complexity and costing constraints.

Let $H = [h_{i,j}]$ be the $N_t \times N_r$ channel matrix. The channel gains between the transmit antenna and the receive antenna are denoted by $h_{i,j}$ for $i=1,2, \dots, N_r$ and $j=1,2, \dots, N_t$ are follow the Nakagami-m fading model.

Let the $L_r \times L_t$ channel matrix after antenna selection be \tilde{H} . The received signals can be expressed by

$$Y = \sqrt{\frac{E_s}{L_t}} \tilde{H}X + N \quad (5.1)$$

Where E_s the energy of the transmitted symbol is, Y is the $L_r \times T$ received signal matrix, X represents the $L_t \times T$ transmitted signal matrix, and T are the block symbol periods. The elements of N are independent identically distributed Gaussian random variables denoted by $CN(0, N_0)$.

Where, N_0 is noise variance.

To maximize the total received signal power for OSTBC transmission, the subset of transmit and receive antennas that yields the largest channel norm should be selected. There are $N = \binom{N_t}{L_t} \binom{N_r}{L_r}$ possible selections of transmit and receive antennas. The j th channel matrix (after antenna selection) out of the N possible antenna subsets, which is denoted as \tilde{H}_j ($1 \leq j \leq N$), is a sub matrix of H formed by selecting certain L_t columns and L_r rows from H . With OSTBC transmission, the maximum-likelihood decoder (with perfect channel information) decomposes the MIMO system to Q independent single-input–single-output (SISO) channels [89]. In the case of the j th antenna subset selection, it can easily be shown that these equivalent SISO channels have the following effective SNR per symbol [90]:

$$\gamma_j = \frac{E_s}{R_s L_t N_0} \|\tilde{H}_j\|_F^2 = \frac{\rho}{R_s L_t} \|\tilde{H}_j\|_F^2 = a \|\tilde{H}_j\|_F^2 \quad (5.2)$$

$J=1, 2, \dots, N$, where, R_s is the symbol rate (in symbol per second), $\rho = E_s/N_0$ is the transmit SNR, and $a = E_s/R_s L_t N_0$. The receive SNR of T-RAS with OSBTC transmission is then equal to

$$\gamma = \max \{\gamma_1, \dots, \gamma_N\} \quad (5.3)$$

Let γ denotes the instantaneous SNR of received output signal. Clearly, selecting the best antenna hence corresponds to selecting the antenna for which this effective SNR is maximized.

For T-RAS with L_r receive selected antenna and L_t transmit selected antenna over Nakgami random variants with fading parameter m and squared mean $\Omega = E[|h_{i,j}|^2]$, where $E[\cdot]$ denote the expectation operator. Therefore, the instantaneous channel gain which can be denoted by $X_{i,j} = |h_{i,j}|^2$, follows a Gamma distribution with probability density function (PDF)

$$p_\gamma(\gamma) = \left(\frac{m}{\Omega}\right)^m \frac{\gamma^{m-1} e^{-\gamma m/\Omega}}{\Gamma(m)}, \gamma \geq 0 \quad (5.4)$$

and with a cumulative distribution function (CDF)

$$P_\gamma(\gamma) = \frac{\gamma(m, \gamma m/\Omega)}{\Gamma(m)}, \gamma \geq 0 \quad (5.5)$$

Where $\Gamma(s) = \int_0^\infty t^{s-1} e^{-t} dt, \text{Re}(s) > 0$, denotes the Gamma function and

$\gamma(s, x) = \int_0^x e^{-t} t^{s-1} dt, \text{Re}(s) > 0$, denotes the incomplete Gamma function. Note that the CDF in

(5.5) can be expressed as

$$P_\gamma(\gamma) = 1 - e^{-\gamma m/\Omega} \sum_{k=0}^{m-1} (\gamma m/\Omega)^k \frac{1}{k!}, \gamma \geq 0 \quad (5.6)$$

for integer values of fading parameter m .

Before every transmission period, antenna selection process determines the transmit antenna and receive antenna pair which will be used for transmission and reception by comparing all combinations of. Simply, using (5.7), indices of transmit and receive antennas are determined in order to maximize the channel gain.

$$\{I_T, I_R\} = \arg \left(\max_{\substack{1 \leq i \leq N_R \\ 1 \leq j \leq N_T}} \{\gamma_{i,j}\} \right) \quad (5.7)$$

We denote the maximum value of $\mathcal{Y}_{i,j}$ by Z , such that the instantaneous received SNR per bit will be $\gamma = \bar{\gamma}Z$, where $\bar{\gamma} = E_s/N_0$ the average SNR. E_s denote the average energy per symbol at the transmitter and N_0 denotes the one sided power spectral density of the additive white Gaussian noise (AWGN) at each receive antenna. With the help of highest order statistics described in [16], the CDF of the output SNR is readily obtained as

$$P_Z(\gamma) = [P_\gamma(\gamma)]^{n_R n_T} \quad (5.8)$$

5.3 Error Performance Analysis of T-RAS/STBC Scheme

In this section, based on the order statistics given in the previous section, the MGF expression of the output SNR is obtained for joint SDT&SC scheme. Then, the average BER analyses have been carried out for BPSK and BFSK modulations.

The received SNR for transmit and receive antennas, selected for transmission and reception, follows a distribution with a CDF given in (5.8). Besides deriving the PDF of the output SNR and using its Laplace transform which will give us the MGF as

$$M_\gamma(s) = \int_0^\infty e^{-s\bar{\gamma}\gamma} f_Z(\gamma) d\gamma \quad (5.9)$$

it is also possible to derive the MGF expression by means of the Laplace transform of the CDF expression. Using the differentiation property of the Laplace transform $L\{f_z(\gamma)\} = s\bar{\gamma}_b L\{F_Z(\gamma)\}$, where $L\{\cdot\}$ denotes the Laplace transform operator, one can easily obtain the MGF as

$$M_\gamma(s) = s\bar{\gamma}_b \int_0^\infty e^{-s\bar{\gamma}_b\gamma} F_Z(\gamma) d\gamma \quad (5.10)$$

Substituting CDF expression in (5.8) into (5.10) results in

$$M_\gamma(s) = s\bar{\gamma}_b \int_0^\infty e^{-s\bar{\gamma}_b\gamma} [F_Z(\gamma)]^{n_R n_T} d\gamma \quad (5.11)$$

By using binomial expansion over the CDF expression in the integrand in (5.11), we obtain the identity

$$[F_Z(\gamma)]^{n_R n_T} = \sum_{p=0}^{n_R n_T} \sum_{k=0}^{p(m-1)} \binom{n_R n_T}{p} (-1)^p \mu_k(p, m) \gamma^k e^{-p\gamma m/\Omega} \quad (5.12)$$

$\mu_k(p, m)$ Denotes the multinomial coefficients given in [91, eq(0.314)]

$$\left(\sum_{k=0}^{m-1} \frac{1}{k!} \left(\frac{m\gamma}{\Omega} \right)^k \right)^p = \sum_{k=0}^{p(m-1)} \mu_k(p, m) \gamma^k \quad (5.13)$$

Where $\mu_0(p, m) = 1$ and $\mu_k(p, m) = \frac{1}{k} \sum_{t=1}^k (t(p+1) - k) (1/t!) (m/\Omega)^t \mu_{k-t}(p, m)$, $k \geq 1$.

Then, the MGF expression of the output SNR in (5.11) can be derived as

$$[F_Z(\gamma)]^{n_R n_T} = \sum_{p=0}^{n_R n_T} \sum_{k=0}^{p(m-1)} \binom{n_R n_T}{p} (-1)^p \mu_k(p, m) \Gamma(k+1) (s\bar{\gamma}_b) \left(s\bar{\gamma}_b + \frac{mp}{\Omega} \right)^{-k-1} \quad (5.14)$$

Since we obtained the MGF expression of output SNR, the derivation of exact BER expressions of BPSK modulations is straightforward. The average BER of BPSK has been defined as a function of MGF expression as [93]

$$p_b(e) = \frac{1}{\pi} \int_0^{\pi/2} M_\gamma \left(\frac{\lambda}{\sin^2 \phi} \right) d\phi \quad (5.15)$$

Where $\lambda = 1$ for BPSK and $\lambda = 0.5$ for BFSK substituting the MGF in (5.14) into (5.15) results in

$$p_b(e) = \frac{1}{\pi} \sum_{p=0}^{n_R n_T} \sum_{k=0}^{p(m-1)} \binom{n_R n_T}{p} (-1)^p \mu_k(p, m) \Gamma(k+1) \int_0^{\pi/2} M_\gamma \left(\frac{\lambda \bar{\gamma}_b}{\sin^2 \phi} \right) \left(\frac{\lambda \bar{\gamma}_b}{\sin^2 \phi} + \frac{mp}{\Omega} \right)^{-k-1} d\phi \quad (5.16)$$

By making the change of variable $t = \sin^2 \phi$ in the integral in (5.16) and using the definition of Appell hyper geometric function given in [17, eq.(3.211)], the exact average BER of BPSK and BFSK signals for the joint SDT&SC scheme in Nakagami- fading channel can be easily obtained as

$$p_b(e) = \frac{1}{\pi} \sum_{p=0}^{n_R n_T} \sum_{k=0}^{p(m-1)} \binom{n_R n_T}{p} (-1)^p \mu_k(p, m) (\lambda \bar{\gamma}_b)^{-k} \frac{\Gamma(b_2) \Gamma(a)}{\Gamma(c)} F_1(a, b_1, b_2; c; 1, -\nu) \quad (5.17)$$

Where the parameters are $a \triangleq k + 0.5$, $b_1 \triangleq 0.5$, $b_2 \triangleq 0.5$, $c \triangleq k + 1.5$, and $\nu \triangleq (mp/\Omega) / \lambda \bar{\gamma}_b$.

Note that F_1 can be easily calculated by using well known software programs such as MATHEMATICA and MAPLE.

Since, exact BER expression in (5.17) does not help much about the observation of the diversity orders obtained by joint SDT&SC scheme, we derive upper bound expressions for the error probabilities which will give us the diversity orders of the systems clearly. We use the high-SNR approximation technique suggested in [93] in order to obtain upper bound expressions for error probabilities of BPSK/BFSK.

The relation between the asymptotic error performance of a system and the behavior of PDF of the output SNR has been well investigated in [93]. One can express the error performance of a modulation technique that has a conditional error probability (CEP) of $Q(\sqrt{k\bar{\gamma}_b})$ as

$$P_E = \frac{2^t a \Gamma(t+1.5)}{\sqrt{\pi}(t+1)} (k\bar{\gamma}_b)^{-(t+1)} + o(\bar{\gamma}_b^{-(t+1)}) \quad (5.18)$$

if it is possible to express the PDF of the output SNR in the form $f_Z(\gamma) = a\gamma^t + o(\gamma^t)$, $a > 0$. The PDF of the output SNR can be obtained easily by differentiating the CDF of the output SNR in (5.8) as

$$f_Z(\gamma) = n_T n_R f(\gamma) [F(\gamma)]^{n_T n_R - 1} \quad (5.19)$$

Then, by using (2) and the series representation of the incomplete Gamma function given in [17, eq.(8.354.1)], (5.19) can be expressed as

$$f_Z(\gamma) = \left(\frac{m}{\Omega}\right)^{mn_T n_R - 1} \frac{mn_T n_R}{\Gamma(m+1)^{n_T n_R}} \gamma^{mn_T n_R - 1} + o(\gamma^{mn_T n_R - 1}) \quad (5.20)$$

So, for joint SDT&SC scheme the parameters are found as $a = (m/\Omega)^{mn_T n_R} mn_T n_R / \Gamma(m+1)^{n_T n_R}$ and $t = mn_T n_R - 1$, after some manipulations as in [89]. Therefore, (18) can be rewritten as

$$P_E = \left(\frac{2m}{\Omega k}\right)^{mn_T n_R} \frac{\Gamma(mn_T n_R + 0.5)}{2\sqrt{\pi}\Gamma(m+1)^{mn_T n_R}} + o(\gamma^{-mn_T n_R}) \quad (5.21)$$

for any modulation technique whose CEP can be described as the linear combination of $Q(\sqrt{k\bar{\gamma}_b})$. For BPSK modulations, $k = 2\lambda$, where is as described before. So, for BPSK modulations, the asymptotic BER performances can be directly obtained as

$$p_b(e) = \left(\frac{2m}{\Omega k \bar{\gamma}_b}\right)^{mn_T n_R} \frac{\Gamma(mn_T n_R + 0.5)}{2\sqrt{\pi}\Gamma(m+1)^{mn_T n_R}} + o(\gamma^{mn_T n_R - 1}) \quad (5.22)$$

Upper bound expression for BPSK/BFSK modulations given in (5.22) show that the joint SDT&SC schemes achieve full diversity order of $mn_T n_R$.

5.4 Chapter Summary

In this chapter, we have derived exact MGF and BER performance results of multiple-input multiple-output (MIMO) systems employing both transmit and receive

antenna selection (TAS/RAS) for BPSK modulations in Nakagami- m fading. Exact bit error rate (BER) expression for binary phase shift keying (BPSK) and binary frequency shift keying (BFSK) modulations are derived by using the moment generating function (MGF)-based analysis method. In this analysis, the transmit-receive link that maximizes the instantaneous received signal-to-noise ratio (SNR) is selected for transmission and reception. We also derive, the upper bounds for exact expressions we have shown that the systems achieve full diversity order, which is the product of the number of transmit antennas, the number of receive antennas and the fading parameter and also shown in exact and upper bounded BER expressions in (5.19) and (5.22), respectively.

Simulation Result and Discussion

In this chapter, we show the selected graphical result to present the error performance of the last three different antenna selection techniques i.e. transmit, receive and joint antenna selection with vary number of antenna at transmitter and receiver side in BPSK modulation under the Rayleigh channel which is the special case of Nakagani channel where $m=1$. In this chapter, we also show the most important differences in terms of performance for their respective antenna selection scheme.

Fig.6.1 plots capacity Vs n_T and n_R which shows the MIMO (multiple-input and multiple-output) system can improve the performance of wireless System in terms of capacity and rate without extra allocation of extra spectrum. MIMO can be used to increase data rate through multiplexing or to improve performance through diversity.

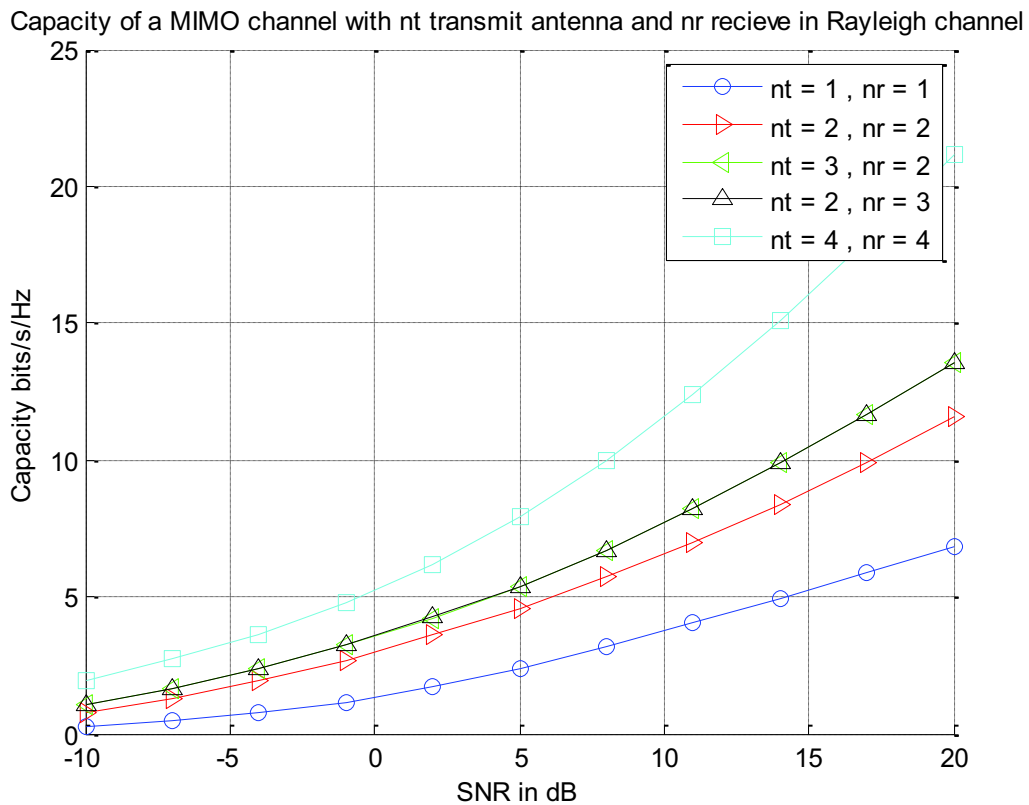


Figure 6.1. MIMO channel capacity with n_T and n_R antenna in Rayleigh channel ($m=1$)

Fig 6.2 shows the MATLAB simulation of bit error probability (BER) of BPSK modulation. In ideal channel, but practically channel is not ideal due to propagation delay error introduces in the system. This curve depicted that over theory and simulation result are exactly same in ideal case.

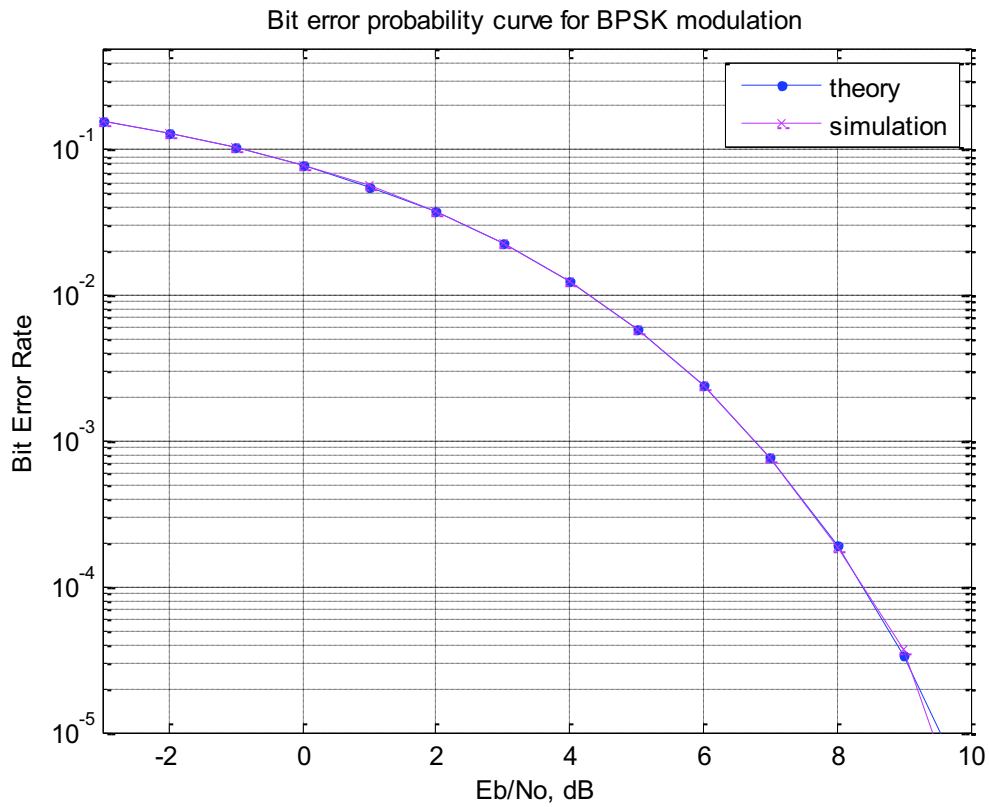


Figure 6.2 Bit error probability of BPSK modulation

After using the channel coding with STC Alamouti code, we get the better performance in the wireless system as clearly shown in fig.6.3 of MATLAB simulated graph. The performance enhance is due to STC schemes combine the channel code design and the use of multiple transmit antennas. By this the encoded data is split into n_T streams that are simultaneously transmitted using n_T transmit antennas. The received signal is a linear superposition of these simultaneous transmitted symbols corrupted by noise and channel-induced ISI. Space-time decoding algorithms as well as channel estimation techniques are incorporated at the receiver in order to achieve both diversity advantages and coding gain.

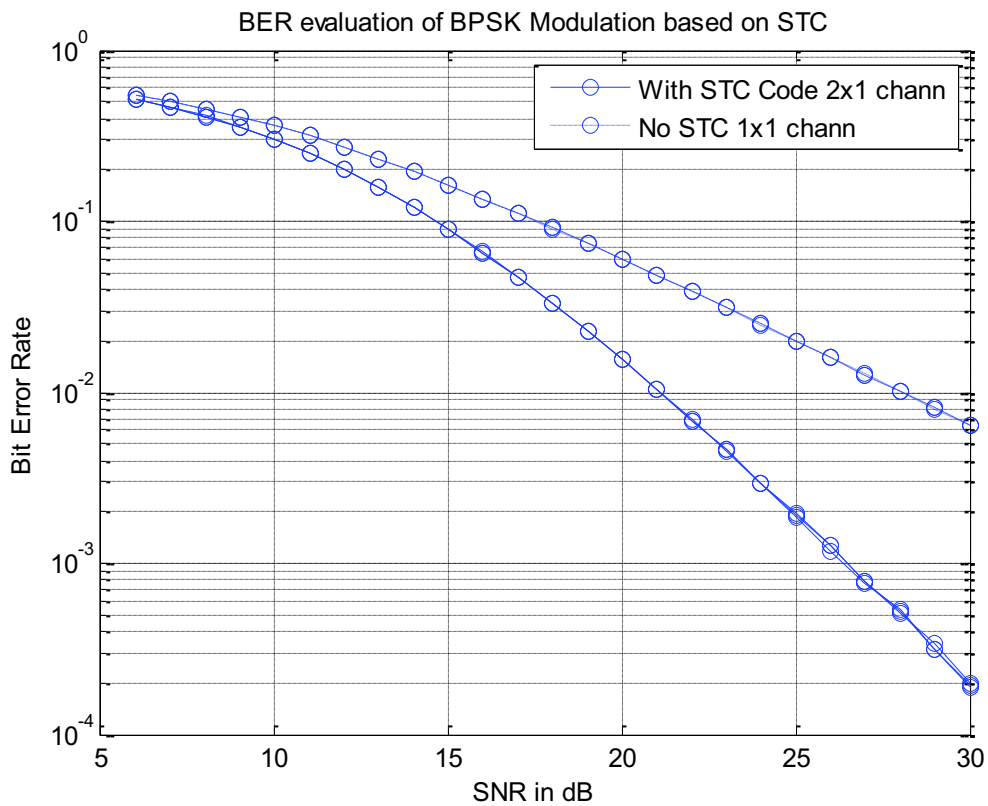


Figure 6.3.Improvement of SNR Vs BER using MIMO/STC code in Rayleigh Channel (m=1)

The performance analysis of receive antenna selection shows by the fig.6.4 and fig.6.5. Here fig.6.4 depicted how the SNR will improve according to number of selected receive antenna.

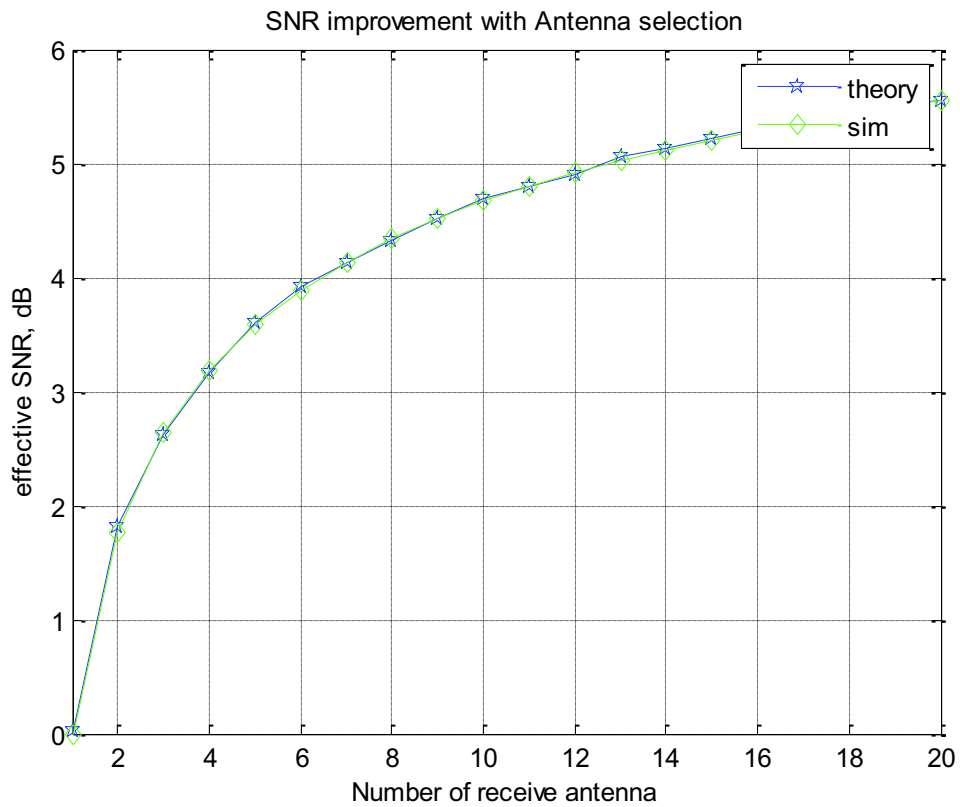


Figure 6.4 Improvement of SNR in MIMO/STBC system with n_R selected antenna in Rayleigh channel ($m=1$)

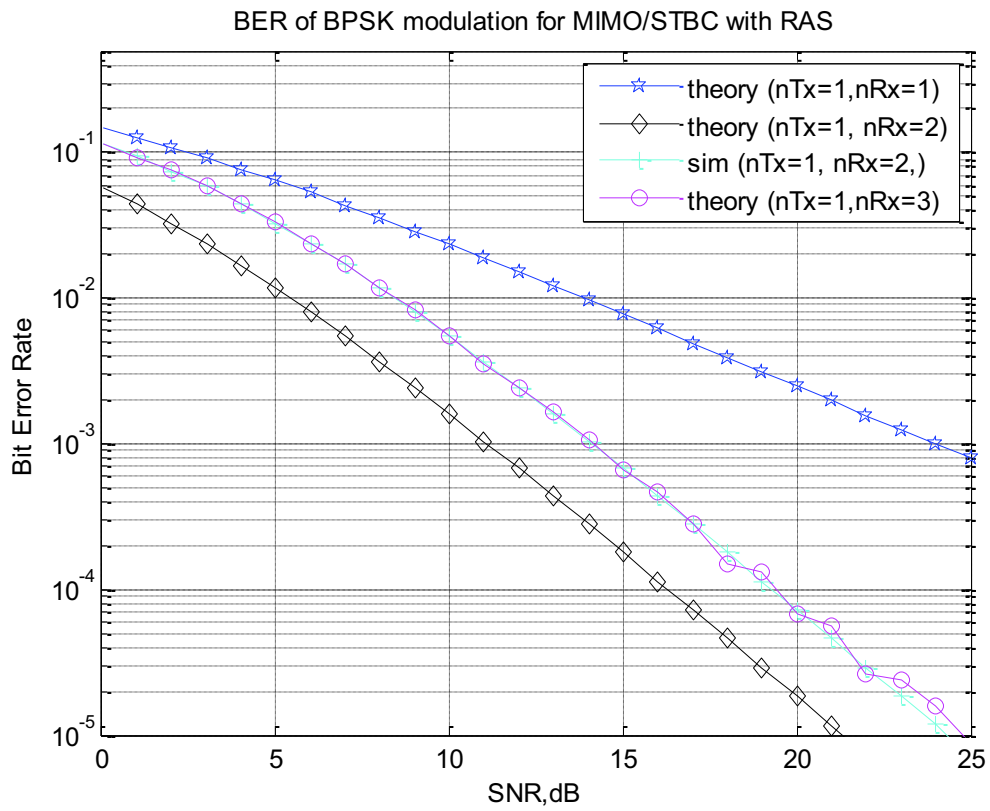


Figure 6.5 SNR Vs BER curve in MIMO/STBC system with RAS in Rayleigh channel ($m=1$)

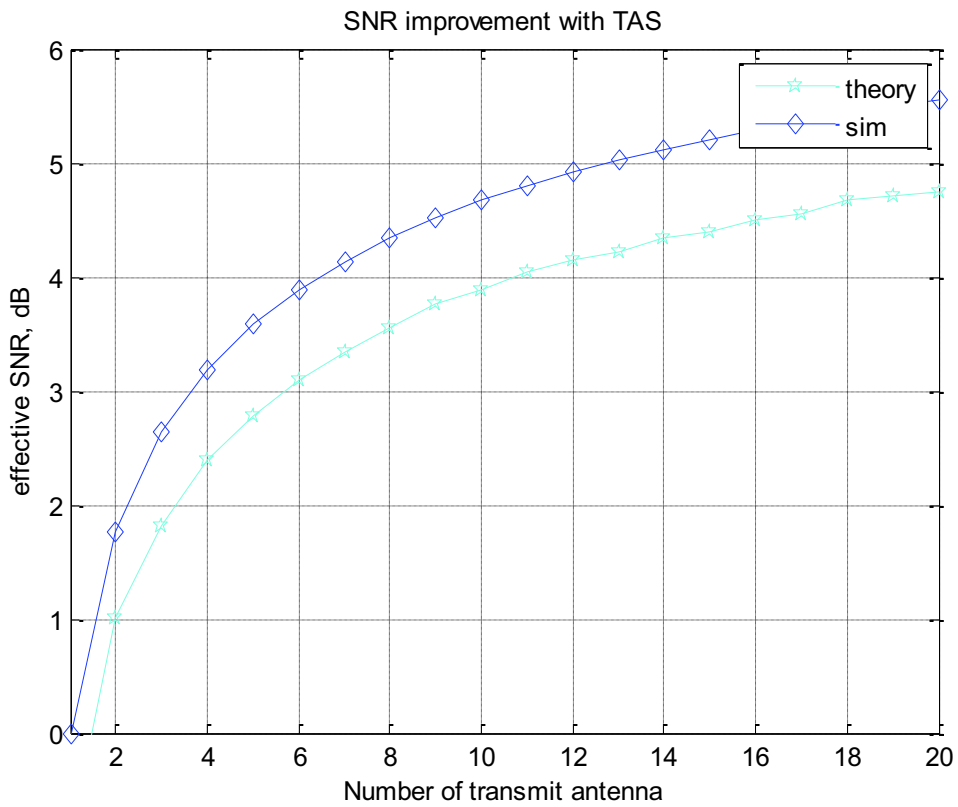


Figure 6.6. Improvement of SNR in MIMO/STBC system with n_T selected antenna in Rayleigh channel ($m=1$)

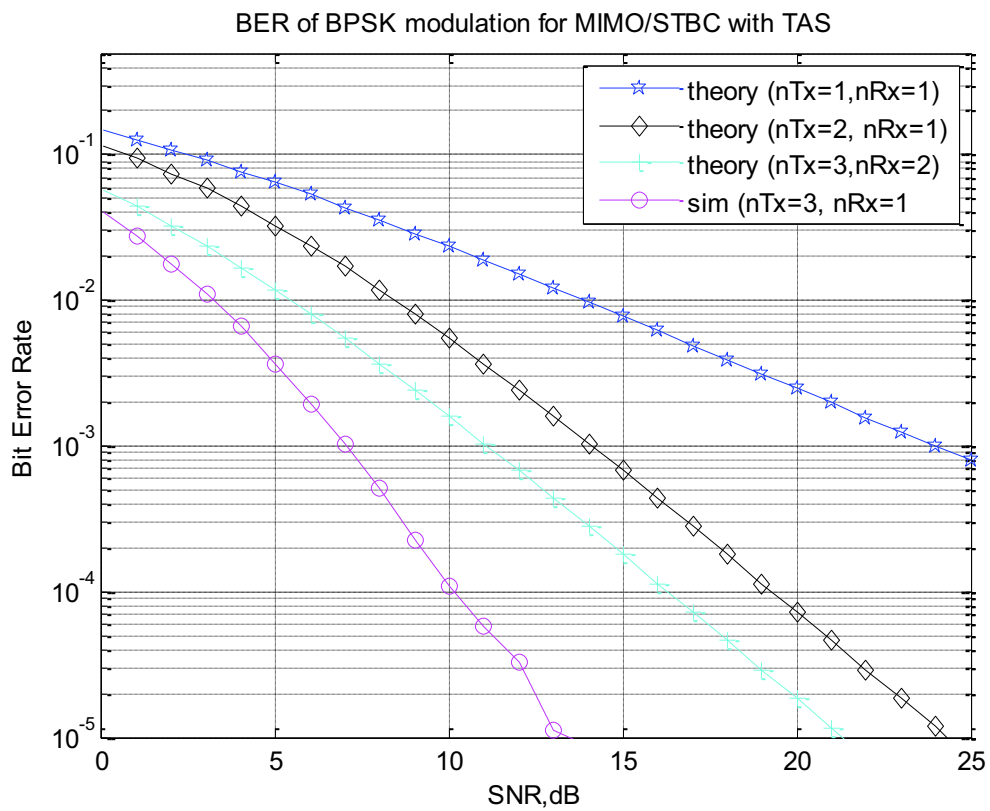


Figure 6.7 SNR Vs BER curve in MIMO/STBC system with TAS in Rayleigh channel ($m=1$)

Fig.6.7 depicts the four possible choices for joint transmit and receive antenna selection. The plot predicts that as the number of transmit and receive antenna selection increase we got a better SNR Vs BER. Clearly, statistical selection can significantly enhance performance 1.5-2 dB. In general, these gains will vary depending on the exact structure of antennas.

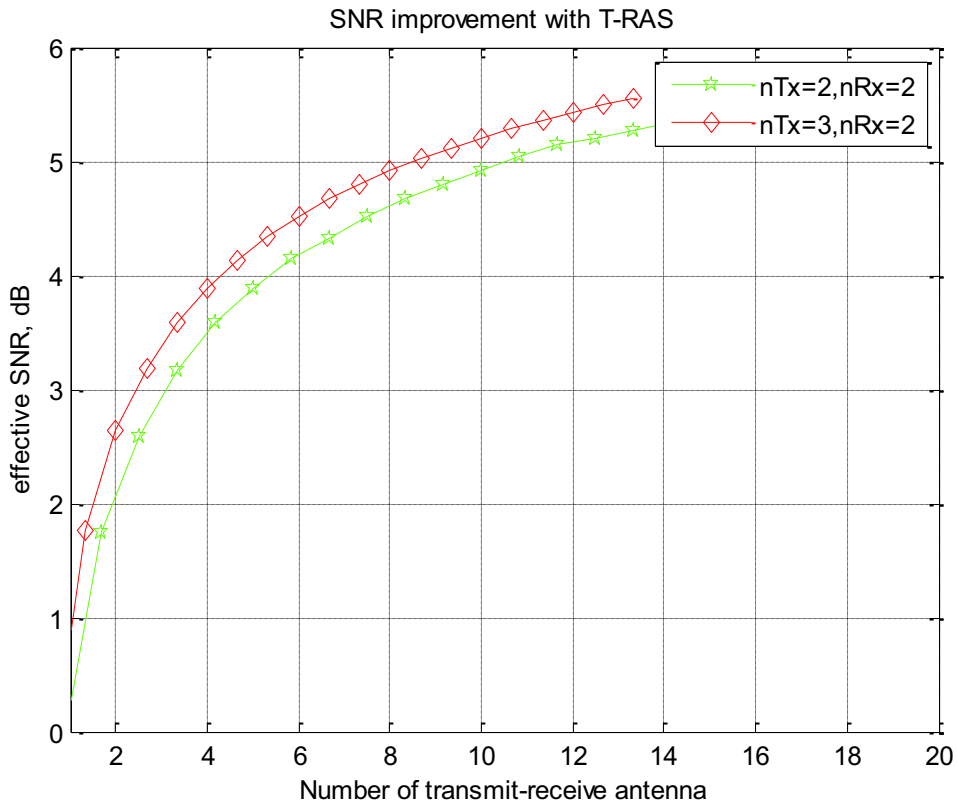


Figure 6.8 Improvement of SNR in MIMO/STBC system with n_R and n_T selected antenna in Rayleigh channel ($m=1$)

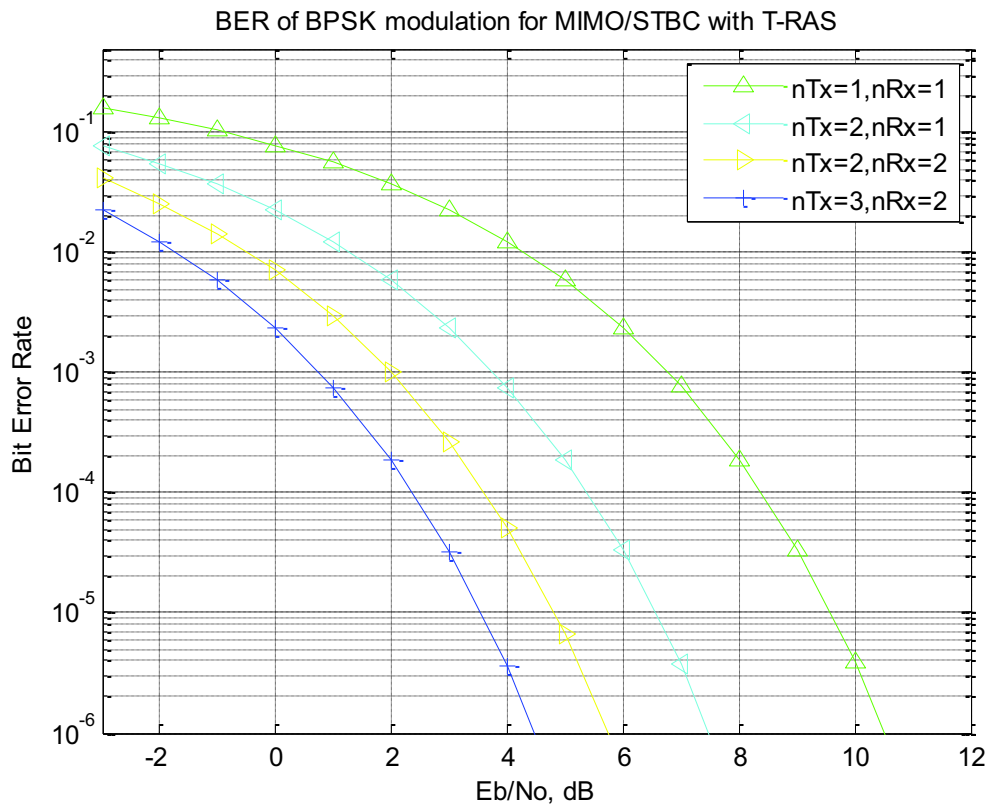


Figure 6.9 SNR Vs BER curve in MIMO/STBC system with T-RAS in Rayleigh channel (m=1)

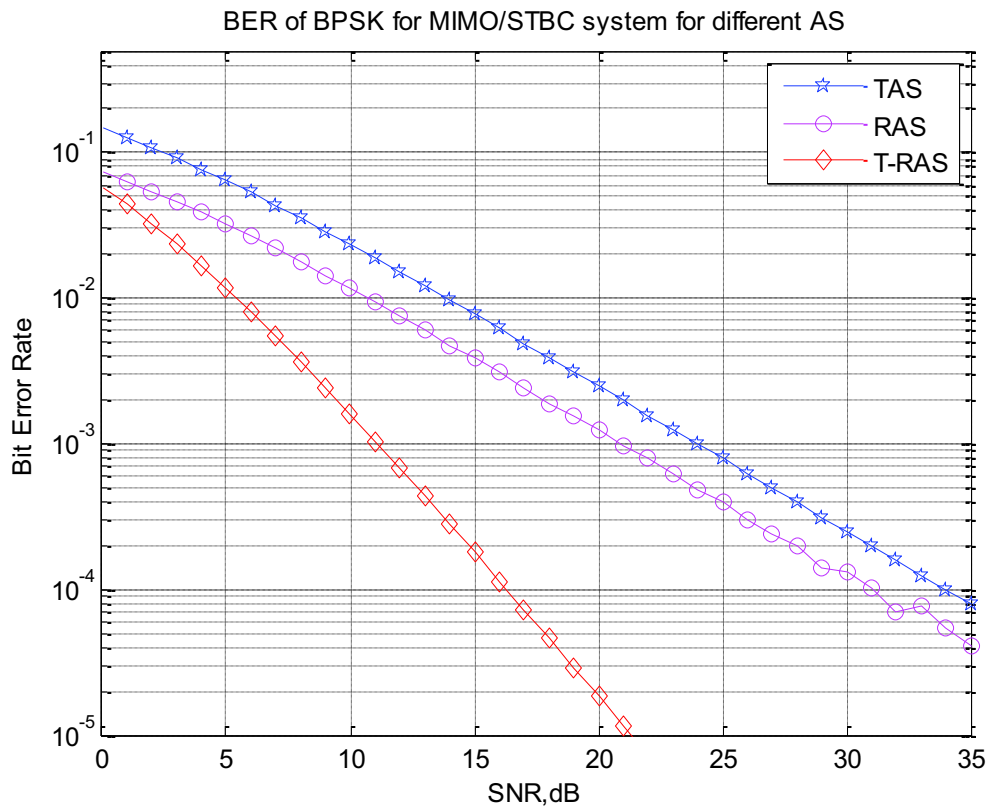


Figure 6.10 SNR Vs BER curve in MIMO/STBC system with all three possible AS in Rayleigh channel ($m=1$)

Conclusion and Future Scope

7.1 Conclusion

This thesis has investigated two MIMO schemes combining maximal-ratio combining and space-time codes with transmit antenna selection for reliable wireless data transmissions over Nakagami-m fading channels. The system model of each scheme was detailed and the error performance was analyzed. Based on the MGF-based and Gaussian Q-functions approaches, the exact expressions for the RAS, TAS and JAS scheme were derived.

Chapter 1 presented the brief introduction of MIMO systems and a challenging issue which was reliable wireless transmission in harsh propagation environments. The antenna selection techniques were used to reduce the implementation costs of MIMO systems. Diversity techniques that are effective approaches to combat the effect of multiple fading were introduced in this chapter. The Alamouti scheme that used two transmit antennas and a simple linear processing to achieve a full diversity order was reviewed as well. This chapter also introduced the research methodology including the MGF-based and Gaussian Q-functions error performance evaluation approaches.

Chapter 2 reviewed the fundamental background materials related to this thesis. Brief introductions of digital communication systems, MIMO systems model and antenna selection techniques were presented. Digital modulations, fading channels, diversity combining techniques, Alamouti scheme and space-time block codes were reviewed. Diversity and coding gain that are the most important parameters quantifying the error performance of a MIMO system were also shown in this chapter.

Chapter 3 analyzed an RAS scheme in which system select an antenna that maximize the received signal SNR over Nakagami-m fading channels. For both Nakagami-m fading channels with arbitrary and integer fading parameters m , the exact BER expressions for BPSK and SER expressions for BPSK modulations were derived by using the MGF-based approach. From the asymptotic BER and SER expressions obtained, it can be shown that the RAS scheme can achieve a full diversity order which is equal to the product of three parameters: the Nakagami fading parameter m , the number of transmits antennas and the number of receive antennas. The numerical results of the RAS scheme with different transmit

and receive antennas over Nakagami- m fading channels with different values of m were presented. The analytical results were verified by the simulation results of chapter 6.

For the RAS scheme, no transmit diversity will be achieved if the feedback link fails. Therefore, a scheme which provides reasonable protection in the case of feedback failure was developed. Chapter 4 presented a scheme in which space-time block codes is combined with transmit antenna selection. In the TAS scheme, two antennas are selected out of all the available transmit antennas. The exact and asymptotic BER expressions for BPSK of the TAS scheme with three and four transmit antennas over Nakagami- m fading channels were derived. It was explicitly shown that the TAS scheme achieves a full diversity order. We also presented the comparison between the RAS scheme and the TAS scheme. That shows the RAS scheme achieved better error performance than the RAS scheme with the same transmit and receive antennas. All the theoretical analysis was verified by simulation results of chapter 6.

Similarly in chapter 6 we have derived exact MGF and BER performance results of joint RAS /TAS scheme for BPSK modulations in Nakagami- m fading channels. Also, by deriving upper bounds for exact expressions we have shown that the systems achieve full diversity order, which is the product of the number of transmit antennas, the number of receive antennas and the fading parameter. As indicated in Fig. 6.2 and Fig. 6.3, the BER performances of diversity schemes can easily achieve great improvements due to higher diversity orders yielded by the increase in the number of available transmit and/or receive antennas in joint AS scheme. For a moderate BER level of $10^{-3}E_b/N_0$ [dB] , the increase in the total number of antennas at transmit and receive ends up to 5 yields SNR gains up to 19 dB as shown in Fig.6.3. Simply, the numbers of transmit antennas and receive antennas which give the same product, provides the same diversity order. Since both sides select only a single antenna, the same diversity order provided by any combination of and at joint AS scheme, corresponds to exactly the same BER performance.

7.2 Future Scope

We conclude with some brief remarks on future extensions of the work presented in this thesis. Future scope can be done on different fields associated with the work discussed in this thesis as:

1. Performance analysis of the systems considering different propagation environments, i.e. changing the wireless channel from Rayleigh to Nakagami-m and Rician fading channels where correlation between the fading coefficients still exist .
2. AS will be tested for other modulation types, such as QAM, FSK, and DPSK.
3. As Alamouti's transmit diversity provides solely a diversity gain, whereas STTC gives both diversity gain and coding gain so it is interesting to analyze the performance of systems employing space-time Trellis code (STTC) at the transmitter.
4. Performance analysis of a system incorporating delay in between transmitter and receiver.

Reference

- [1] I. E. Telatar, "Capacity of multi-antenna Gaussian channels," *Europ. Trans. Telecommun.*, vol. 10, no. 6, pp. 585–595, Nov./Dec. 1999.
- [2] G. J. Foschini and M. J. Gans, "On limits of wireless communications in a fading environment when using multiple antennas," *Wireless Pers. Commun.*, vol. 6, no. 3, pp. 311–335, Mar. 1998.
- [3] J. H. Winters, "On the capacity of radio communication systems with diversity in a Rayleigh fading environment," *IEEE J. Select. Areas Communication*, vol. 5, pp. 871–878, June 1987.
- [4] G. J. Foschini, "Layered space-time architecture for wireless communication in a fading environment when using multi-element antennas," *Bell Labs Tech. J.*, vol. 1, no. 2, pp. 41–59, Autumn 1996.
- [5] Winters, "The Diversity Gain of Transmit Diversity in Wireless Systems with Rayleigh Fading," *IEEE Transactions on Vehicular Technology*, Volume: 47, Issue: 1, Pages: 119 - 123, Feb. 1998.
- [6] V. Tarokh, N. Seshadri and A.R. Calderbank, "Space-Time Codes for High Data Rate Wireless Communication: Performance Criterion and Code Construction," *IEEE Transactions on Information Theory*, Volume: 44, Issue: 2, Pages: 744 - 765, March 1998.
- [7] Gesbert, M. Shafi, Da-shan Shiu, P.J. Smith and A. Naguib, "From Theory to Practice: An overview of MIMO Space-Time Coded Wireless Systems," *IEEE Journal on Selected Areas in Communications*, Volume: 21, Issue: 3, Pages: 281 - 302, April 2003.
- [8] Y. Chen and C. Tellambura, "Performance analysis of three-branch selection combining over arbitrarily correlated rayleigh-fading channels," *IEEE Trans. Communication*, vol. 4, no. 3, pp. 861–865, May 2005.
- [9] Annamalai, K. Gautam, and C. Tellambura, "Theoretical diversity improvement in GSC(N,L) receiver with nonidentical fading statistics," *IEEE Trans. Communication*, vol. 53, pp. 1027–1035, June 2005

- [10] G. Karagiannidis, "Performance analysis of SIR-based dual selection diversity over correlated Nakagami-m fading channels," *IEEE Trans. Veh. Technol.*, vol. 52, no. 5, pp.1207 – 1216, Sept. 2003.
- [11] N. Sagias, G. Karagiannidis, D. Zogas, P. Mathiopoulos, and G. Tombras, "Performance analysis of dual selection diversity in correlated Weibull fading channels," *IEEE Trans. Commun.*, vol. 52, no. 7, pp. 1063 – 1067, July 2004
- [12] S. Thoen, L. Van der Perre, B. Gyselinckx, and M. Engels, "Performance analysis of combined transmit-SC/receive-MRC," *IEEE Trans. Commun.*, vol. 49, no. 1, pp. 5 – 8, Jan. 2001
- [13] D. Love, "On the probability of error of antenna-subset selection with space-time block codes," *IEEE Trans. Commun.*, vol. 53, pp. 1799 –1803, Nov. 2005
- [14] D. Gore and A. Paulraj, "MIMO antenna subset selection with space time coding," *IEEE Trans. Signal Processing*, vol. 50, no. 10, pp. 2580– 2588, Oct. 2002
- [15] Z. Chen, J. Yuan, B. Vucetic, and Z. Zhou, "Performance of Alamouti scheme with transmit antenna selection," *Electron. Lett.*, vol. 39, no. 23, pp. 1666–1668, Nov. 2003.
- [16] Z. Chen, B. Vucetic, J. Yuan, and Z. Zhou, "Performance of Alamouti scheme with transmit antenna selection," in *Proc. IEEE PIMRC'04*, vol. 2, Barcelona, Spain, Sept. 2004, pp. 1135–1141.
- [17] M. Nakagami, "The m-distribution, a general formula of intensity distribution of rapid fading," in *Statistical Methods in Radio Wave Propagation*, W. G. Hoffman, Ed. Pergamon Press, 1960, pp. 3–36.
- [18] H. Suzuki, "A statistical model for urban radio propagation," *IEEE Trans. Commun.*, vol. 25, pp. 673–680, July 1977.
- [19] M. K. Simon and M.-S. Alouini, "A unified approach to the performance analysis of digital communications over generalized fading channels," *Proc. IEEE*, vol. 86, pp. 1860–1877, Sept. 1998.
- [20] H. Exton, "Multiple Hypergeometrical Functions and Applications". *Sussex, England: Ellis Horwood*, 1976.

- [21] Z. Wang and G. B. Giannakis, "A simple and general parameterization quantifying performance in fading channels," *IEEE Trans. Commun.*, vol. 51, no. 8, pp. 1389–1398, Aug. 2003.
- [22] M.S.Alouini and M. K. Simon, "Performance of coherent receivers with hybrid SC/MRC over Nakagami-m fading channels," *IEEE Trans. Veh. Technol.*, vol. 48, pp. 1155–1164, July 1999.
- [25] C. E. Shannon, "A mathematical theory of communication," *BellSyst. Tech. J.*, vol. 27, pp. 379–423, July 1948.
- [26] J. G. Proakis, *Digital Communications*, 3rd ed. McGraw-Hill, 1995.
- [27] A.Goldsmith, *Wireless communications*, 1st ed. Cambridge University Press, August 2005.
- [28] S. G. Wilson, *Digital Modulation and Coding*. Prentice Hall, August 1995.
- [29] B. Vucetic and J. Yuan, *Space-time Coding*. John Wiley & Sons, 2003.
- [30] J. B. Andersen, "Antenna arrays in mobile communications: gain, diversity, and channel capacity," *IEEE Antennas Propagat. Mag.*, vol. 42, pp. 12–16, Apr. 2000.
- [31] S. Sanayei and A. Nosratinia, "Antenna selection in MIMO systems," *IEEE Commun. Mag.*, vol. 42, pp. 68–73, Oct. 2004
- [32] M. K. Simon and M.-S. Alouini, *Digital Communication over Fading Channels: A Unified Approach to Performance Analysis*. New York: John Wiley & Sons, 2000.
- [33] J. Doble, *Introduction to radio propagation for fixed and Mobile Communications*. Artech House, Boston, 1996.
- [34] Y. Zhang and M. Fujise, "Performance analysis of wireless networks over Rayleigh fading channel," *IEEE Trans. Commun.*, vol. 55, pp. 1621–1632, Sept. 2006.
- [35] J. Wang, M. K. Simon, M. P. Fitz, and K. Yao, "On the performance of space-time codes over spatially correlated Rayleigh fading channels," *IEEE Trans. Commun.*, vol. 52, pp. 877–881, June 2004.
- [36] P. A. Dighe, R. K. Mallik, and S. S. Jamuar, "Analysis of transmit-receive diversity in Rayleigh fading," *IEEE Trans. Commun.*, vol. 51, pp. 694–703, Apr. 2003.
- [37] J. Yuan, Z. Chen, B. Vucetic, and W. Firmanto, "Performance and design of spacetime coding in fading channels," *IEEE Trans. Commun.*, vol. 51, pp. 1991–1996, Dec. 2003.

- [38] Z. Chen, J. Yuan, and B. Vucetic, "Improved space-time trellis coded modulation scheme on slow Rayleigh fading channels," *Electron. Lett.*, vol. 51, pp. 440–441, Mar. 2001.
- [39] [50] Z. Chen, B. Vucetic, J. Yuan, and Z. Zhou, "Performance analysis of space-time trellis codes with transmit antenna selection in Rayleigh fading channels," in *Proc. IEEE WCNC'04*, Atlanta, GA, Mar. 2004.
- [40] D. Chizhik, J. Ling, P. W. Wolniansky, R. A. Valenzuela, N. Costa, and K. Huber, "Multiple-input-multiple-output measurements and modeling in Manhattan," *IEEE J. Select. Areas Commun.*, vol. 21, pp. 321–331, April 2003.
- [41] [41] J. B. Andersen, "Antenna arrays in mobile communications: gain, diversity, and channel capacity," *IEEE Antennas Propagat. Mag.*, vol. 42, pp. 12–16, Apr. 2000
- [42] [52] U. Charash, "Reception through Nakagami fading multipath channels with random delays," *IEEE Trans. Commun.*, vol. 27, pp. 657–670, Apr. 1979.
- [43] [53] Y. Ma and C. C. Chai, "Unified error probability analysis for generalized selection combining in Nakagami fading channels," *IEEE J. Select. Areas Commun.*, vol. 18, pp. 2198–2210, Nov. 2000.
- [44] [54] L. L. Yang and L. Hanzo, "Performance of generalized multicarrier multicarrier DSCDMA over Nakagami-m fading channels," *IEEE Trans. Commun.*, vol. 50, pp. 956–966, June 2002.
- [45] G. Femenias, "BER performance of linear STBC from orthogonal designs over MIMO correlated Nakagami-m fading channels," *IEEE Trans. Veh. Technol.*, vol. 53, pp. 307–317, Mar. 2004.
- [46] G. Efthymoglou and V. Aalo, "Performance of RAKE receivers in Nakagami fading channel with arbitrary fading parameters," *Electron. Lett.*, vol. 31, p. 16101612, Aug. 1995.
- [47] G. Efthymoglou, V. Aalo, and H. Helmken, "Performance analysis of coherent DSCDMA systems in a Nakagami fading channel with arbitrary parameters," *IEEE Trans. Veh. Technol.*, vol. 46, pp. 289–297, May 1997.
- [48] T. Eng and L. B. Milstein, "Coherent DS-CDMA performance in Nakagami-fading environment," *IEEE Trans. Commun.*, vol. 43, pp. 1134–1143, Feb./Mar./Apr. 1995.

- [50] D. G. Brennan, "Linear diversity combining techniques," *Proc. IRE*, vol. 47, pp. 1075–1102, June 1959.
- [49] N. C. Beaulieu and C. Cheng, "Efficient Nakagami-m fading channel simulation," *IEEE Trans. Veh. Technol.*, vol. 54, no. 2, pp. 413–424, Mar. 2005.
- [51] J. D. Gibson, Ed., *The Mobile Communications Handbook*, 1st ed. CRC Press, 1996.
- [52] [61] V. A. Aalo, "Performance of maximal-ratio diversity systems in a correlated Nakagami-fading environment," *IEEE Trans. Commun.*, vol. 43, pp. 2360–2369, Aug. 1995.
- [62] V. A. Aalo, T. Piboongunon, and G. Efthymoglou, "Another look at the performance of MRC schemes in Nakagami-m fading channels with arbitrary parameters," *IEEE Trans. Commun.*, vol. 53, pp. 2002–2005, Dec. 2005.
- [63] Y. Ma, R. Schober, and S. Pasupathy, "Effect of channel estimation errors on MRC diversity in Rician fading channels," *IEEE Trans. Veh. Technol.*, vol. 54, pp. 2137–2142, Nov. 2005.
- [64] A. Shah and A. M. Haimovich, "Performance analysis of maximal ratio combining and comparison with optimum combining for mobile radio communications with cochannel interference," *IEEE Trans. Veh. Technol.*, vol. 49, pp. 1454–1463, July 2000.
- [65] Q. T. Zhang, "Maximal-ratio combining over Nakagami fading channels with an arbitrary branch covariance matrix," *IEEE Trans. Veh. Technol.*, vol. 48, pp. 1141–1150, July 1999.
- [53] S. Million, B. Shah, and S. Hinedi, "Comparison of two maximal ratio combining techniques in antenna arraying," *IEEE Trans. Commun.*, vol. 44, pp. 1599–1609, Nov. 1996.
- [53] X. Qi, M. S. Alouini, and Y. C. Ko, "Closed-form analysis of dual-diversity equalgain combining over Rayleigh fading channels," *IEEE Trans. Wireless Commun.*, vol. 2, pp. 1120–1125, Nov. 2003.
- [54] M. S. Alouini and M. K. Simon, "Performance analysis of coherent equal gain combining over Nakagami-m fading channels," *IEEE Trans. Veh. Technol.*, vol. 50, pp. 1449–1463, Nov. 2001.

- [54] L. Zheng and D. N. C. Tse, "Diversity and multiplexing: A fundamental tradeoff in multiple-antenna channels," *IEEE Trans. Inform. Theory*, vol. 49, no. 5, pp. 1073–1096, May 2003.
- [55] [74] V. Tarokh, N. Seshadri, and A. R. Calderbank, "Space-time codes for high data rate wireless communication: Performance criterion and code construction," *IEEE Trans. Inform. Theory*, vol. 44, pp. 744–765, Mar. 1998.
- [56] S. M. Alamouti, "A simple transmit diversity technique for wireless communications," *IEEE J. Select. Areas Commun.*, vol. 16, no. 8, pp. 1451–1458, Oct. 1998.
- [57] V. Tarokh, H. Jafarkhani, and A. R. Calderbank, "Space-time block codes from orthogonal designs," *IEEE Trans. Inform. Theory*, vol. 45, no. 5, pp. 1456–1467, July 1999
- [58] V. Tarokh, H. Jafarkhani, and A. R. Calderbank, "The application of orthogonal designs to wireless communication," in Proc. IEEE Information Theory Workshop, Killarney, Ireland, June 1998, pp. 46–47.
- [59] "Space-time codes for high data rate wireless communication: Performance criteria in the presence of channel estimation errors, mobility, and multiple paths,"
- [60] "Space-time block coding for wireless communications: performance results," *IEEE J. Select. Areas Commun.*, vol. 17, no. 3, pp. 451–460, Mar. 1999.
- [61] A.F.Molisch and M. Z. Win, "MIMO systems with antenna selection," *IEEE Microwave Mag.*, vol. 5, pp. 46-56, Mar. 2004.
- [62] M. Gharavi-Alkhansari and A. B. Gershman, "Fast antenna subset selection in MIMO systems," *IEEE Trans. Signal Processing*, vol. 52, pp. 339-346, Feb. 2004.
- [63] A. Gorokhov, D. A. Gore, and A. Paulraj, "Receive antenna selection for MIMO spatial multiplexing: theory and algorithms," *IEEE Trans. Signal Processing*, vol. 51, pp. 2796-2807, Nov. 2003.
- [64] D. J. Love, "On the probability of error of antenna-subset selection with space-time block codes," *IEEE Trans. Commun.*, vol. 53, no. 11, pp. 1799 – 1803, Nov. 2005.
- [65] S. Kaviani and C. Tellambura, "Closed-form BER analysis for antenna selection using orthogonal space-time block codes," *IEEE Commun. Letters*, vol. 10, no. 10, pp. 704 – 706, Oct. 2006.

- [66] X. N. Zeng and A. Ghrayeb, "Performance bounds for space-time block codes with receive antenna selection," *IEEE Trans. Inf. Theory*, vol. 50, no. 9, pp. 2130 – 2137, Sept. 2004.
- [67] W. Li and N. C. Beaulieu, "Effects of channel-estimation errors on receiver selection-combining schemes for Alamouti MIMO systems with BPSK," *IEEE Trans. Commun.*, vol. 54, no. 1, pp. 169 – 178, Jan. 2006.
- [68] H. A. David, *Order Statistics*. John Wiley & Sons, 1970.
- [69] I. S. Gradshteyn and I. M. Ryzhik, *Table of Integrals, Series, and Products*, 6th ed. San Diego, CA: Academic, 2000.
- [70] M. K. Simon and M.-S. Alouini, *Digital Communication over Fading Channels: A Unified Approach to Performance Analysis*. New York: John Wiley & Sons, 2000.
- [71] H. Shin and J.H. Lee, "Performance analysis of space-time block codes over keyhole Nakagami-m fading channels," *IEEE Trans. Veh. Technol.*, vol. 53, no. 2, pp. 351–362, Mar. 2004
- [72] J.W.Craig, "A new, simple, and exact result for calculating the probability of error for two-dimensional signal constellations," in *Proc. IEEE MILCOM'91*, Boston, MA, Oct. 1991, pp. 571–575
- [73] [26] Z. Chen, J. Yuan, and B. Vucetic, "Analysis of transmit antenna selection/maximal ratio combining in Rayleigh fading channels," *IEEE Trans. Veh. Technol.*, vol. 54, no. 4, pp. 1312–1321, July 2005.
- [75] H. Shin and J. H. Lee, "Performance analysis of space-time block codes over keyhole Nakagami-m fading channels," *IEEE Trans. Veh. Technol.*, vol. 53, no. 2, pp. 351–362, Mar. 2004.
- [76] S. Thoen, L. V. der Perre, B. Gyselinck and M. Engels, "Performance analysis of combined transmit-SC/receive-MRC," *IEEE Trans. Commun.*, vol. 49, pp. 5–8, Jan. 2001.
- [77] L. Yang and J. Qin, "Performance of Alamouti scheme with transmit antenna selection for M-ary signals," *IEEE Trans. Wireless Commun.*, vol. 5, pp. 3365–3369, Dec. 2006.

- [78] Z. Chen, J. Yuan and B. Vucetic, "Analysis of transmit antenna selection/maximal-ratio combining in Rayleigh fading channels," *IEEE Trans. Vehic. Technol.*, vol.54, pp. 1312–1321, Jul. 2005.
- [79] X. Cai, G. B. Giannakis, "Performance analysis of combined transmit antenna selection diversity and receive generalized selection combining in Rayleigh fading channels," *IEEE Trans. Wireless Commun.*, vol.3, pp. 1980–1983, Nov. 2004.
- [80] D. A. Gore and A. J. Paulraj, "MIMO antenna subset selection with space-time coding," *IEEE Trans. Sign. Process.*, vol. 50, pp. 2580–2588, Oct. 2002.
- [81] T. Gucluoglu and T. M. Duman, "Performance analysis of transmit and receive antenna selection over flat fading channels," *IEEE Trans. Wireless Commun.*, vol. 7, pp. 3056–3065, Aug. 2008.
- [82] N. R. Sollenberger, "Diversity and automatic link transfer for TDMA wireless access link," in *Proc. GLOBECOM*, Houston, TX, Nov. 29Dec.2,1993,pp.532-536.
- [83] L. Yang and J. Qin, "Performance of Alamouti scheme with transmit antenna selection for M-ary signals," *IEEE Trans. Wireless Commun.*, vol. 5, pp. 3365–3369, Dec. 2006.
- [84] S. Kaviani and C. Tellambura, "Closed-form BER analysis for antenna selection using orthogonal space-time block codes," *IEEE Commun. Letters*, vol. 10, pp. 704–706, Oct. 2006.
- [85] S. R. Meraji, "Performance analysis of transmit antenna selection in Nakagami-m fading channels," *Wireless Pers. Commun.*, vol. 43, pp. 327–333, Oct. 2007.
- [86] Z. Chen, J. Yuan, Y. Li and B. Vucetic, "Error performance of maximal-ratio combining with transmit antenna selection in flat Nakagami-m fading channels," *IEEE Trans. Wireless Commun.*, vol.8, pp. 424–431, Jan. 2009.
- [87] J.M. Romero-Jerez and A. J. Goldsmith, "Performance of multichannel reception with transmit antenna selection in arbitrarily distributed Nakagami-m fading channels," *IEEE Trans. Wireless Commun.*, vol.8, pp. 2006–2013, Apr. 2009.
- [88] M. Nakagami, "The m-distribution: a general formula of intensity distribution of rapid fading," in *Statistical Methods in Radio Wave Propagation*, W. C. Hoffman, Ed. Oxford, U.K.: Pergamon, 1960, pp. 3–36.

- [89] G. Zang and G. Li, "Performance analysis of orthogonal space-time block codes over hadowed Rician fading channels," in Proc. IEEE ITW, Chengdu, China, Oct. 2006, pp. 453–457.
- [90] A. Miiller and J. Speidel, "Orthogonal space-time block codes with receive antenna selection: Capacity and SER analysis," in Proc. 2nd CHINACOM, Shanghai, China, Aug. 2007, pp. 574–578.
- [92] M. K. Simon, M. S. Alouini, Digital Communications over Fading Channels. New York: John Wiley&Sons, 2005.
- [93] Z. Wang and G. B. Giannakis, "A simple and general parameterization quantifying performance in fading channels," *IEEE Trans. Commun.*, vol. 51, pp. 1389---1398, Aug. 2003